In practice, a confidence interval was calculated by fitting statistics to the 500 generated discharge scenarios. By trial and error, it has appeared that a useful synthesis could be based on a lower limb of the interval taken as the 30 % quantile and the upper one as the 95 % quantile. These quantiles were chosen so that the range of future discharges was wide enough to include the observed discharge most of the time. Also, below the 30 % quantile, the scenarios frequently reverted to the zero rainfall scenario which is the natural recession from the current hour status, when rain definitively stops, see Figure 4.3.14 (b) and (c).

Obviously, using such statistics does not prevent one from considering some of the extreme scenarios, but proves more useful as a first tool.

This sytem has been "played" off-line on all the events of the Gardons data set, in an attempt to reproduce real-time conditions. Obviously, both TOPMODEL and the Rainfall Generator had been already calibrated on this set of events, therefore altering slightly the value of this validation test.

A complete example is provided for a multi peak event where a sequence of 12 hour ahead forecast is provided for some critical time-steps during the event (Figure 4.3.15). More details can be found in Lardet and Obled (1994), and only conclusions will be presented.

Results can be summarized as follows:

a) the system provides reliable information up to a lead-time of 4 hours, and often 6hours . Indeed, rainfall scenarios are only significantly conditioned by past observed rainfall for a couple of future coming hours only. Taking into account a delay of almost 2 hours between rainfall and discharge at the outlet of the catchment, it means that discharge scenarios can be actually well conditionned during 4 hours. At this short lead-time, generated discharge scenarios can be considered as reliable forecasts.

b) the system provided useful information for decision-making for lead-times up to 12h. At these longer lead-times, generated scenarios can be considered as potential future discharges, or climatologically likely discharges, but not as forecast, since the conditioning is weakened. For example, it can give an idea of possible future

discharges if it continues to rain after the flood peak, even if it is more likely that rain stops . In some such cases, the range of future discharge scenarios may be very wide, which reflects the fact the hydrological system is mainly driven by its last inputs.When these inputs are uncertain, the response can only be very uncertain.

c) results are very dependent on the time-step in a rainfall event at which generations are considered. Indeed, the quality of the results, (in terms of a narrow range for the discharge confidence interval), is not constant throughout an event. At some time, the meteorological situation conditions the rainfall generation very well (e.g. just after a storm peak, when rainfall can only dampen for a few hours) but at other times, conditioning is weaker and the range of future discharges becomes wider.

d) the rising part of a hydrograph is quite well predicted by the upper limb of the confidence interval used whilst the lower limb is more useful when discharges are receeding. Thus, the problem is to determine exactly when the discharge peak will or has occured. But this can be solved only by using a meteorological model.

e) even if the rainfall-runoff model is considered good, the uncertainties related to such a model cannot be ignored and should be added to the confidence interval suggested by the scenarios. This was not done in the work presented here because the aim was only to investigate the usefulness of a stochastic rainfall generator. These uncertainties are obviously more important at lead-times of more than 6 h, but could be neglected in a first step at lead-times up to 4 h.

f) it was noticed that other meteorological information could be added to the model to obtain a still better conditioning of the scenarios by the observed situation. The present conditioning is performed by the observed past only. However, existing meteorological forecast could suggest an expected range of possible future rainfall volumes (over the next 12 h for example). In such case, this can be assimilated by the rainfall generator which would then be used as a disaggregation model of these suggested volumes to give still more realistic scenarios of rainfalls and discharges. An example is provided for the biggest event available, with the confidence interval based on past rainfall only (see Figure 4.3.14(d)), or complemented by a 12 hour forecast specifying that total rainfall will be between 50 and 150 mm (see Figure 4.3.14(e)).

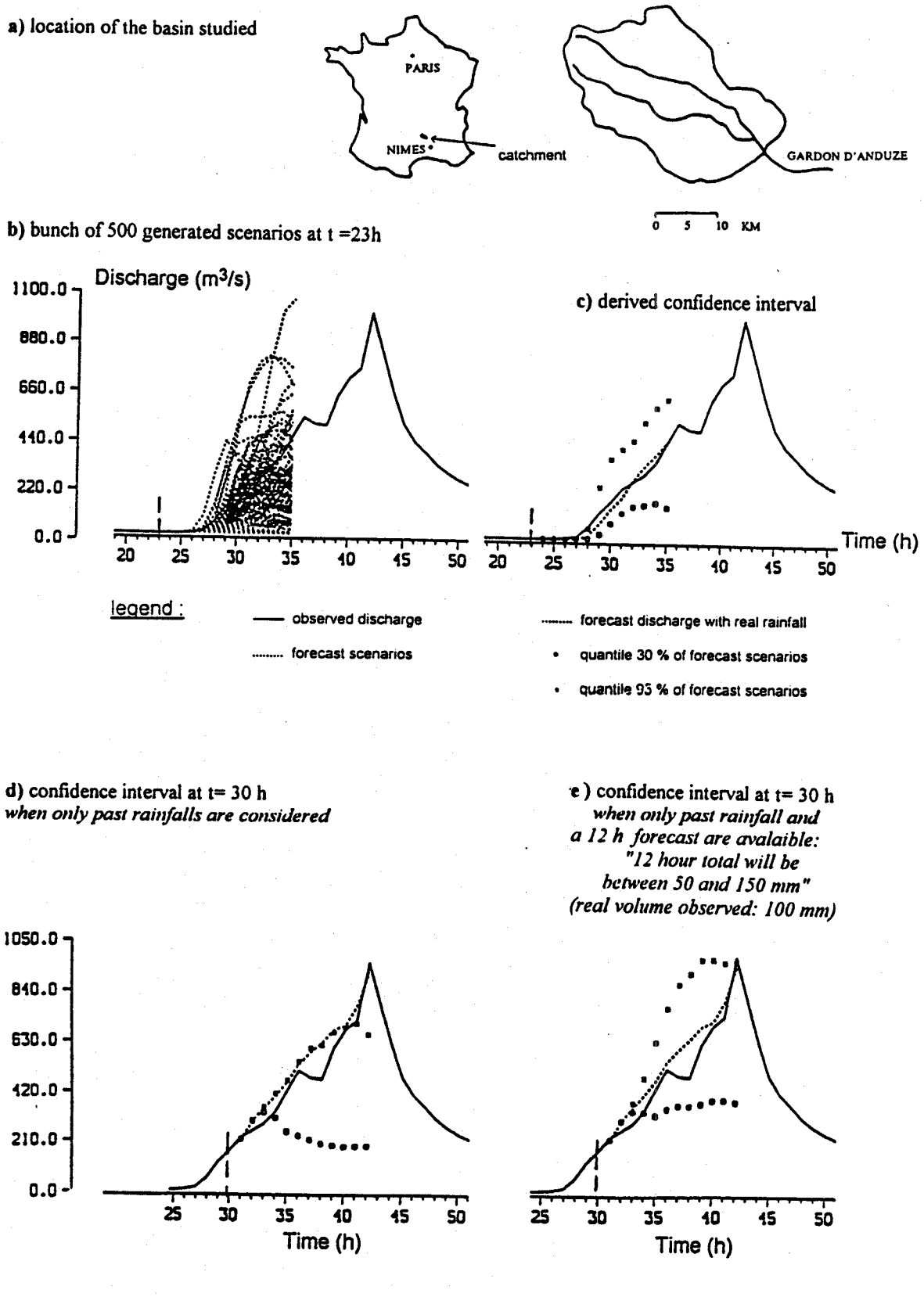

Figure 4.3.14 - Example of generated scenarios and derived confidence intervals

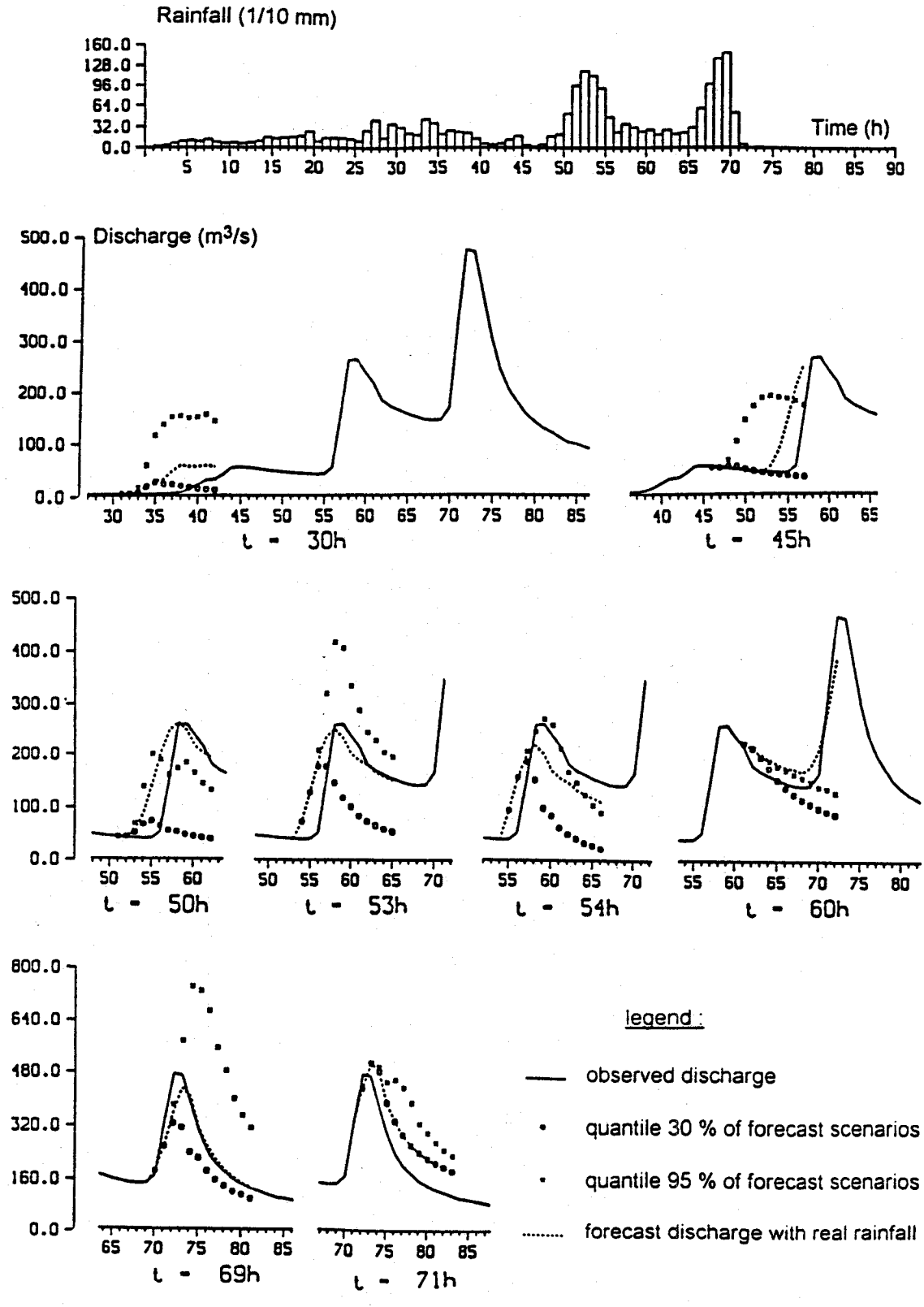

Figure 4.3.15 - Example of discharge confidence intervals issued during a multi-peak event

In conclusion, it has been shown that this rather simple method already shows a significant improvement over a pure hydrologic forecasting system. This was not expected, nor is it a widespread concept in the hydrologic community. Furthermore, it still seems far from complete development.

4.4 CONCLUSIONS

Various problems and methodological options arise when a rainfall-runoff model is operated for real-time flood forecasting. These are summarised below to help the non-expert user in model development and use.

Choice and collection of data

At first, it may be sufficient to collect the longest possible record of data for the most significant events (of the range which is feared to produce trouble making flooding i.e. an order of magnitude of two to three per year). So, our suggestion will be to perform first an exploratory analysis on event data, even if the implementation choice is to run the model continuously (see below).

The time step to be used is roughly around one hour, coming down to half an hour for basin areas of some 10 km^2, and two or three hours when approaching 10.000 km^2.

There are two important things about the quality of data. One is the density of the raingauge network (or the availability of radar information), to get a good estimate of the true input variable i.e. the basin average rainfall. Some rules of thumb deduced from geostatistical analysis of rainfall fields suggest one gauge per ~25 km^2 x (time step in hours) without getting below one gauge per ~80 km^2 x (time step in hours). If this density is not accessible, there is a strong chance that the gross input rainfall is poorly estimated, so it will be hard to get a proper estimate of effective rainfall and quick runoff. In any case a preliminary study of the area should be made, given that the required density depends on several factors, among which is the spatial correlation of precipitation fields.

The second issue is the quality of discharge data, especially for high or extreme values. Obviously, reproducing those "observed" values will be the aim of any model, whatever its type. If these values are wrong or biased due to poor instrumental procedures or to poor extrapolation of rating curves for example, the model will do its best to reproduce those wrong values. In particular a problem is frequently found in the calibration and updating of rating curves that may lead to extensive extra work involving hydrological analyses in order to match hystorical with real-time level data.

Event-based vs continuous operation

There is no definite position to be maintained in the use of event-based versus continuous models, since it depends very much on external constraints such as the wishes of the demanding service or the context of available on-line data.

A continuous operational model offers the guarantee that the system is permanently ready to respond to a sudden rain event, in that it does not require initialization. It is obvious that in this case a real time data acquisition system is needed but in any event, this is an essential pre-requisite for a real time flood forecasting system. Besides, in actual operation, the model may not be run continuously in real time, since a long antecedent dry period may be quickly reprocessed at the onstart of a new event, so long as the data has continued to be collected in the interim, which is usually the case. Although such a model requires continuous series, discontinuities often arise e.g. from breaks in the gauge, maintenance periods etc., and therefore an automatic real time data reconstruction system must be available. In the European Flood Forecasting Operational Real Time System (EFFORTS) (E. Todini & Partners, 1992), the algorithm described in Section 4.3.2 is implemented in order to automatically rebuild missing data.

On the other hand, event-based models may often provide the same level of performance for wet periods only with a slightly simpler structure but at the cost of a very careful and sensitive initialisation. Several ways will be explored to cope with this requirement, later on. In the case of event based models, the only strong recommendation is to select one of those for which initialisation can be reasonably controlled and understood (like in TOPMODEL, where it relies only on pre-event baseflow, if there is some) and provide an organization to ensure that the system and operators can be quickly brought on-line.

The basin response function

Parabollic transfer functions, such as the ones in the ARNO model (Todini, 1996) can be developed. In this case calibration must be performed based on physical grounds by taking care of the speed and the attenuation of the flood waves produced by the runoff over the hillslopes and in the channels.

Alternatively a transfer function identification approach for the routing of runoff can be used. This method can be used, as long as the transfer function has been based on a substantial sample of events of sufficient quality.

If one derives the function only from input output data, this may be substantiated first by a qualitative screening of the "purest events" (single peaked, with short intense rainfalls). However, a more complete screening of all major events, either long or multi-peaked, requires the help of an objective method, as much independent of a priori model as possible. Among existing identification techniques, the alternate iterative FDTF-ERUHDIT method has proved objective and robust enough to be as much free as possible of a priori assumptions (particularly on the loss function or water accounting part of the process), and flexible enough to accommodate many options.

A strategy for running these analyses has been derived from experience, consisting in three steps:

(a) First a rough-hewing of the transfer function, ordinate per ordinate, is made to detect its general shape. This requires at least 12 to 15 flood events, preferably more. The poorer the data, the more floods are needed. Instabilities in the transfer function, like secondary peaks are often an index of poor data quality or a difficult catchment.. Often, a recession analysis is useful to approximate the response length and to decide if an extra filtering of the baseflow is required (which is only partially performed by the FDTF-ERUHDIT method).

(b) Next, the invariance of the transfer function must be considered. The FDTF-ERUHDIT tool can still be used in an exploratory mode, to test whether event subsamples, stratified according to different criteria (e.g. rain intensities, initial discharges, etc...) and gathering at least eight or ten events, do not show excessive time-variance of their respective transfer function. These trials allow one to measure

the degree of robustness in using a unique transfer function, or suggest a parametrisation for making it time-variable (e.g. according to the discharge level).

(c) Finally, a refined average transfer is derived, sometimes smoothed by ARMAX fitting (on discharges or discharges variations). Simultaneously, a set of excess rainfall series is derived by deconvolution. The presence of instabilities (like succession of high and low values) often reveals problems in the original data. Otherwise, the deconvoluted excess rainfalls may serve as a hint for what a loss model should produce, and may guide its choice.

Choice of a loss or production function

This choice should hopefully be based on extensive instrumentation and experimental work at the basin scale. However, this is more often based on a priori assumptions or model availability. This choice will also interact with our capacity to initialise or control the internal state of the model.

If a predominantly Hortonian generation is assumed, where excess runoff is controlled by infiltration capacity, this means that antecedent conditions must focus on topsoil wetness. This variable is known to be highly spatially varying, and difficult to access at the basin scale except through very rough indexes like the antecedent precipitation index. Models like SCS, SACRAMENTO and SWATCH, are good representatives of this type of model.

If, on the other hand, the development of contributing areas is a sustainable assumption, excess runoff becomes mainly controlled by aquifer seepage. This means that antecedent conditions rely on full soil wetness or near-surface aquifer storage. This variable is known to correlate pretty well with recession flows, unless the latter are influenced or disappear totally. Models employing this concept are essentially simplified aquifer models; TOPMODEL, and eventually ARNO, are representative of this class.

Calibration and initialisation

Whatever the model chosen, a large degree of pragmatism is required for calibration. The parameters of the model should have, as far as possible, a physical meaning. Automatic calibration should be avoided since most of the time it is unable to estimate sets of physically meaningful parameters and to discriminate among convergent sub-basins.

Another problem will arise in real-time operation, even with a "good" model, namely its initialisation at the start of a new event. As has already been discussed in the choice of the production model , depending on the dominant processes, the critical initial state may be the topsoil humidity or the upper aquifer level.

The first way explored here was the updating of this variable by Kalman filtering, responding to the first reactions of the basin discharge to the starting event. This proved very unstable and must be discarded. An error correction model, superimposed on the loss model itself, does better, although it does not change the potentially poor initialisation used.

A better way is to run the model continuously, hoping that the model performs well enough to be in the proper state at the onstart of the next event. This requires some extra complexity, since the water accounting (involving processes such as actual evapotranspiration or aquifer drainage) must be reproduced more precisely than in the case of the model running on events only.

This does not mean that one can abandon a permanent checking of the model, which is usually based on observed streamflows. Running continuously does guarantee fully a proper state for the model. A potentially more economical way could consist of running the model at larger time steps (e.g. daily) during those recession periods. This has been explored in this project. It involves running the model in continuous-time on a daily basis, extracting the values of state variables and initialising the model on the final shorter time step (e.g. one hour) through these initial values. Prediction of initial states though model operation on a daily basis is very accurate for models with a small number of parameters (three to five) and state variables (two or three), such as the simplified TOPMODEL. For other models with a larger number of parameters (more than ten) and state variables (more than five) predictions are generally accurate for those states that are directly related

to the slow response of the basin. So, for such models (i.e., SACRAMENTO, TANK, ARNO, etc.) one or two initial states need to be tuned or filtered during real-time operation.

Calibration based on inappropriate data

Historical data records that are inappropriate (in the sense of being sparse) for model identification is not an uncommon situation in the design phase or the first stages of operation of a flood forecasting system. Small response times of small and medium-sized basins (with areas up to several hundreds of km^2) require small time steps (up to few hours) while the bulk of the available data has been obtained through non-recording devices as a series of daily observations. Continuous records are sparse and they have often been obtained for some significant flood events for the needs of a flood study in the area. The long series of daily data can be effectively used to identify the model selected on a daily basis. The transfer function of the model can be directly identified based on multi-event data set that can be extracted from the continuous-time records. With this transfer function and a production function derived from the daily model, and a model can be obtained (called derived model). Extensive computer experiments have shown that this model is an acceptable alternative to a model identified on a set of appropriate data.

Lumped vs distributed: hints for semi-distribution

It has been seen in Chapter 3 that when rainfall falls over almost the whole catchment and is spread in time and space, then the damping capacity of the basin due to integration is sufficient to smooth the effects of this variability. If the dominant processes are interflow and saturation excess overland flow, only a small part of the basin contributes directly, while a large part of the water goes first into the topsoil which probably smooths its spatio-temporal variability. In this rather common case, a lumped treatment performs as well as a distributed one.

However, it may happen that:

(a) rainfall is very localised, i.e. the wetted area is quite limited, it does not last for a long period of time (compared with the response time), and covers only part of the basin, (e.g. a particular tributary), and/or that

(b) rainfall displays little temporal variability, i.e. large intensities last long enough to prevent the given subcatchment to recover, and the drainage network is too short to dampen the effect from the isolated basin.

In both cases, the transfer function that controls the response is no longer that of the complete catchment, but that of the tributary on which the rainfalls. This happened for example in the catastrophic flood of Vaison la Romaine in France (22nd September 1992), when it was not the whole Ouveze catchment (580 km^2) that was wetted, but three downstream subcatchments close to the outlet totalling only 120 to 150 km^2 (see Figure 4.3.16(a)). This lasted for three to four hours, while common rain events move and stay hardly more than an hour and a half. In another catastrophe occurring in the city of Nîmes in 1988, a stationary cell remained for more than six hours with very constant intensities of about 40 to 50 mm/h.

The lack of spatio-temporal spread in big rain events seems more hazardous than a large variability. In such cases where only part of the basin is specifically hit by a long lasting cell, the transfer to consider is that of the subbasin, especially when it runs off close to the global outlet.

This leads to another remark concerning the network structure of the basin: When the point of interest for a forecast is located immediately downstream of the confluence of two main tributaries, then it is better to identify each tributary's transfer function separately (which means two or more gauging stations). Roughly, it seems already worth considering separately any tributary coming close to the outlet when its size exceeds 10% of the total catchment. For example, on the Upper Loire River catchment (867 km^2 - see Figure 4.3.16 (b)) which threatens the city of Brives-Charensac, the Aubepin right bank tributary (~170 km^2) needs special attention.

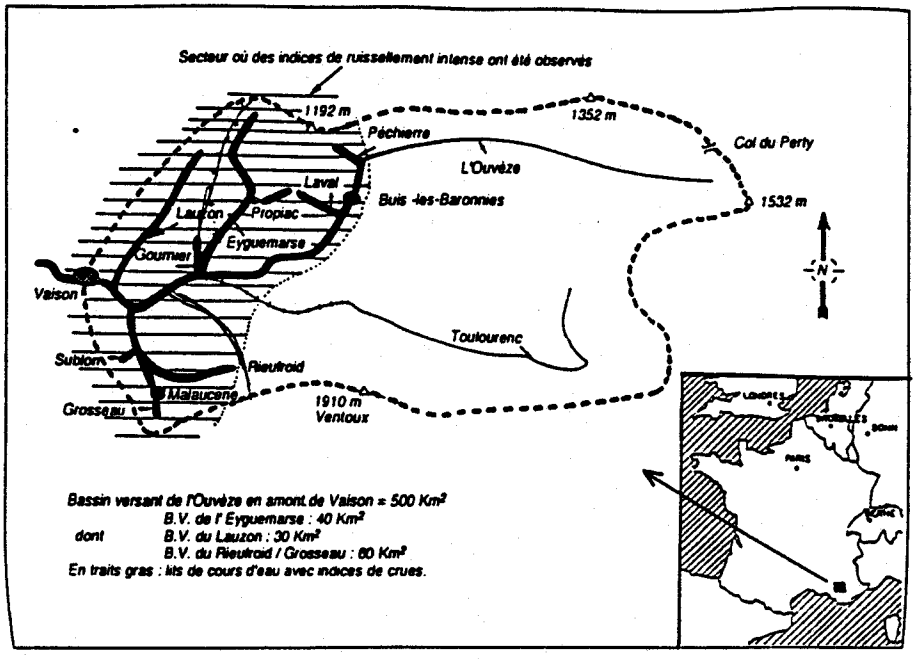

a) Ouvèze basin (580km²), in South france,
striken by a catastrophic localised event in 1992

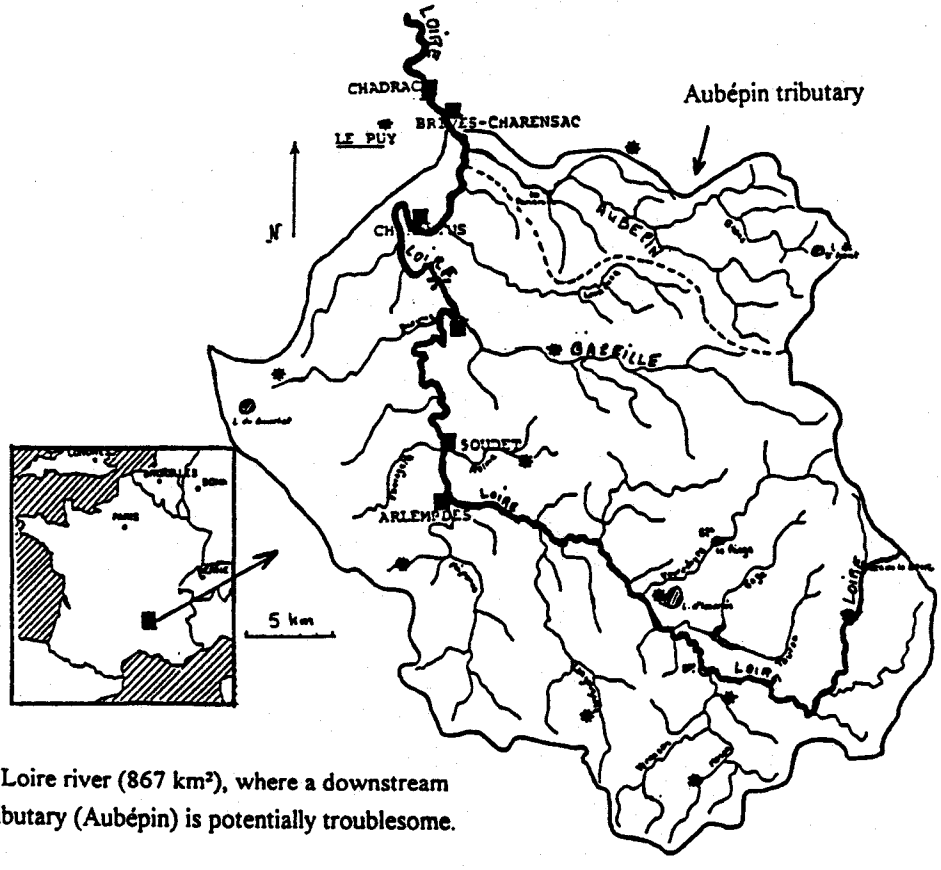

b) Upper Loire river (867 km²), where a downstream
tributary (Aubépin) is potentially troublesome.

Figure 4.3.16 - Examples of basins where the global response may reduce to that of a downstream tributary

As a rule of thumb, if an hourly or half-hourly time step is used, a splitting into subbasins down to 10 or 15% of the whole basin area when located in the vicinity of the outlet, or 50 km^2 as an order of magnitude, (provided rainfall can be properly estimated for each subbasin) seems sufficient to avoid those particular cases when the overall basin transfer function degenerates for a particular event into that of a single tributary. Figures 4.3.17(a) and 4.3.17(b) show examples of basins used in this project where no splitting is required (Réal Collobrier at Pont de Fer and Sieve at Fornacina). On the other hand two other basins used in the project (Gardon d'Anduze or Paillon at Nice shown in Figure 4.3.18) show a network structure likely to display those particular effects.

A recommended procedure could consist in running routinely at the larger scale of interest (e.g. for a basin of 527 km^2, to run a global model at 500 km^2), but to keep ready a model of any subbasin (e.g. a tributary of 63 km^2 delivering its discharge close to the outlet). Any time when there is doubt about a possibly concentrated and stationary system, this secondary model could be run and compared with the whole-basin model. If raingauge networks have a density not allowing one to track such situations, qualitative radar imagery can easily suggest if it is worth (or not) decreasing the scale considered. So a nested structure of basins, organised according to a hierarchy that considers only those with a significant degree of potential hazard, can compete with a fully distributed, or a fully split structure (i.e., where all the basins considered are at the same scale, e.g. $\sim$40 km^2, and then linked to each other).

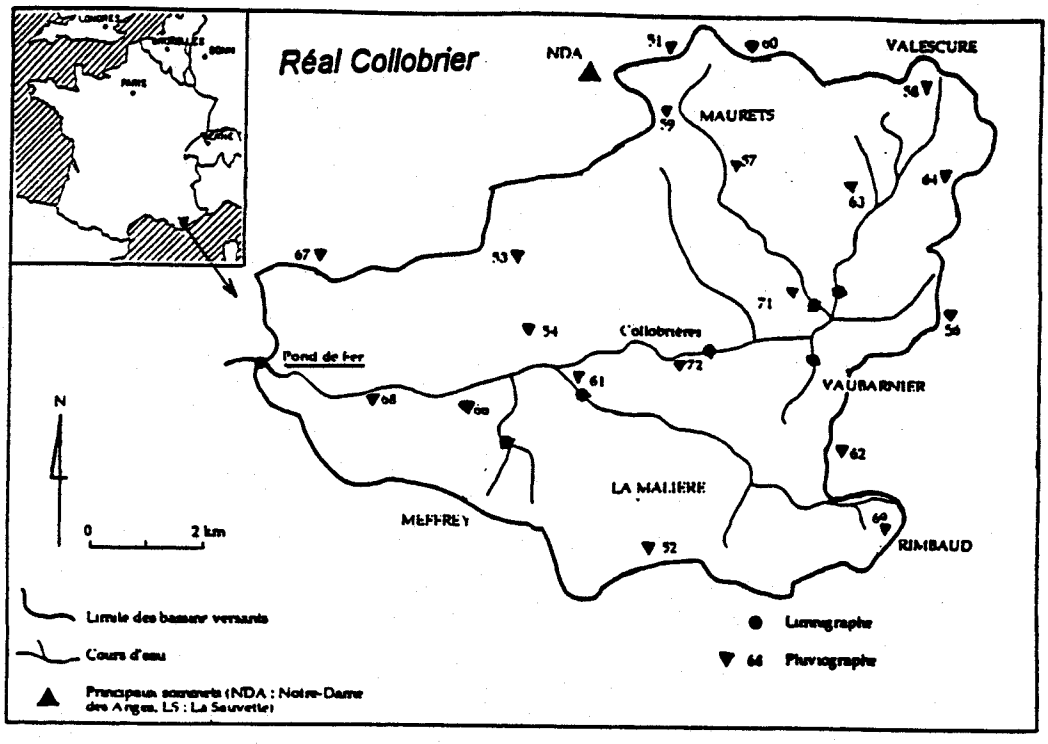

a) Réal Collobrier (71 km²), in South france,

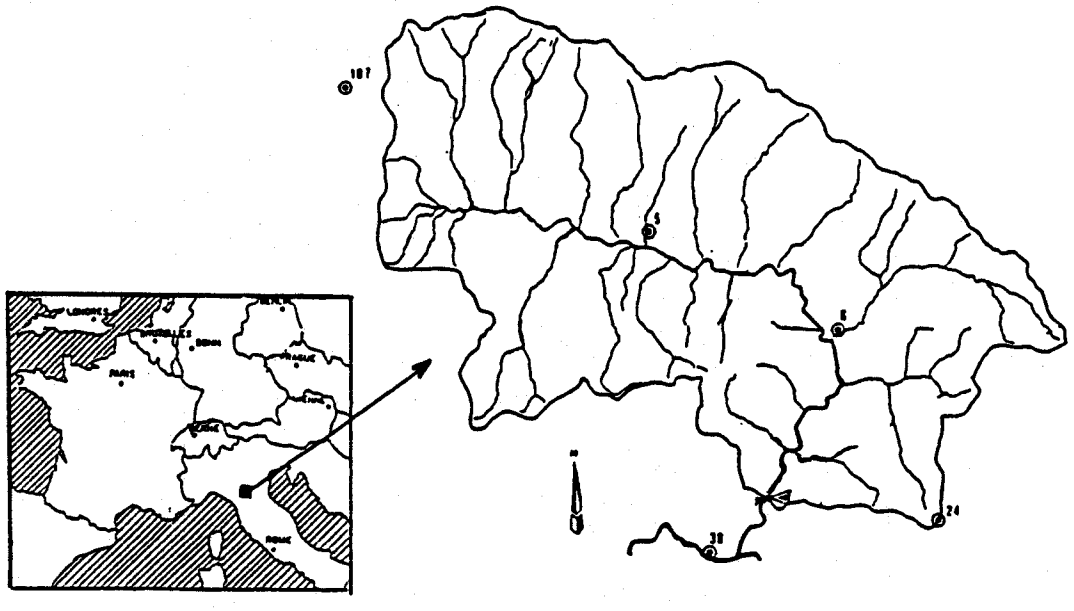

b) Sieve (840 km²), in Central Italy

Figure 4.3.17 - Examples of basins where the global response may prove sufficient for a downstream forecast

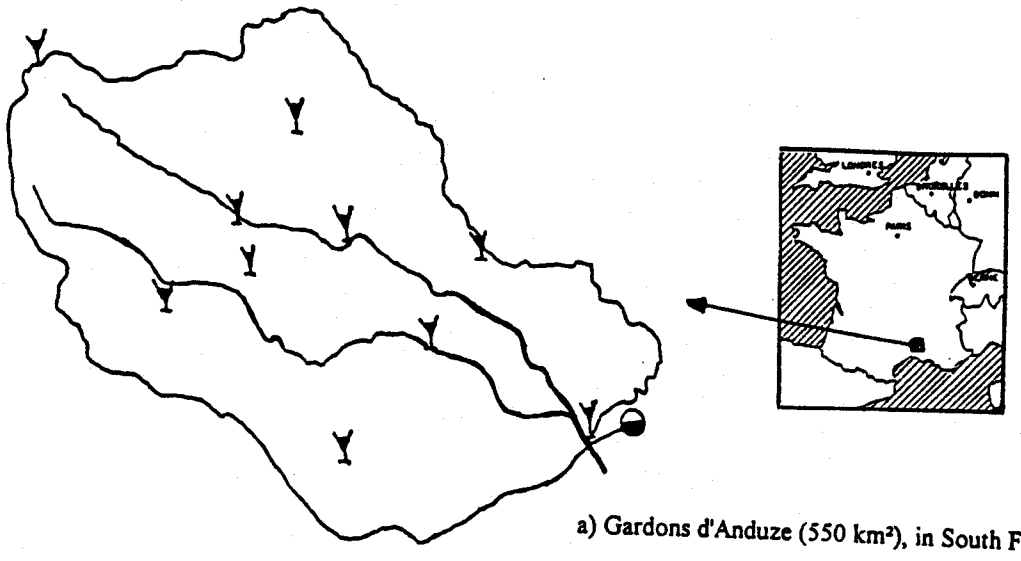

a) Gardons d'Anduze (550 km²), in South France,

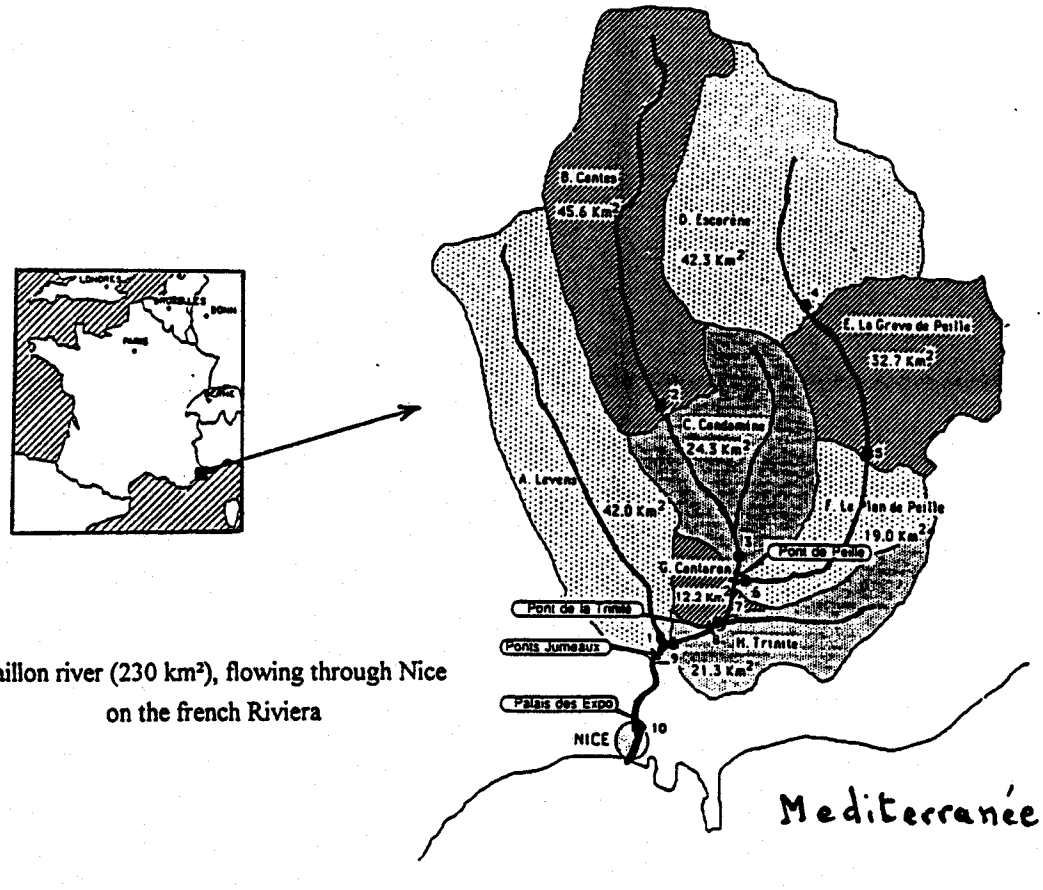

b) Paillon river (230 km²), flowing through Nice on the french Riviera

Figure 4.3.18 - Typical examples of basins with network structure that would require some splitting

Rainfall scenarios for real-time operation

It has long been claimed that for medium sized, quickly responding streams, the availability of rainfall information is critical for issuing forecasts with sufficient lead-times. Until reliable QPFs produced by mesoscale-meteorological models become routinely available, synthetically generated rainfall scenarios can increase the lead time by some (precious) hours, as it has been shown here.

Until now, only single input scenarios have been tested. However they can already be conditioned by the observed past, and also by the information available on the near future (meteorological forecast, probabilistic QPFs).

No doubt, the more sophisticated rainfall models as described in Chapter 2 will soon allow scenarios of spatial rainfall on more than one a priori fixed catchment. This approach will allow a swift move from the present situation where no (or very crude) future rainfall is entered in the hydrological models, to a hopeful future where excellent QPFs (both in volume, timing and localisation), will become available.

Real-time updates of Flood Forecasts

There are three commonly used means of updating forecasts, usually embedded in a Kalman Filter. They are described as follows:

- updating the state variables (which typically describe the amount of water stored in various natural reservoirs);
- modifying the parameters of the rainfall-runoff model from observed and computed flows;
- using a physically based rainfall-runoff model, which once calibrated is left alone to compute current and future flows which are then corrected by the Kalman Filter using the most recently observed values.

The first two approaches pose non-linear estimation problems, usually dealt with by using Extended Kalman Filters. In particular, the second approach (in which the non-linear model parameters are modifed on a regular basis) may lead to numerical instability, usually because many of the parameters are not observable.

The third method is unconditionally stable, being a linear smoothing of the output from a non-linear model, which already has high precision and has been calibrated on sensible physically based premises. The Kalman Filter then raises the precision of the estimates from a (reasonable) 85% to a very useful 99% for one-step-ahead forecasts which slowly decays to 90 to 95% accuracy twelve steps ahead.

Model intercomparison

The main conclusion that may be drawn from the intercomparison of the ARNO model whith the TOPMODEL is that both models are expected to give results of the same quality. The ARNO model appears slightly more complex to calibrate than TOPMODEL. However, TOPMODEL may fail to correctly represent the unsaturated zone.

REFERENCES

Bergström, S., 1976, Development and Application of Conceptual Runoff Model for Scandinavian Catchments, SMHI. Nr. RHO 7, Norrköping.

Bertoni J.C., Tucci C.E. and Clarke R.T. 1992. Rainfall-based real-time forecasting, J. of Hydrol., 131, p. 313-319.

Beven, K.J. and Kirkby, M.J., 1979. A physically based variable contributing area model of basin hydrology, Hydrol. Sci. Bull., 24, 43-69.

Beven, K.J., 1986. Runoff production and flood frequency in catchments of order n: an alternative approach, in Scale problems in hydrology, Gupta et al. (ed.), Reidel Publishing Company, Dordrecht, pp. 107-131.

Brath A. , Burlando P. and R. Rosso, 1988. Sensitivity analysis of real-time flood forecasting to on-line rainfall predictions. International Workshop on Natural disasters in European-Mediterranean countries.Perugia Italy 1988. Proceedings published by UNESCO 1989. 20 p.

Burnash, R.J.C, Ferral, K.L. and McGuire, R.A., 1973. A generalized streamflow system: conceptual modeling for digital computers, Report, Joint Federal State River Forecast Center, U.S. National Weather Service, and California Department of Water Resources, Sacramento.

De Lainė, R.J., 1970. Deriving the Unit Hydrograph without using rainfall data, J. Hydrol., 10, 379-390.

Delleur, J.W.D., and Obled, Ch., 1985. Flash flood forecasting in the Cevennes Region in France: a case study, proceedings of the Vth World Congress on Water Resources, Brussels, Belgium, IWRA publ., 871-881.

Duband, D., Nalbantis, I., Obled, Ch., Tourasse, P. and Rodriguez, J.Y., 1990. Unit Hydrograph revisited: the first differenced transfer function (FDTF) approach, in Hydrology of Mountainous Areas, IAHS Publ., No 190, (editor L. Molnar), proceedings of the _trbské Pleso workshop, Czechoslovakia (June 1988).

Duband, D., Obled, Ch. and Rodriguez, J.Y., 1993. Unit Hydrograph revisited: an alternate iterative approach to U.H. and effective precipitations identification, *J. Hydrol., 150*, 113-149.

E. Todini & Partners - Consulting Engineering Srl , 1992 - The FUCHUN River Project, A Computer Based Real Time System.

Franchini, M. and Pacciani, M, 1991. Comparative analysis of several conceptual rainfall-runoff models. J. Hydrol., 122, 261-219.

Georgakakos K.P. 1986a. A generalized stochastic hydrometeorological model for flood and flash-flood forecasting. 1. Formulation. Water Resour. Res. 22(13): 2083-2095.

Georgakakos K.P. 1986b. A generalized stochastic hydrometeorological model for flood and flash-flood forecasting. 1. Case Studies. Water Res. 22(13): 2096-2106.

Gouy, D., 1991. Comparaison de deux méthodes d'identification de la fonction de transfert et des pluies efficaces. Application au bassin du Gardon d' Anduze, Mémoire de DEA (Master Thesis) - Université J. Fourier-LTHE-Grenoble-39 p.+annex.

Gresillon, J.M., Lemeillour, F., Neyret-Jigot, J.M. et Obled, Ch., 1994. Variabilité de la fonction de transfert d'un bassin versant. Analyse des causes et essais d'interprétation, Société Hydrotechnique de France - 23èmes Journées de l'Hydraulique, Nîmes, 1994.

Gresillon, J.M.G., 1994. Contribution a l'étude des écoulements de crue dans les petits bassins versants, Thesis for Habilitation Diploma. INPG-UJF-Lab. LTHE. 157 p.

Imhoff, A.C., 1993. Modélisation hydrologique opérationnelle. Application de la chaîne DPFT+TOPMODEL à un bassin versant méditerranéen: le Paillon de Nice, (Diploma Thesis) Ecole Polytechnique Fédérale de Lausanne, 53p.

Lardet P. 1992. Prévision des crues: contribution à l'utilisation opérationelle de modèles pluie-débits. Ph. D. Thesis, Institut National Polytechnique de Grenoble.

Lardet P. and Ch. Obled 1994. Real-time flood forecasting using a stochastic rainfall generator (accepted for publication in the J. of Hydrology)

Lardet, P., 1990. Etude comparative de deux modèles pluie-débit globaux: DPFT et GR3H. Applications aux bassins de Réal Collobrier et du Rio Alenquer, Mémoire de DEA (Master Thesis) - Université J. Fourier Grenoble.

Lebel T. 1984. Moyenne spatiale de la pluie sur un bassin versant: estimation optimale, génération stochastique et gradex des pluies extrêmes. Ph. D. Thesis, Institut National Polytechnique de Grenoble.

Loague, K.M., and R.A. Freeze, 1985. A Comparison of Rainfall-Runoff Modelling Techniques on Small Upland Catchments, Water Resources Research, 21, 229-248

Mehra, R.K., 1974. Topics in Stochastic Control Theory: Identification in Control and Econometrics: Similarities and Differences, Ann. Econ. Social Measures, 3, 21-47.

Murphy, A.H., 1992. Climatology, persistence, and their linear combination as standards of reference in skill scores, Weather Forecasting, 7, 692-698

Nalbantis, I., 1987. Identification de modèles pluie-débit du type hydrogramme unitaire: développement de la méthode DPFT et validation sur données générées avec et sans erreur, Thèse de doctorat INPG, Grenoble..

Nalbantis, I., 1994a. Use of multiple-time-step information in rainfall runoff models, submitted for publication to the Journal of Hydrology.

Nalbantis, I., 1994b. Use of multiple time-steps in rainfall runoff models: evaluation on synthetic data, paper presented at the XIXth General Assembly of the European Geophysical Society, Grenoble, 25-29 April 1994.

Nalbantis, I., Obled, Ch. and Rodriguez, J.Y., 1994. Unit Hydrograph and effective precipitation identification: testing the FDTF-ERUHDIT method through synthetic data, submitted for publication to the Journal of Hydrology.

Newbold, P. and Granger, C.W.J., 1974. Experience with forecasting univariate time series and the combination of forecasts, J. of R. Statist. Soc. A, 137, 131-165.

Obled Ch. and Wendling J., 1991. Development of TOPMODEL: applications to Mediterranean catchments. Role of rainfall spatial variability and further simplifications for operational use. Technical Report TR n°89 CRES Center for Research on Environmental Systems - University of Lancaster 300p.

Roche, P.A., et Tamin, R., 1987. La combinaison de modèles: un moyen de limiter l'impact des perturbations en prévision des crues, Revue Internationale des Sciences de l'eau, vol 3(2), 57-65.

Rodriguez, J.Y., 1989. Modélisation pluie-débit par la méthode DPFT: développements de la méthode initiale et extension à des cas bi-entrées, Ph. Thesis INPG, Grenoble.

Roux, J.P., 1993. Modélisation des écoulements notamment dans les bassins de montagne de la zone méditerranéenne, DEA Report (Master Thesis)

Sempere-Torres, D. et Obled, Ch., 1990. Modélisation pluie-débit de bassins à relief accidenté: le rôle de la variabilité spatiale de la pluie, International Conf. on Hydrology in Mountainous Regions; AIH-IAHS Lausanne 27 Aug-1 Sept 1990, Publ. AIHS No 193, 645-654.

Sempere-Torres, D., Rodriguez, J.Y. and Obled, Ch., 1992. Using the DPFT approach to improve Flash Flood Forecasting Models, Natural Hazards, 5, 17-41, Kluwer Academic Publlshers.

Sugawara, M., 1976. The flood forecasting by a series storage type model, Int. Symp. on Floods and their computation, Leningrad.

Sugawara, M., 1979. Automatic calibration of the tank model, Hydrol. Sci. Bull., 24(3), 375-388.

Sugawara, M., Watanabe, I., Ozaki, E. and Katsuyame, Y., 1983. Reference manual for the TANK model, National Research Center for Disaster Prevention, Japan

Todini E., Bossi A., 1986. PAB (Parabolic And Backwater) an unconditionally stable flood routing scheme particularly suited for real time forecasting and control, J. of Hydraulic Res. Vol.24, n.5 pp.405-424.

Todini, E., 1988. Rainfall-runoff modeling- Past, present and future. J. Hydrol., 100: 341-352.

Turner, J.E., Dooge, J.C.I. and Bree, T., 1989. Deriving the Unit Hydrograph by root selection, *J. Hydrol., 110*, 137-152.

WMO 1992, "Simulated Real-Time Intercomparison of Hydrological Models. OHR-38. WMO n. 779.

Young, P.C., 1974. Recursive Approach to Time Series Analysis, Bull. Inst. Math. Appl., 12 (5/6), 209-224.

5 FLOOD ROUTING: MODELLING AND FORECASTING

5.1 INTRODUCTION

A flood routing model is an essential component of a real time flood forecasting system; it is a mathematical model able to predict the changing magnitude of a flood wave as it propagates through a river system: propagation along the channels is influenced by the downstream boundary condition, usually only locally, and mainly by the geometric properties of the channels: the "macroscopic" geometry (measurable with a topographic survey) and the "friction properties" (regularity, sinuosity, vegetation, bed forms, ...) which are not directly measurable but can be deduced from measurements of the water flow (levels and velocities) during past flooding periods.

For real-time operation, it is necessary to forecast water levels (sometimes also velocities or discharges) at some points of interest along the channels at an appropriate time interval, called "lead time". Forecasting is based on already available observations: water levels (and rarely velocities or discharges) at the boundaries, at the points of interest, or at other points along the channels. As flood wave celerity is usually of a few km/h, observations of water levels or discharges at the boundaries up to a certain time is sufficient for forecasting the evolution of the flood level at a point at the interior for a rather long leading time but with gradually diminishing accuracy; if this is not sufficient, it becomes necessary to be able to forecast discharges coming in from the catchments at the upstream boundaries, and sometimes also the "exit" condition at the downstream boundaries.

Flood-routing models decribe the water motion in a more or less simplified form. The so called "hydraulic" models operate with a spatio-temporal resolution (usually more than a hundred of meters and seconds) too coarse for describing details about the velocity or pressure distribution. As a consequence these models use not more than two spatial horizontal coordinates and not more than three state variables: water level elevation and two components of the horizontal mean velocity: this kind of hydraulic model is called two-dimensional, or also "shallow water". A great simplification is obtained when only one spatial coordinate along the channel and one horizontal mean velocity are retained: this kind of model is called one-dimensional, or also "fluvial".

Sometimes, when the inundated areas are crisscrossed by dikes, roads, etc. they are represented as a set of interconnected cells, connected also with the main river. It is then assumed that the water surface is nearly horizontal within a cell and that the discharge exchanged by adjacent cells depends only on the water surface elevation in these cells. For the main river itself a one-dimensional model is used; this kind of model is called "quasi two-dimensional" or mixed 1/2 dimensional.

The theoretical foundation for all these models is the set of partial differential equations expressing balances of volumes and momentum, considering as external forces gravity and frictional effects (sometimes wind is accounted for). Due to mathematical complexities of the differential equations, their analytical solution is possible only for theoretical cases, and their numerical solution had to wait one century to become feasible, as a result of advances in computing equipment and improved numerical techniques. Difficulties in their application are still present no more for mathematical or computational reasons, but because they require topographic and hydrographic measurements for describing properties of the channels and the overflow areas, which is a very expensive task for a natural river, whose geometrical and frictional properties are highly variable in space and not constant in time.

Moreover, even when a recent and reliable description of the channels is available and a "detailed" (two, quasi-two,one-dimensional) model using that description has been calibrated, this model is often adopted only for building up simpler ones to be used in the on-line forecasting procedure, as already pointed out by Cunge, Holly and Vervey (1980) and shown in "River flow modeling and forecasting" edited by Kraijenhoff and Moll (1986).

For these reasons, various simplified wave propagation models continue to be developed; these models have been categorized by Fread (1985) as:

(1) purely empirical spatio-temporal correlation of water levels or discharges;
(2) linearization of the Saint Venant equations;
(3) hydrological, based on an approximate relation between flow and storage;
(4) hydraulic, based on a simplified version of the conservation of momentum equation.

As was pointed out in Cunge (1980): "The use of models based on simplified equations

may lead to difficulties in practice, most often because of one of two factors: developments in the river basin and the limited range of applicability of simplified methods". The first reason is typical of "empirical" and "hydrological" models whose parameters are not clearly related with the channel physical characteristics and are therefore estimated through a statistical calibration; the second reason applies also to simplified "hydraulic" models, which, in Cunge's opinion: "can describe the flood propagation along steep rivers reasonably well, but cannot be used when the longitudinal free surface slope is small".

In the following, a fairly full development of the basic equations of motion for one and two dimensional models is given, with particular derivations emphasizing the background to the hydraulic models adopted in AFORISM. This is done, not because there are no other models, but because the Parabolic and Backwater (PAB) model was adopted for 1-Dimensional hydraulic modelling and the Integrated Finite Difference Scheme was adopted to model the 2-Dimensional Hydraulic Flood-routing problems in this study.

5.2 ONE-DIMENSIONAL MODELS FOR REAL-TIME USE.

The model adopted for 1-Dimensional hydraulic modelling of flow in Rivers was PAB. The back-ground and development of the model are described in the following section.

5.2.1 The PAB model for one dimensional Flow Routing

The equations that govern the one-dimensional propagation of a flood wave in a river reach, known as De Saint Venant equations, in the absence of outflows or lateral inflows distributed along the channel, may be written:

$$\begin{cases} \dfrac{\partial Q}{\partial x} + \dfrac{\partial A}{\partial t} = 0 \\ \dfrac{\partial z}{\partial x} + \dfrac{1}{g}\left[\dfrac{Q}{A}\dfrac{\partial (Q/A)}{\partial x} + \dfrac{\partial (Q/A)}{\partial t}\right] + J = 0 \end{cases} \tag{5.2.1}$$

where:

Q flow

A area of wetted section

Z height of water surface in relation to a horizontal plane

R hydraulic radius

x abscissa running along axis of water course

t time coordinate

J distributed loss, per unit of weight and unit of length, due to perimeter resistance and expressible according to Manning as:

$$J = \frac{n^2 Q^2}{A^2 R^{\frac{4}{3}}}$$

n roughness coefficient according to Manning.

In most practical applications, for studying flood propagation in natural water courses, the inertial terms are considerably lower than the friction loss terms and liquid profile slope terms and are moreover of opposite sign. In reality this is not entirely true in some particular problems where the frictional loss slope is very small and of the same order as the inertial terms, as happens for example in the case of estuaries under the influence of tides however these exception are relatively rare in applications.

On the assumption that the inertial terms are negligible, the equation system becomes:

$$\begin{cases} \frac{\partial Q}{\partial x} + \frac{\partial A}{\partial t} = 0 \\ \frac{\partial z}{\partial x} = -J \end{cases} \tag{5.2.2}$$

and may be reduced in the form of a parabolic equation in the single depended variable, flow:

$$\frac{\partial Q}{\partial t} = D\frac{\partial^2 Q}{\partial x^2} - C\frac{\partial Q}{\partial x} \tag{5.2.3}$$

where:

$$D = \frac{Q}{2JB} \tag{5.2.4}$$

$$D = \frac{Q}{A}\left(1 + \frac{2}{3}\frac{A}{BR}\frac{\partial R}{\partial z}\right) + \frac{D}{B}\frac{\partial B}{\partial x} \qquad (5.2.5)$$

where:

D: the diffusivity coefficient

C: the convectivity coefficient

B: the surface width

The equation (5.2.3) is a differential equation of the second order of the almost linear type. From an analytical viewpoint it is simpler to consider the coefficients C and D as constant so as to transform the equation (5.2.3) into a linear diffusive-convective equation, within a Δt time interval, and to take account of their temporal variability by linearizing the equation around a fresh profile of the water course at every time step.

The fact that the equation (5.2.3) is now of the linear type makes it possible to apply the principle of superposition. Basically it is possible to identify the solution to the equation (5.2.3) for an impulse and then to express every other solution by means of the convolution integral. With regard to this problem, the boundary conditions set are:

$$\begin{aligned} &\text{I)} \quad Q(0,t) = \delta(t) \quad t > 0 \quad \{\text{where } \delta(t) \text{ is the Dirac delta function}\} \\ &\text{II)} \quad Q(x,t) = 0 \quad x \to +\infty \\ &\text{III)} \quad Q(x,0) = 0 \end{aligned} \qquad (5.2.6)$$

Condition (I) indicates that the wave flowing into the reach under study is represented by a Dirac delta function. Condition (II) states that the flow disturbance is eliminated moving downstream at a sufficiently large distance. Condition (III) is consistent with the assumption of linearity accepted and expresses the fact that the disturbance is superimposed on the pre-existing outflow condition without interfering with it.

The solution to equation (5.2.3) on the basis of the boundary conditions (5.2.6), with C>0 and D>0 (Hayami, 1951), (Dooge, 1973), (Todini e Bossi, 1986) is:

$$U_{\Delta x} = \frac{\Delta x}{\sqrt{4\pi D t^3}} e^{-\frac{(\Delta x - C t)^2}{4Dt}} \qquad (5.2.7)$$

where Δx is the distance between the section considered and the section further upstream in which a flow variation is found.

Therefore, for any variation in flow upstream, while the other boundary conditions remaining unaltered, the solution to equation (5.2.3) is obtained through the convolution integral:

$$Q(x+\Delta x;t) = \int_0^t Q(x,t-\gamma)\, u_{\Delta x}(\gamma)\, d\gamma \qquad (5.2.8)$$

In practical applications equation (5.2.8) is used in discretized form. This means that the integral is replaced with a summation, the function Q(x,t) is sampled at time interval Δt, and finally $u_{\Delta x}(t)$, which represents the impulse response of the system, is replaced by the discretized form of the unit hydrograph for a square impulse of Δt duration, in other words by the Δt duration pulse response function.

To calculate the latter we proceed as follows. Note, first of all, that the response in continuous form to a rectangular pulse of Δt duration is:

$$P_{\Delta x}(t) = \frac{F(t) - F(t-\Delta t)}{\Delta t} \qquad (5.2.9)$$

where:

$$F(t) = \int_0^t u_{\Delta x}(\gamma) d\gamma = N\left(-\frac{\Delta x - Ct}{\sqrt{2Dt}}\right) + e^{\frac{\Delta x C}{D}} N\left(-\frac{\Delta x + Ct}{\sqrt{2Dt}}\right) \qquad (5.2.10)$$

where:

$$N(\bullet) = \frac{1}{\sqrt{2\pi}} \int_{-\infty}^{+\infty} e^{-\frac{\vartheta^2}{2}} d\vartheta$$

Therefore its discretized form is:

$$\overline{U}_{\Delta x}(i) = \overline{U}_{\Delta x}(t \Leftrightarrow t+\Delta t) = \frac{1}{\Delta t} \int_t^{t+\Delta t} U_{\Delta x}(\gamma)\, d\gamma = \frac{1}{\Delta t}[IU(t+\Delta t) - IU(t)] \qquad (5.2.11)$$

where:

$$IU(t) = \int_0^t U_{\Delta x}(\gamma)\, d\gamma$$

is the (continuous) step-response function. It turns out that

$$\overline{U}_{\Delta x}(i) = \frac{1}{\Delta t^2}\left[IF\{(i+1)\Delta t\} - 2IF\{(i)\Delta t\} + IF\{(i-1)\Delta t\}\right] \qquad (5.2.12)$$

where

$$IF(t) = \int_0^t F(\gamma)\, d\gamma = \frac{1}{C}\left[(Ct - \Delta x)\, N\left(-\frac{\Delta x - Ct}{\sqrt{2Dt}}\right) + (Ct + \Delta x)\, e^{\frac{\Delta x C}{D}}\, N\left(-\frac{\Delta x + Ct}{\sqrt{2Dt}}\right)\right]$$

In conclusion equation (5.2.8) becomes, in discrete form:

$$Q(x + \Delta x, k) = \sum_{i=1}^{r} Q(x, k - i + 1)\, \overline{U}_{\Delta x}(i) \qquad (5.2.13)$$

where r indicates the number of time intervals corresponding to the hydraulic system memory.

As already stated, this equation is valid provided $U_{\Delta x}(i)$ does not vary over time, or rather that C and D remain unchanged over time. Should one wish to take account of their variability at each time interval, the following $U_{\Delta x}(i)$ successive responses will be obtained for the different time intervals k and equation (5.2.13) becomes:

$$Q(x + \Delta x, k) = \sum_{i+1}^{r} Q(x, k - i + 1)\, \overline{U}_{\Delta x, k}(i) \qquad (5.2.14)$$

In sum, to solve the non-linear problem of unsteady flow (i.e. to determine the functions Q(x,t) and Z(x,t)), the basic idea of the PAB model is to associate with equation (5.2.14) a constant flow profile (reconstructed for slowly changing flow from downstream to upstream on the assumption of variable flow with x) around which equation (5.2.3) can be linearized at each Δt so as to update the values of the coefficients C and D that will then be considered constant during the next time interval.

In more detail the PAB method procedure is as follows:

1) to define, at time t=0, the value of the flow in all the cross sections used to describe the geometry of the water course.

2) to calculate the downstream level, on the basis for example of the outflow scale, and to reconstruct the constant flow profile with the variable flow with x.

3) To calculate the mean values of the estimated coefficients C and D in the sections between the reference sections used for the flow propagation.

4) To propagate downstream the inflow upstream, based on the selected reference sections.

5) To increment by one time interval and repeat the procedure starting from point 2.

It is worth noting that the PAB scheme, described here, has the advantage of separating flow propagation from level propagation.

In fact this separation makes it possible to propagate the flow on a subgroup of cross sections, known as reference sections, while the levels are calculated in all the geometric description cross sections.

Finally, the flow at each time interval for all the geometric description sections is calculated on the basis of the assumption of linear variation of the flow value in the reference sections.

Steady flow backwater profile computation in PAB.

As described above, the PAB model calculation is based, at each time interval, on the updating of the diffusivity and convectivity parameters obtained by calculating a backwater profile with time constant, but spatially varied, flow.

Consider the dynamic equation of spatially gradualy varied flow, inferred by applying the momentum theorem:

$$\frac{\partial}{\partial x}\left(z_f + \frac{p}{\gamma} + \frac{\beta Q^2}{2gA^2}\right) = -\frac{\tau}{\gamma R} \qquad (5.2.15)$$

where:

z_f height of bottom of current section;

p hydrostatic pressure on bottom of section;

γ specific weight of the water;

Q outflow rate;

A wetted area;

β relevance coefficient of momentum flow defined as:

$\beta = \frac{\int v^2 dA}{Q^2 / A}$ where v is the velocity of the current that crosses the elementary area dA;

τ tangential force, in the opposite direction to the flow, bearing on the wetted perimeter area C;

R A/C: hydraulic radius;

C wetted perimeter area;

x current abscissa.

The term connected with the action of resistance to flow by friction may be expressed (Manning):

$$\frac{\tau}{\gamma R} = J = \frac{n^2 Q^2}{A^2 R^{\frac{4}{3}}} \qquad (5.2.16)$$

One can also write:

$$Q = \frac{R^{\frac{2}{3}} A J^{\frac{1}{2}}}{n} = K\sqrt{J} \tag{5.2.17}$$

where K is the hydraulic conductance.

Therefore:

$$J = \frac{Q^2}{K^2}$$

And, given

$$y = \frac{p}{\gamma}$$

where y is the depth of the current in relation to the bottom, we may write:

$$\frac{\partial}{\partial x}\left(z_f + y + \frac{\beta Q^2}{2g A^2}\right) = -\frac{Q^2}{K^2} \tag{5.2.18}$$

The reconstruction of the constant flow profile in slow current conditions implies the solution of the differential equation (5.2.18) on the basis of the perimeter conditions represented by the function Q(x), the water level in the section furthest downstream and knowledge of the geometric characteristics.

The integration of equation (5.2.18) in the case of a natural water course can only be carried out numerically. It follows therefore that the constant flow model is adapted and represented by the following equation:

$$z_{f2} + y_2 + \beta_2 \frac{Q_2^2}{2gA_2^2} = z_{f1} + y_1 + \beta_1 \frac{Q_1^2}{2gA_1^2} + \int_{x_1}^{x_2} J(x)dx \tag{5.2.19}$$

where the bases 1 and 2 indicate the downstream section and the upstream section respectively.

The cross sections of a natural bed are generally relatively irregular; in particular they present a marked distinction between incised bed and berm.

In these conditions representing the current merely by the overall area and wetted perimeter values, the mean velocity and a single roughness coefficient value, may lead to insufficiently reliable results.

Hence in the case of currents that are essentially one-dimensional but not transversally homogeneous, such as the currents under consideration, it is best to consider the generic cross section as a composite section.

Integration of the constant flow equation

When, for each cross section, one has a table containing the bottom height of the section and also the values of A, K, ß and Q_c, where Q_c is the critical flow, for depth y values scanned regularly (e.g. 20 cm.) from 0 to a maximum value related to the height of the top of the banks.

The quantity Q_c has been included in the table in order to check that the solution sought is actually in slow current ($Q<Q_c$).

Considering again the equation (5.2.19), assume that the friction function J(x) is expressible in linear form, namely:

$$\int_{x_1}^{x_2} J(x)dx = \frac{J_1 + J_2}{2}\Delta x \qquad (5.2.20)$$

where: $\Delta x = x_2 - x_1$. And given:

$$z = z_f + y$$

we have:

$$z_2 + \beta_2 \frac{Q_2^2}{2gA_2^2} - J_2 \frac{\Delta x}{2} = z_1 + \beta_1 \frac{Q_1^2}{2gA_1^2} - J_1 \frac{\Delta x}{2} \qquad (5.2.21)$$

With reference to the generic integration step, the right-hand side of the equation (5.2.21) is completely known, while on the left-hand side Z_2 is unknown, A_2 and J_2 being expressible as a function of Z_2.

The search for Z_2 consists therefore in the search for zero in the function:

$$f(z_2) = z_2 + \beta_2 \frac{Q_2^2}{2gA_2^2} - J_2 \frac{\Delta x}{2} - F_1 \qquad (5.2.22)$$

where:

$$F_1 = z_1 + \beta_1 \frac{Q_1^2}{2gA_1^2} + J_1 \frac{\Delta x}{2}$$

The search for zero in function (5.2.22) is performed using the bisection method, since there are two z_2 starting values between which the correct solution in slow current will certainly be bounded.

The first derives from the assumption that in the upstream section the flow Q_2 flows under critical conditions; it follows that

$$F_2 = z_2 + \beta_2 \frac{Q_2^2}{2gA_2^2}$$

assumes the lowest possible value in the field of slow currents while J_2 assumes the highest possible value.

The following two cases are possible:

(a) $$F_2 \geq F_1 + J_2 \frac{\Delta x}{2}$$

(b) $$F_2 < F_1 + J_2 \frac{\Delta x}{2}$$

Case (a) indicates that there is no solution in sub-critical flow and that the solution is to be found therefore as critical flow or as supercritical flow.

This situation (in a water course with the flow rate of a river) is found only locally or in general for high flow rate values, while the mean outflow rate is of the subcritical type. It is assumed that a local approximation can be made and suppose, in case (a), that the outflow arises in critical conditions.

In the second case, where a solution exists to equation (5.2.19) in sub-critical flow conditions, the z_2 starting values for applying the bisection method are defined as follows:

$$z_{2s} = z_{2c}$$

where s = left, d=right

$$z_{2d} = F_1 + J_{2c}\frac{\Delta x}{2}$$

where J_{2c} and z_{2c} refer to the critical conditions in the upstream section.

Note that the solution z_2 in sub-critical flow will definitely be greater than z_{2c} and certainly less than $F_1 + J_{2c}\frac{\Delta x}{2}$

The bisection method is thus applied in the following way.

Beaing in mind that:

$$F(z_{2s}) \le 0$$
$$F(z_{2s}) \ge 0$$

The first choice of z_2^1 is

$$z_2^1 = \frac{z_{2s} + z_{2d}}{2}$$

if $f(z_2^1) < 0$ this gives:

$$z_{2s} = z_2^1$$

if $f(z_2^1) > 0$, this gives:

$$z_{2d} = z_2^1$$

and accordingly on the second attempt, z_2^2: is given by:

$$z_2^2 = \frac{z_{2s} + z_{2d}}{2}$$

In general, this continues until $f(z_2^i) \approx 0$ with a given precision.

In order to speed up the calculation procedure and thus reduce the programme execution time, the following measures are taken.

First of all every attempt value $y_2^i = z_2^i - z_{f2}$, which is almost certain not to be tabulated, is approximated by means of the closest lower or higher y value, given in the table.

Hence interpolations for calculation of the geometric quantities are avoided.

The bisection method proceeds, as described above, until z_{2s} and z_{2d} correspond to two successive y_2 values given in the table.

At this stage z_2 is obtained as:

$$z_2 = z_{2s} + (z_{2d} - z_{2s}) \frac{f(z_{2s})}{f(z_{2s}) + f(z_{2d})}$$

Before concluding, further clarification is required with regard to the proposal:

$$\int_{x_1}^{x_2} J(x)\,dx = \frac{J_1 + J_2}{2} \Delta x \qquad (5.2.23)$$

adopted for the numerical integration of equation (5.2.19).

By a simple development in Taylor series of the function J(x), truncated at the end of the second order, and further integration between sections 1 and 2 over Δx distance, it is easy to obtain:

$$\Delta h \approx \frac{J_1 + J_2}{2} \Delta x + \frac{1}{12} \frac{\partial^2 J}{\partial x^2} \Delta x^3 \qquad (5.2.24)$$

The second term in the second member of (5.2.24) is the integration error committed by solving (5.2.19) with the assumption (5.2.23), an error which is obviously related to the calculation rate, and which is added to the error due to the incomplete geometric description of the bed between sections 1 and 2.

This error is the more marked the greater the curvature of the function J(x) in the reach

considered; this is a situation found generally upstream of a section in which a critical or near critical condition is encountered.

An approximate expression of this error is given by:

$$E = \left[J^2 \frac{J - S_0}{\left(1 - F^2\right)^2} \right] \frac{\Delta x^3}{12} \qquad (5.2.25)$$

where S_0 is the slope of the bed and F is the Froude number:

$$F = \sqrt{\frac{Q^2 B}{g A^3}}$$

Expression (5.2.25) may be calculated approximately in the downstream section 1 where the hydraulic condition is known and provides an order of magnitude of the error committed by making a spatial step along Δx starting from section 1.

Having assigned the maximum value of the error admitted, it is then possible to obtain the order of magnitude of the corresponding maximum spatial step Δx_0.

Should Δx_0 be less than x an intermediate calculation section must be introduced between sections 1 and 2 whose geometric characteristics are obtained by interpolation of sections 1 and 2.

Once the intermediate section solution has been obtained, a fresh is made from this point upstream, repeating the procedure using the method described above.

Calculation of the hydraulic parameters of a composite section

The calculation of the overall hydraulic parameters of a composite cross section must be tackled by dividing the section under study into subsections, in which the parameters may be considered sufficiently homogeneous, and then by appropriately averaging their values.

The cross section of a water course may be divided, for example, into several subsections, each of which has a different roughness coefficient value. In this case, using for example

the Manning formula, it is possible to calculate the mean velocity in each subsection and, therefore, the flow corresponding to it.

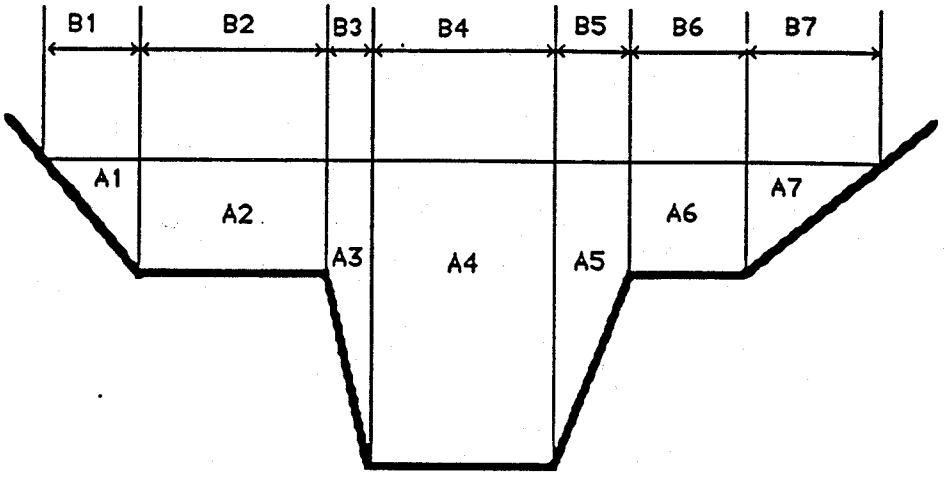

The total flow is accordingly the sum of the flows corresponding to the various subsections, while the mean velocity of the whole section is equal to the relation between the total flow and the total area.

Making v_1, ..., v_n the mean velocity in the n subsections; A_1, ..., A_n the area of the subsections; K_1, ..., K_n the conductance coefficients of the subsections. Suppose that the slope of the total loads line is the same for all the subsections.

Hence:

$$v_1 = \frac{K_1}{A_1} J^{\frac{1}{2}}, \ldots\ldots, v_n = \frac{K_n}{A_n} J^{\frac{1}{2}}$$

$$Q = VA = \sum_{i=1}^{n} v_i A_i = J^{\frac{1}{2}} \sum_{i=1}^{n} k_i$$

Hence the conductance coefficient for the whole section is:

$$K = \sum_{i=1}^{n} k_i$$

The coefficient ß of the total section is obtained, on the assumption of constant velocity in

each subsection, by the relation:

$$\beta = \frac{\int v^2 dA}{Q^2/A} = \frac{\sum_{i=1}^{n} \frac{k_i^2}{A_i}}{\frac{K^2}{A}}$$

The coefficients C and D in equation (5.2.3) may be expressed as:

$$D = \frac{K^2}{2QB}$$

$$C = \frac{D}{B}\frac{\partial B}{\partial x} + \frac{Q}{KB}\frac{\partial K}{\partial z}$$

where B is the surface width.

Finally, to calculate the critical flow for a certain water depth value, bearing in mind that the distribution of velocity in the subsections is assumed to be uniform:

$$Q_c = \sum_{i=1}^{n} \sqrt{\frac{gA_i^3}{B_i}}$$

where B_i is the surface width of the i-th subsection.

5.3 OVERLAND FLOW: A TWO-DIMENSIONAL MODELLING APPROACH

5.3.1 Introduction

The aim of this section is to describe the equations governing two-dimensional overland flow and, in particular, the numerical schemes used to resolve them.

The establishment of a plan and the definition of possible actions aimed to the improvement of the hydraulic conditions of a given flood prone area, in order to mitigate the risk and the effects of flooding, requires the knowledge of the hydraulic levels that could be reached during extreme flood events. In view of its importance, many studies -

which will be referred to later - have been devoted to this subject.

This section focuses primarily on the assumptions that have led to a class of simplified models, the parabolic models, which seem quite adequate for the solution of most problems encountered in practice.

The first furst of the section includes basic equations in the continuum, according to the Eulerian theory, for the description of phenomena occurring in fluids. The aim of the Eulerian approach is to determine the characteristics of flow (dependent variables) by investigating fixed positions at each point in the space occupied by a fluid; thus velocity and pressure, and - where relevant - density, are a funciton of the coordinates of the investigation point and of time (independent variables). This concept is set against the other theory, propounded by Lagrange, according to which the phenomena are studied by analyzing the behaviour of a given fluid particle in its motion through space; i.e. the coordinates of the particle (dependent variables) are defined as functions of given initial values of time (independent variables).

The second part of the section of the paper is concerned with an examination of numerical methodologies, and in particular the method of finite differences, the method of integrated finite differences and the method of finite elements for solving the approximate model referred to.

5.3.2. Basic equations of mass and momentum balance

The indefinite equations of mass and momentum balance, expressing respectively the principle of the conservation of mass and the conditions of dynamic equilibrium at each point in time for an incompressible fluid are, according to the classic literature (Citrini D. and Noseda G. (1975) and Marchi E. and Rubatta A., (1981)) and others, as follows:

$$\mathrm{Div}\ \mathbf{v} = 0 \tag{5.3.1}$$

$$\frac{d\mathbf{v}}{dt} = \mathbf{F} - \frac{\mathrm{grad}\ \mathbf{p}}{\rho} + \nu \nabla^2 \mathbf{v} \tag{5.3.2}$$

Equation (5.3.2) is commonly known as the NAVIER-STOKES equation. Applying the rule of Eulerian derivation, equations (5.3.1) and (5.3.2), in terms of components, can be written as:

$$\frac{\partial u}{\partial x} + \frac{\partial v}{\partial y} + \frac{\partial w}{\partial z} = 0 \tag{5.3.3}$$

$$\frac{\partial u}{\partial t} + u\frac{\partial u}{\partial x} + v\frac{\partial u}{\partial y} + w\frac{\partial u}{\partial z} = F_1 - \frac{1}{\rho}\frac{\partial p}{\partial x} + \nu\nabla^2 u \tag{5.3.4}$$

$$\frac{\partial v}{\partial t} + u\frac{\partial v}{\partial x} + v\frac{\partial v}{\partial y} + w\frac{\partial v}{\partial z} = F_2 - \frac{1}{\rho}\frac{\partial p}{\partial y} + \nu\nabla^2 v \tag{5.3.5}$$

$$\frac{\partial w}{\partial t} + u\frac{\partial w}{\partial x} + v\frac{\partial w}{\partial y} + w\frac{\partial w}{\partial z} = F_3 - \frac{1}{\rho}\frac{\partial p}{\partial z} + \nu\nabla^2 w \tag{5.3.6}$$

where u,v,w and F_1, F_2, F_3 represent, respectively, the components of velocity and mass force referred to the mass unit in directions x, y and z; p, ν, ρ and t are respectively pressure, kinematic viscosity, fluid density and time; the symbol ∇^2 is the Laplace operator. The indefinite equation of momentum balance (5.3.2), completed by the equation of continuity of mass (5.3.1), by the equation of state (which for an incompressible fluid is ρ =cost), by the relations between stresses and strains which, still under the assumption of an incompressible fluid, make it possible to arrive at the equation of motion in the form (5.3.2), and by the boundary and initial conditions typical of the specific process of motion considered enables the determination of the characteristic elements of motion at each point in time, providing a complete and detailed description.

This result, which is certainly the most complete solution of the dynamic problem, is extremely difficult to achieve because of the many obstacles encountered in the integration of the system of differential equations with partial derivatives on real world domains. On the other hand it should also be noted that such a detailed description of the phenomena is generally not required vis-à-vis the solution of many practical problems.

Partial differential equations of two-dimensional free surface flow

The basic partial differential equations on which this paper concentrates may be derived from the equations (5.3.3) to (5.3.6) describing mass and momentum balance.

Integration of the equation (5.3.3) over the liquid height h of a generic cross section and applying the Leibnitz rule, as in Pinder F.F. and Gray, W.G.(1977), Chen C. and Chow V.T. (1971), Chow V.T.and Ben-Zvi A. (1973), Lai C. (1986), Di Silvio G. (1978), leads to:

$$\frac{\partial h}{\partial t} + \frac{\partial (Uh)}{\partial x} + \frac{\partial (Vh)}{\partial y} = q \qquad (5.3.7)$$

where possible inflows and/or outflows (rainfall, infiltration, evaporation, etc...) were considered and where U and V represent the mean velocities along the vertical depth in the x and y direction respectively.

In the case of almost horizontal flows, the vertical component of velocity and acceleration can be ignored, and under this assumption Lai, C. (1986) eq. (5.3.6) reduces to the form:

$$\rho F_3 - \frac{\partial p}{\partial z} = 0 \quad ; \quad F_3 = -g \qquad (5.3.8)$$

Integrating with respect to z and selecting the atmospheric pressure p_0 over the water surface as the integration constant, leads to:

$$p = \rho g (H - z) + p_0 \qquad (5.3.9)$$

where H is the water surface elevation. Then, using eq. (5.3.9) and assuming p_0 to be everywhere constant, the following expressions can be found:

$$\frac{\partial p}{\partial x} = \rho g \frac{\partial H}{\partial x} \qquad (5.3.10a)$$

$$\frac{\partial p}{\partial y} = \rho g \frac{\partial H}{\partial y} \qquad (5.3.10b)$$

Equations (5.3.4) and (5.3.5) can be integrated over the liquid height h, as with the equation

of continuity of mass, and applying once more the Leibnitz rule, and taking into account equations (5.3.10a) and (5.3.10b) with the further assumption $F_1=F_2=0$,the equations of momentum balance become:

$$\frac{\partial (U h)}{\partial t} + \frac{\partial (U^2 h)}{\partial x} + \frac{\partial (U V h)}{\partial y} + g h \frac{\partial h}{\partial x} = g h (S_{0x} - S_{fx}) + D_{lx} \qquad (5.3.11)$$

$$\frac{\partial (V h)}{\partial t} + \frac{\partial (V^2 h)}{\partial y} + \frac{\partial (U V h)}{\partial x} + g h \frac{\partial h}{\partial y} = g h (S_{0y} - S_{fy}) + D_{ly} \qquad (5.3.12)$$

where S_{0x} and S_{0y} are the components of the bottom slope in the two directions x and y respectively; S_{fx} and S_{fy} are the head loss components in the same directions; D_{lx} and D_{ly} account for possible lateral inflows and/or outflows [5].

A detailed examination of the equations of mass (5.3.7) and of momentum balance (5.3.11) and (5.3.12) are given, for example, in Abbott, M.B. (1979) Cunge, J.A. (1975), Abbott, M.B. and Cunge, J.A. (1975), Daubert A. and Graffe, O. (1967).

Moreover the problem of numerical solution of these equations has been addressed by many authors. An extensive study of the various methods is provided by Chintu Lai (1986), Katopodes and Strelkoff (1978, 1979). The method of finite differences can be found in Grubert's study (1976) and more recently in Fennema and Chaudry (1989) The method of integrated finite differences can be found in Narasiman and Witherspoon (1976), Narasimhan et al. (1978), Pacciani (1987), Calò (1987). The method of finite elements can be found not only in classic texts [41], [22] or in a general overview paper such as the one by Ralph Ta-Shun Cheng (1978), but also in Fugazza and Gallati (1977), Katopodes (1980), Katopodes (1984), Hossenipour and Amein (1984), Vansnick and Zech (1984) and Akanbi and Katopodes (1988).

In the present paper, in order to provide a general overview of the problem while reducing the complexity of the derivation, following the works undertaken by Xanthopoulos and Koutitas (1976), and by T.V. Hromadka ii et al. (1985) and J.D. De Vries et al. (1986), equations (5.3.7), (5.3.11) and (5.3.12) have been simplified; in particular, in the equations of continuity of momentum per unit of weight (5.3.11) and (5.3.12) the dynamical terms (i.e. the derivatives of momentum with respect to time), as well as the kinetic terms (i.e. the derivatives of velocity with respect to x and y) can been neglected without a great loss of

accuracy in the description of the two dimensional flow pattern. By ignoring, without loss of generality, the terms D_{lx} and D_{ly} resulting from possible inflows and/or outflows, a simplified form of the equation of momentum can be found in which the surface water slope coincides with the friction slope.

Furthermore, expressing the load losses according to Manning's formula, as indicated by Xanthopoulos and Koutitas (1976) for two-dimensional problems, and by Akan and Yen (1981) and Hromadka et al. (1986) for mono-dimensional problems, the following equations are obtained:

$$\frac{\partial h}{\partial x} = S_{0x} - \frac{n_x^2 U^2}{h^{4/3}} \tag{5.3.13}$$

$$\frac{\partial h}{\partial y} = S_{0y} - \frac{n_y^2 V^2}{h^{4/3}} \tag{5.3.14}$$

Obtaining from these latter two equations the velocity components U and V and replacing them in the equation of mass balance (5.3.7), the following final expression is obtained:

$$\frac{\partial}{\partial x}\left(K_x \frac{\partial H}{\partial x}\right) + \frac{\partial}{\partial y}\left(K_y \frac{\partial H}{\partial y}\right) + q = \frac{\partial H}{\partial t} \tag{5.3.15}$$

where:

$$K_x = \frac{\dfrac{h^{5/3}}{n_x}}{\left(\dfrac{\partial H}{\partial x}\right)^{1/2}} \quad ; \quad K_y = \frac{\dfrac{h^{5/3}}{n_y}}{\left(\dfrac{\partial H}{\partial y}\right)^{1/2}} \tag{5.3.16}$$

with q representing external net flow exchanges (inflows-outflows)

In this paper the solution of eq. (5.3.15) or of the equivalent system (5.3.7), (5.3.13), (5.3.14) are based upon the method of finite differences, the method of finite integrated differences and the method of finite elements.

The method of finite differences

Under this method, the domain is discretized in a finite number of points which form a regular mesh grid in which the approximate value of the solution is determined, as shown in the classic literature Abbott, M.B. 1979, Lapidus L., Pinder G.F. 1982. In the following case, since the unknown h varies with the spatial coordinates x and y and with time t, the scheme is the one shown in Figure 5.3.1 in which the spatial coordinates are indicated with the symbol i for the x direction and symbol j for the y direction; time is counted with n multiples at interval Δt.

Referring to the system (5.3.7), (5.3.13), (5.3.14), the equation of continuity (5.3.7), using a general form of the finite temporal differences, integrated between the instant $n.\Delta t$ and the instant $(n+1).\Delta t$, takes the form:

$$\frac{h_{i,j}^{n+1} - h_{i,j}^{n}}{\Delta t} + \varepsilon\left(\frac{\partial (Uh)}{\partial x} + \frac{\partial (Vh)}{\partial y} - q\right)^{n+1} + (1-\varepsilon)\left(\frac{\partial (Uh)}{\partial x} + \frac{\partial (Vh)}{\partial y} - q\right)^{n} = 0 \qquad (5.3.17)$$

with q accounting for external inflows and/or outflows.

The method becomes explicit for $\varepsilon=0$; in this case the unknown height h at interval $(n+1)$ Δt, can be expressed explicitly as a function of known quantities at time $n\,\Delta t$; nevertheless the procedure requires that certain stability conditions be satisfied. On the other hand, if $\varepsilon>0$, the unknown height is defined implicitly; this method involves more complex computations but it does offer the advantage of furnishing stable solutions (with $0.5\leq\varepsilon\leq1$). Lastly, in the case of $\varepsilon=0.5$ the centered implicit scheme (CRANK-NICOLSON) is obtained, in which the disadvantage of relatively complicated calculations is compensated by an enhanced degree of accuracy of the solution.

For the replacement of spatial partial derivatives with finite incremental relations, again with reference to Figure 5.3.1, one of the following forms can be used.

In these latter expressions there is a truncation error connected with the substitution of the tangent at point (i,j) with the chord; in eq. (5.3.18) this is centered around the point itself, in eq. (5.3.19) it refers to the previous Δx interval and, lastly, in eq. (5.3.20) it refers to the next interval. Similar expressions may be written for the other spatial coordinate y.

$$\frac{\partial (Uh)}{\partial x} \cong \frac{1}{2\Delta x} [(Uh)_{i+1,j} - (Uh)_{i-1,j}] \tag{5.3.18}$$

$$\frac{\partial (Uh)}{\partial x} \cong \frac{1}{\Delta x} [(Uh)_{i,j} - (Uh)_{i-1,j}] \tag{5.3.19}$$

$$\frac{\partial (Uh)}{\partial x} \cong \frac{1}{\Delta x} [(Uh)_{i+1,j} - (Uh)_{i,j}] \tag{5.3.20}$$

The values of the velocity components $U_{i,j}$ and $V_{i,j}$ can be obtained, once more by applying one of schemes (5.3.18), (5.3.19) and (5.3.20), from equations (5.3.13) and (5.3.14). As far as the water free surface depth values h are concerned, the average values within the interval can be assumed.

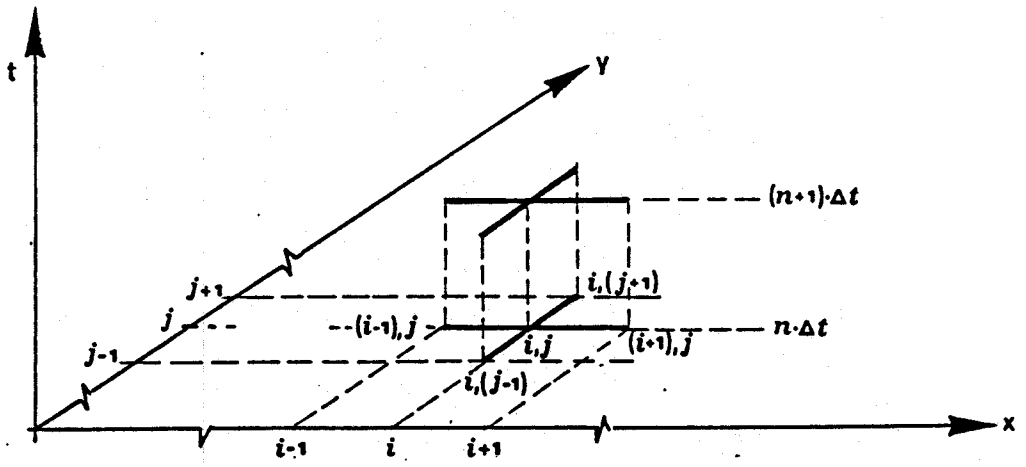

Figure 5.3.1 - The Finite Differences Mesh

The method of integrated finite differences

Eq. (5.3.15) is integrated over a surface element with an area S_i and boundary H.

$$\int_{S_i} \left[\frac{\partial}{\partial x}\left(K_x \frac{\partial H}{\partial x}\right) + \frac{\partial}{\partial y}\left(K_y \frac{\partial H}{\partial y}\right)\right] \, dS_i + \int_{S_i} q \, dS_i = \frac{\partial}{\partial t} \int_{S_i} H \, dS_i \qquad (5.3.21)$$

Applying the theorem of divergence, the first term on the left part of eq. (5.3.21) is transformed into a line integral. For the remaining two elements in the expression it is assumed that $q_i$and H_i are the mean values assumed by the respective quantities over S_i, thus obtaining:

$$\int_L \left(K_x \frac{\partial H}{\partial x} \, i + K_y \frac{\partial H}{\partial y} \, j\right) dL + q_i \, S_i = S_i \frac{\partial H_i}{\partial t} \qquad (5.3.22)$$

The basic aim of integrated finite differences is to discretize the total domain of the flow in subdomains or conveniently small "elements", and to assess the mass balance in each element as shown in eq. (5.3.22).

In physical terms, the line integral in eq. (5.3.22) represents the total flow through the boundary of the element, whereas the second term, on the left hand side in eq. (5.3.22), represents the external flow exchanges. Therefore the first element represents, globally, the accumulation of mass within element S_i. The term on the right hand side transforms, on element S_i, the accumulated quantity into a corresponding mean variation of the water potential.

In order to illustrate the method, the whole domain is divided into polygonal cells (Dirichlet tassellation, better known to hydrologists as Thiessen polygons Sloan S.W. (1987), Bear J. (1979)), whose mean properties are associated with the nodal point i inside the element (see Figure 5.3.2). To ensure the highest degree of precision, the interfaces between the elements must be perpendicular to the lines joining the nodal points and they must intersect such lines at their median point Bear J. (1979), Narasimhan T.N., Witherspoon P.A. (1976).

It is further assumed that the function H changes linearly among the nodal points and that its point value coincides with the mean value. Therefore eq. (5.3.22) becomes:

$$\sum_{m=1}^{M} K_{i,m} \frac{H_m - H_i}{d_{i,m}} B_{i,m} + q_i S_i = S_i \frac{\partial H_i}{\partial t} \qquad (5.3.23)$$

where:

$d_{i,m}$ is the distance between the nodes i and m;

$K_{i,m}$ is the inverse of the resistance along the line $d_{i,m}$;

$B_{i,m}$ is the breadth of the interface between the cell i and the cell m.

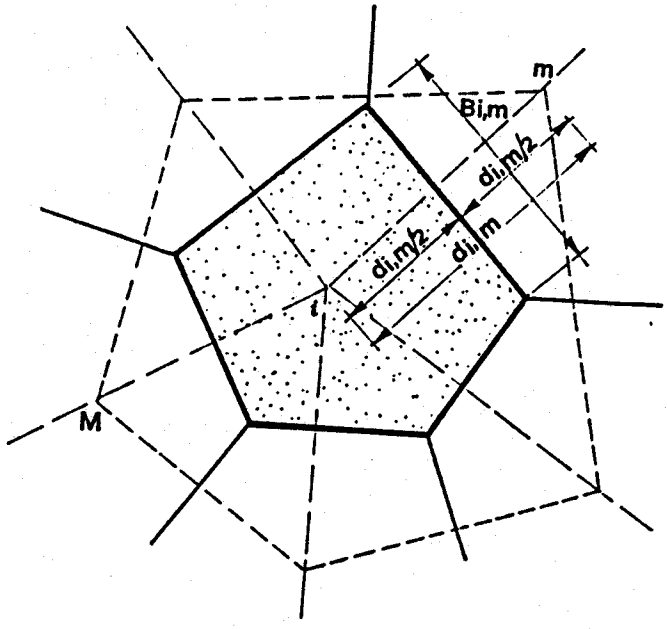

Figure 5.3.2 - The Integrated Finite Differences Mesh

Eq. (5.3.23) can be rewritten as:

$$\sum_{m=1}^{M} U_{i,m} (H_m - H_i) + q_i S_i = S_i \frac{\partial H_i}{\partial t} \qquad (5.3.24)$$

where $U_{i,m} = (K_{i,m} B_{i,m})/d_{i,m}$ is the conductivity of the interface of separation between the elements i and m and represents the quantity of fluid transferred for a unit potential difference between the nodal points i and m Narasimhan T.N., Witherspoon P.A. (1976).

With regard to discretization over time, eq. (5.3.24) takes the following general form:

$$\sum_{m=1}^{M} [\, \varepsilon\, U_{i,m}^{t+\Delta t} + (1-\varepsilon)\, U_{i,m}^{t} \,] \{ [\, \varepsilon\, H_m^{t+\Delta t} + (1-\varepsilon)\, H_m^{t} \,] - [\, \varepsilon\, H_i^{t+\Delta t} + (1-\varepsilon)\, H_i^{t} \,] \} +$$

$$+ [\, \varepsilon\, q_i^{t+\Delta t} + (1-\varepsilon)\, q_i^{t} \,]\; S_i = \frac{S_i}{\Delta t} (H_i^{t+\Delta t} - H_i^{t}) \qquad (5.3.25)$$

With ε=0, ε=1 and ε=0.5, eq. (5.3.25) leads to previously cited schemes: explicit, fully implicit and centered (CRANK- NICOLSON).

The method of finite elements

According to this method, as abundantly described in the classic literature Zienkiewicz O.C. (1977), Dhatt G., Touzot G., (1985), Becker E.B., Carey G.F.,Oden J.T. (1986), the domain of definition of the problem is divided into a certain number of subdomains or elements; the intersection points of the division lines (mesh) are called nodes. At these points the approximate value of the solution is determined; with this value, by means of linear combinations, it is possible to obtain the value of the unknown function, again in approximate form, at every point in the domain. Eq. (5.3.15) can be written in the form:

$$f(H) = \frac{\partial}{\partial x}\left[K_x (H) \frac{\partial H}{\partial x} \right] + \frac{\partial}{\partial y}\left[K_y (H) \frac{\partial H}{\partial y} \right] + q - \frac{\partial H}{\partial t} \qquad (5.3.26)$$

and, defining with:

$$H^*(x,y,t) = \sum_{j=1}^{N} H_j(t)\; \Phi_j(x,y) \qquad (5.3.27)$$

an unknown approximation of the solution sought H(x,y,z), given N known base functions $\Phi_j(x,y)$, and the N unknown nodal values H_j, then the application of the GALERKIN method leads to the imposition of orthogonality condition between the residue $f(H^*)$ and the N base functions:

$$\int_{\Omega} f(H^*)\ \Phi_i\ d\Omega = 0 \qquad i = 1, 2, \ldots, N \tag{5.3.28}$$

which can be written in full as:

$$\int_{\Omega} \left\{ \frac{\partial}{\partial x} \left[K_x (H^*) \frac{\partial H^*}{\partial x} \right] + \frac{\partial}{\partial y} \left[K_y (H^*) \frac{\partial H^*}{\partial y} \right] + q - \frac{\partial H^*}{\partial t} \right\} \Phi_i\ d\Omega = 0$$

$$i = 1, 2, \ldots, N \tag{5.3.29}$$

Figure 5.3.3 shows the general base function $\Phi_i(x,y)$ for the i-th node and all the functions taking the form $\psi_{i,e}(x,y)$ which constitute it Becker E.B., Carey G.F.,Oden J.T. (1986). The example in the figure refers to triangular linear elements which offer the advantage, over quadrangular elements for example, of complete interpolating polynomials to the maximum degree which increases the approximation of the method as described in Becker E.B., Carey G.F., Oden J.T. (1986) and Reddy J.N. (1986).

Resuming the procedure, first the formula of integration by parts (1st identity of GREEN) is applied to eq. (5.3.29) in order to eliminate the second derivatives and, then, in view of the non-linearity, the equation is resolved by using one of the iterative methods, such as Newton-Raphson or others Huyakorn P.S., Pinder G.F. (1983).

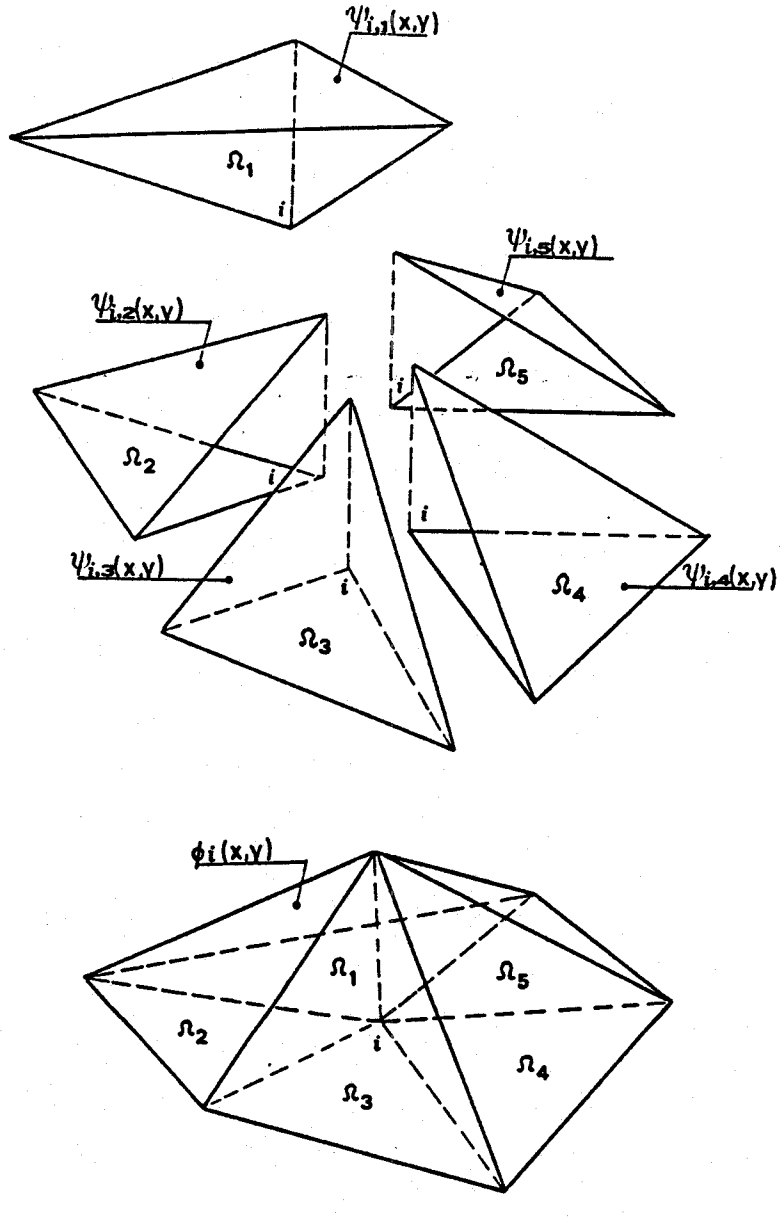

Figure 5.3.3 - The Finite Elements Base Function representation

5.4 COMBINED 1 AND 2 DIMENSIONAL FLOOD PLAIN MODELLING

The formulation described in Section 5.2 and 5.3 are pulled together in this section to make a practical tool. The work was done by EPFL-IATE in conjunction with UNIBO-ICI, and the material is substantially the contribution of Consuegra to the EPFL-IATE Report.

5.4.1 Introduction

The 1987 and 1993 flood damages in several European countries and North American regions clearly demonstrate the need for an adequate flood mapping and damage assessment methodology. Decision makers need flood risk maps to approve land development schemes in flood prone areas. Because of evident economic and political implications, flood maps should be as accurate as possible.

Marco (1992) provides an extensive review of flood risk mapping procedures. He indicates that standards on flood risk mapping are only available in the United States of America while European experience is quite divided by national or regional differences. He notes that the European Community (EC) has not yet implemented such standards. Flood risk delineation requires adequate hydraulic models and suitable methods to assess flood damages.

The following paragraphs describe the developments regarding the hydraulic flood plain modelling and the construction of the required Digital Terrain Model (DTM) supporting the flood delineation procedures. The impact assessment component of the project and the Geographical Information System (GIS) framework to assess damages is described later in this Section.

Several hydraulic models have been reported in the literature ranging from improved one dimensional routing, accounting for compound channel effects (Abiba and Townsend, 1992), lateral spill and filling of storage cells (Labadie, 1992) to complex two dimensional finite element models (Galland et al., 1991). Two dimensional diffusive approximations of the Saint Venant equations solved with finite difference methods have also been proposed (Reitano, 1992).

Labadie (1992) states that the application of two dimensional models can be significantly enhanced if river reaches (structures lines) and the flood plain domain are treated with the same hydraulic equations. The best solution should be to keep the predominant one dimensional component of channel flow and combine it with two dimensional propagation in the flood plain. Labadie (1992) also indicates that the definition of storage cells and their proper connection to the river cross-sections is not an easy task. Reitano (1992) stresses that land modeling and loading of related data is very demanding and requires a specific pre-processing support software allowing the generation of the cell grid. Adequate post-processors are also needed to visualize the flood maps.

However, two dimensional models are seldom applied in common engineering practice because reliable Digital Terrain Models (DTM) are rarely available. Flood maps are generally based upon the extrapolation of water stages for a given design flow and contouring the flood plain points lying below the calculated water surface elevation. In flat flood plains (slope less than 0.1%) this approach generally overestimates the extent of flooding. Traditional DTMs are in raster format and neglect the effects of obstacles to flow circulation such as embankments or dikes. An adequate consideration of such break lines is rarely found in the literature. A Triangular Irregular Network (TIN) based DTM appears to be best suited for flood mapping in flat areas. It is well recognised that a TIN is the only available method which explicitly accounts for such break lines.

5.4.2. Flood plain hydraulic modelling

Mapping of flood characteristics required the development of a specific hydraulic model. The latter should simultaneously simulate one dimensional propagation in the main channels and two dimensional flood routing in the flood plain. The connection between channels and flood plains requires adequate hydraulic equations. As already mentioned, the DTM supporting hydraulic computations should account for break lines.

In this study, debris flows, sediment transport and dike failures were not analysed. These features are particularly important in mountainous regions. In flat areas the dike failure problem remains. A literature survey indicated that dike failure is a very complex problem (Zatta, 1993). Two important features have to be predicted. The first one relates to the

location of the breach while the second concerns the failure mode. Consequently, it was decided not to consider this problem in the initial development of the proposed hydraulic model.

Basic equations

For both river flow and flood plain flow, the diffusive wave approximation of the full Saint-Venant equations is used. In the flood plain, shallow wave theory is assumed to apply while in the channel, flood routing is based on traditional cross-sections. The equations in both cases are solved with an integrated time centred finite difference scheme (Giammarco et al., 1994).

It can be assumed that the diffusive approximation of the Saint-Venant equations is applicable to the flood plain since routing is essentially controlled by gravity and friction forces. However, there is no general agreement with respect to channel flow. Henderson (1966) considers inertia terms to be negligible in most cases, others like Ahn et al. (1993) argue that such simplifications induces errors between 5 to 10% that could be easily avoided. De Vries et al. (1979) indicate that inertia terms should not be neglected for the analysis of tidal effects. For the purpose of this study, it was considered that flood waves in flat valleys are relatively slow and state changes occur over long periods of time. Therefore, the diffusive approximation was considered to be acceptable.

The two dimensional diffusive approximation of the Saint-Venant equations can be written as follows:

$$\frac{\partial uh}{\partial x} + \frac{\partial vh}{\partial y} + \frac{\partial H}{\partial t} - q = 0 \qquad (5.4.1)$$

For an infinitesimal element, equation (5.4.1) can be written in terms of flows:

$$\frac{\partial Q_x}{\partial x} dx + \frac{\partial Q_y}{\partial y} dy + \frac{\partial H}{\partial t} dydx - qdxdy = 0 \qquad (5.4.2)$$

where: H = water surface elevation at the control element (m)
u,v = velocities in the x and y directions (m/s)
h = water depth in the control element (m)
q = external inflows (m/s)
Q_x = flow rate in the x direction (m^3/s)

The motion equations can be written as follows:

$$Sf_x + \frac{\partial H}{\partial x} = 0 \tag{5.4.3}$$

$$Sf_y + \frac{\partial H}{\partial y} = 0 \tag{5.4.4}$$

where: Sf_x = friction slope in the x direction

According to Manning's formula and equations (5.4.3 and 5.4.4), the following expression may be derived if the velocity components of u along y and v along x are neglected:

$$Q_x = -\frac{R_x^{2/3}}{n_x} hdy\sqrt{\frac{\partial H}{\partial x}} \quad Q_y = -\frac{R_y^{2/3}}{n_y} hdx\sqrt{\frac{\partial H}{\partial y}} \tag{5.4.5}$$

where: $R_{x,y}$ = hydraulic radius in the x and y directions
$n_{x,y}$ = Manning's roughness coefficient in the x and y directions
$Q_{x,y}$ = flow rates in the x and y directions

Substituting (54.5) into (5.4.2) leads to a partial differential equation which is only a function of H.

$$\left(\frac{\partial}{\partial x} K_x \frac{\partial H}{\partial x}\right)dxdy + \left(\frac{\partial}{\partial y} Ky \frac{\partial H}{\partial y}\right)dxdy + qdxdy = \frac{\partial H}{\partial t} dxdy \tag{5.4.6}$$

where:

$$K_x = \frac{R_x^{2/3} h}{n_x \sqrt{\frac{\partial H}{\partial x}}} \quad K_y = \frac{R_y^{2/3} h}{n_y \sqrt{\frac{\partial H}{\partial y}}} \tag{5.4.7}$$

Integrating equation (5.4.6) over a given domain S, leads to the following equation:

$$\iint_S \left(\frac{\partial}{\partial x} K_x \frac{\partial H}{\partial x} + \frac{\partial}{\partial y} K_y \frac{\partial H}{\partial y} \right) dxdy + \iint_S q dxdy = \iint_S \frac{\partial H}{\partial t} dxdy \tag{5.4.8}$$

Equation (5.4.8) can be integrated over a sub domain S_i of contour length L_i assuming that q and H are average values over S_i. The first term on the left hand of (5.4.8) can be transformed into a line integral resulting from an integration by parts and the application of the Green's theorem to eliminate the second derivatives of H.

$$\oint_{L_i} \left(K_x \frac{\partial H}{\partial x} \vec{x} + K_y \frac{\partial H}{\partial y} \vec{y} \right) . dL + q_i S_i = S_i \frac{\partial H}{\partial t} \tag{5.4.9}$$

The term in the line integral describes the components in the xy co-ordinate system of the flow vector which is perpendicular to the contour limits (L_i) of the sub domain S_i. The line integral may be interpreted as the sum of all flow exchanges along the contour of the sub domain.

Consequently, equation (5.4.9) is a mass balance equation for the sub domain S_i since $q_i S_i$ is equal to the net inflow and the right hand side term represents the corresponding change in storage. If the entire domain is subdivided into polygonal cells using the Thiessen method and assuming that the mean properties of each mesh can be represented by its nodal point (i), it can be easily demonstrated that equation (5.4.9) can be written as follows:

$$\sum_{j \in M_i} K_{ij} B_{ij} \frac{H_j - H_i}{d_{ij}} + q_i S_i = S_i \frac{\partial H_i}{\partial t} \tag{5.4.10}$$

where: M_i = set of nodes connected to node (i)

d_{ij} = distance between nodes (i) and (j)

S_i = polygon surface for node (i)

B_{ij} = interface length between nodes (i) and (j)

K_{ij} $\Rightarrow$ is obtained from equation (5.4.7) when substituting the xy derivatives of H by the slope of the water surface profile along the [i↔j] direction which is perpendicular to the Thiessen polygon facet, the length of which is B_{ij}.

Equation (5.4.10) can be solved with a time centred scheme where Δt is the selected time step, R_m and h_m are respectively the hydraulic radius and the water depth at the interface between the polygons for nodes (i) and (j) and n_{ij} is the Manning's roughness coefficient along the (i↔j) direction:

$$\left[\left(\alpha \sum_{j \in M_i} \frac{R_m^{2/3} h_m B_{ij}}{n_{ij}} \sqrt{\frac{Hj - H_i}{d_{ij}}}\right) + \frac{S_i}{\Delta t} H_i\right]^{t+\Delta t} =$$

$$\left[\left(-(1-\alpha) \sum_{j \in M_i} \frac{R_m^{2/3} h_m B_{ij}}{n_{ij}} \sqrt{\frac{Hj - H_i}{d_{ij}}}\right) + \frac{S_i}{\Delta t} H_i\right]^{t} + \qquad (5.4.11)$$

$$S_i \left[(1-\alpha) q_i^t + \alpha q_i^{t+\Delta t}\right]$$

Equation (5.4.11) can be written in a (N_i*N_i) matrix form where N_i is the number of nodes. The unknowns of the problem are $H_i^{t+\Delta t}$.

Computing transmissivities and cell volumes

In the channel, control volumes are defined according to the location of cross sections (Figure 5.4.1). For each channel cell, the surface S_i is calculated as a function of cross section characteristics and the length of the control volume L_i (Figure 5.4.2).

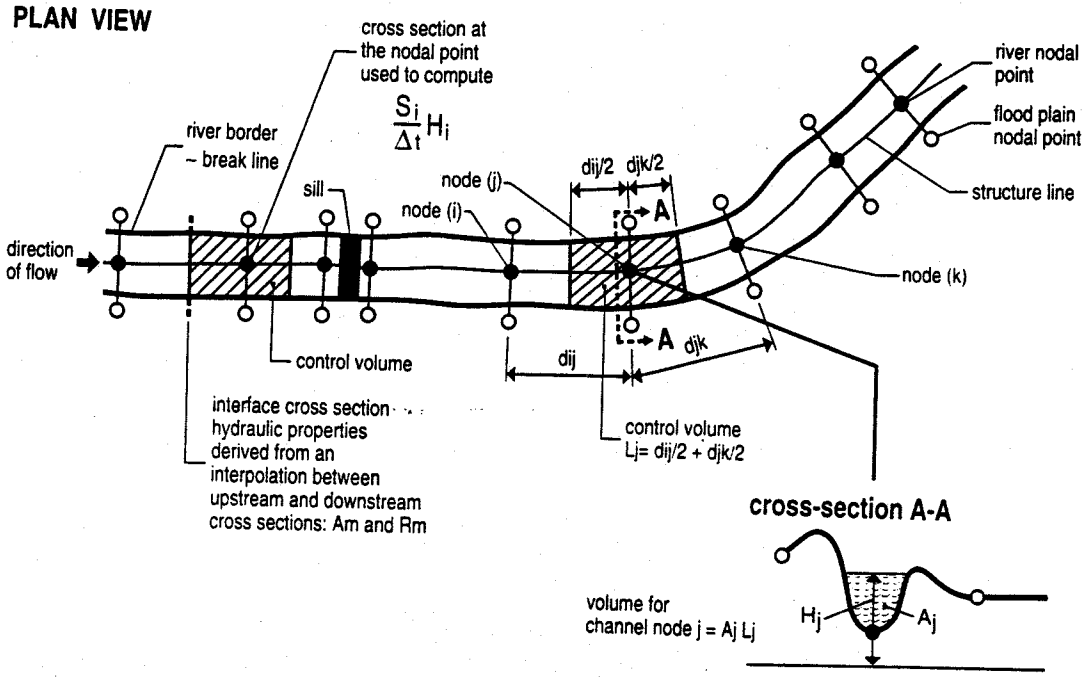

Figure 5.4.1. Layout of control volumes in the river (structure line)

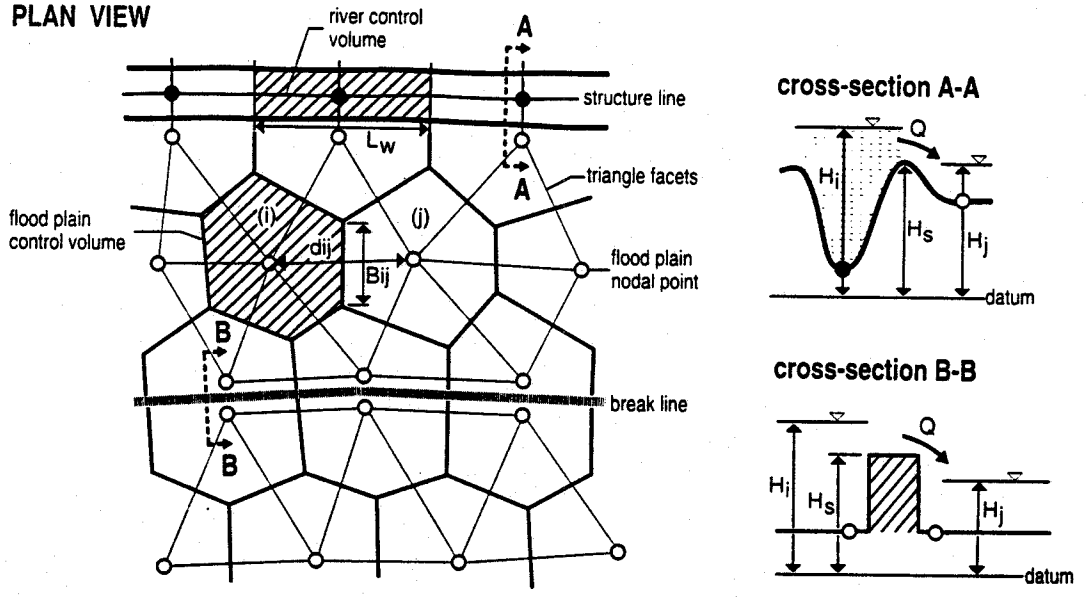

Equations:

Unsubmerged $Q = C_1 L_w (H_i - H_s)^{2/3} \sqrt{2g}$

Submerged $Q = C_2 L_w (H_i - H_s) (H_i - H_j)^{1/2} \sqrt{2g}$

Figure 5.4.2. Layout of control volumes in the flood plain

Transmissivities between channel nodes are computed with the following equation:

$$T_{ij} = \frac{1}{n_{ij} d_{ij} \sqrt{\frac{H_j - H_i}{d_{ij}}}} R_m^{2/3} A_m \qquad (5.4.12)$$

where: A_m = wetted surface at the interface cross section of the control volumes for the channel nodes (i) and (j) [m^2].

The flow (Q) between nodes (i) and (j) is equal to:

$$Q_{ij} = T_{ij}(H_j - H_i) \qquad (5.4.13)$$

The direction of flow is defined by the sign of the difference between H_j and H_i. Transmissivities have to be computed at the interface cross-section between two channel control volumes. A specific interpolator was developed to derive the main hydraulic relations at each interface cross-section.

To compute R_m and A_m in equation (5.4.12) it is necessary to assume a particular water surface profile between the upstream and downstream channel nodes. At present a linear profile is used. This hypothesis seems to be adequate since comparisons between the model used and a full solution of the Saint-Venant equations provided very close results (Vitalini, 1993).

Hydraulic structures such as weirs, sills or bridges can be included in the channel description (Vitalini, 1993). Nodes have to be defined upstream and downstream of the structure (Figure 5.4.1). The transmissivity between these two nodes is then computed using the proper hydraulic equations. The advantage of this approach is that the river DTM relies exclusively on traditional cross sections and a standard definition of hydraulic structures.

The flood plain domain is subdivided into polygonal cells (Figure 5.4.2). The domain discretization method will be described in paragraph 3. For each control volume equation (5.4.11) is also solved. The volume in each flood plain cell is simply given by the product of the cell surface S_i and the water surface elevation H_i. The transmissivities between flood plain nodes are computed with equation (5.4.12) after substituting the average depth Y_m

for R_m at the interface and the product $Y_m.B_{ij}$ for A_m. For flood plain cells, a hyperbolic profile is assumed between connected nodes. This assumption may be somewhat arbitrary and should be investigated further. Recent improvements in this direction have already been suggested by Giammarco and Todini (1994).

Lateral spill over a river embankment can be computed on the basis of a classical weir equation accounting for submerged or unsubmerged conditions. Spilling from one compartment to another can be treated in a similar manner (Vitalini, 1993).

Solving the mass balance equation

Equation (5.4.11) must be solved iteratively because of the link between T_{ij} and the water surface elevation (H_i). Figure 5.4.3 describes the method implemented to solve equations (5.4.11, 5.4.12 and 5.4.13).

At a given time (t), the water surface elevations of equation (5.4.1) are the initial conditions of the problem. Iterations start with a forecast at time $t+\Delta t$ of H_i, on the basis of which transmissivity T_{ij} can be computed half a time step ahead. At the moment, the predicted $H_i^{t+\Delta t}$ are assumed to be equal to the computed water surface elevations at time (t). The matrix system obtained from Equation (5.4.11) can be solved for water surface elevations at time $t+\Delta t$. Its solution is carried out by means of a modified iterative conjugate gradient method (Todini, 1991).

The newly computed $H_i^{t+\Delta t}$ define new transmissivities (T_{ij} in equation 12) and new flows (Q_{ij} in equation 13) between all nodes. The latter are again used to solve equation (5.4.11) for H_i. Iterations stop when the maximum differences between successively computed values of Q_{ij} are below a specified tolerance:

$$max\left|Q_{ij}^{k+1} - Q_{ij}^{k}\right| \leq \varepsilon \qquad (5.4.14)$$

where $Q_{ij}^{(k+1)}$ is the flow between two nodes at the current iteration (k+1) and $Q_{ij}^{(k)}$ is the flow between the same two nodes at the previous numerical iteration (k) (Figure 5.4.3).

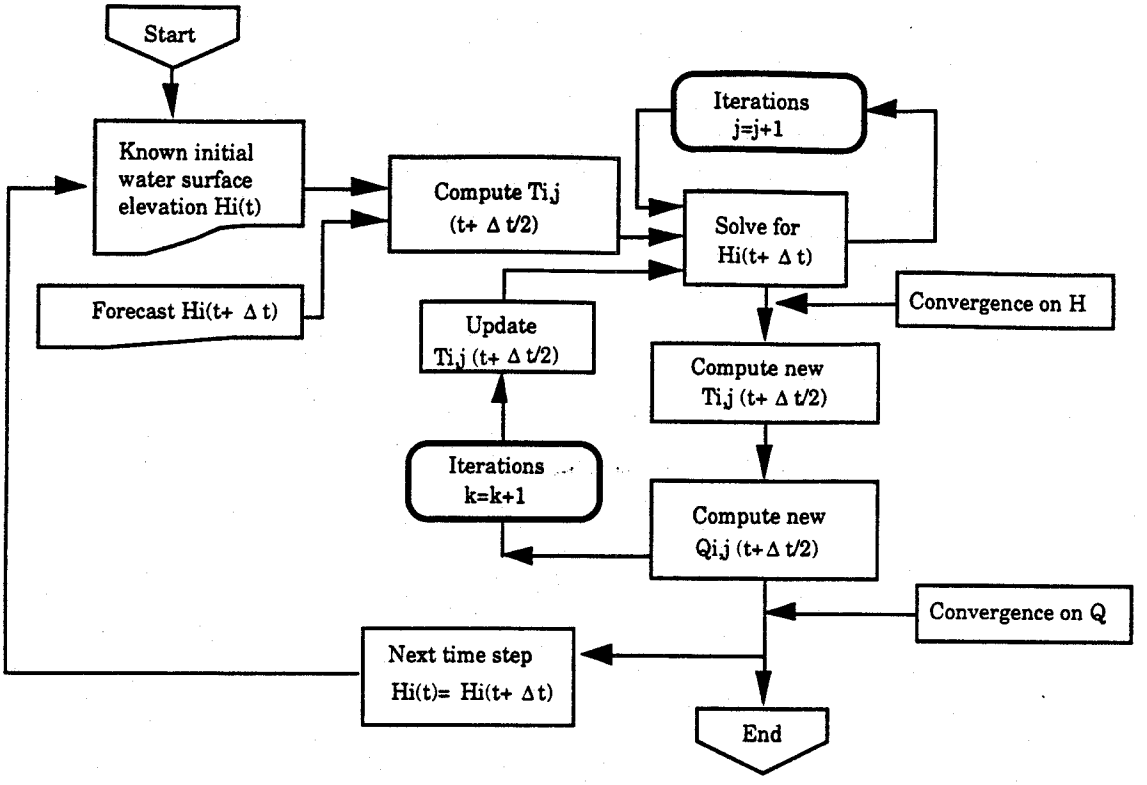

Figure 5.4.3. Iterative solution of equations (5.4.11, 5.4.12 and 5.4.13)

For each iteration, the solution of equation (5.4.11) computes the maximum value of the absolute difference $(Q_{ij}^{(k+1)}-Q_{ij}^{(k)})$ for all connected nodes. Iterations stop when this difference is less than a user defined tolerance ε.

The solution of equation (5.4.11) is stable. Di Giammarco and Todini (1994) have prooven that water surface elevations and flows computed from equation (5.4.11) are equivalent to those computed with more sophisticated approaches. However, the definition of stability criteria to optimise the selection of computational time steps needs further investigation. To reduce the number of iterations between t and t+Δt, two modifications have been implemented. The first one relates to the forecasting of $H_i^{t+\Delta t}$ while the second regards the convergence criteria on flows.

Instead of using the values of H_i^t as the first estimates for those corresponding to time t+Δt, it was felt that a linear forecast based on the two previous values of H_i at times t-Δt and t was a better solution as illustrated in Figure 5.4.4.

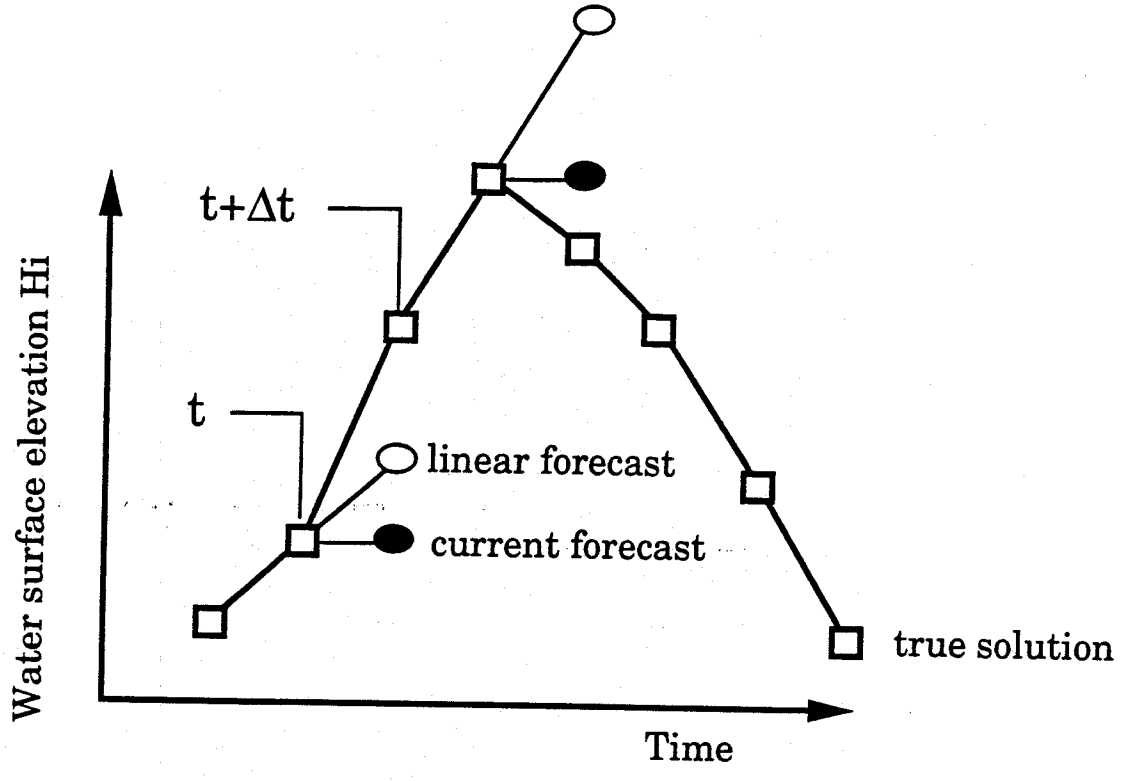

Figure 5.4.4. Improvement of the forecast of $H_i^{t+\Delta t}$

It is evident that for the rising and recession limbs of the hydrograph, the proposed linear forecast will be improved and consequently the number of iterations on Q_{ij} will decrease. However it is also obvious, that when the hydrograph will present inflection points (for instance the peak), the linear forecast is worst than assuming that $H_i^{t+\Delta t}=H_i^t$. Improving the forecasts for the water surface elevations for the next time step is still an open question that requires further investigations.

The convergence criteria in equation (5.4.14) ignores the order of magnitude of computed flows. For high flow values it is not necessary to reach such degrees of accuracy. Another convergence criteria was subsequently proposed. It can be written as follows:

$$max\left|1-\frac{Q_{ij}^{k+1}}{Q_{ij}^{k}}\right| \leq \varepsilon \qquad (5.4.15)$$

For low flows ≤ 0.1 m^3/s, equation (5.4.14) is used while equation (5.4.15) is preferred for higher values. In the first case e ~10^{-6} while in the second a value around 10^{-3} is considered

to be satisfactory. This improvement reduced significantly the number of iterations for all the tested scenarios. Equation (5.4.15) prooved to be usefull for trouble shooting. Most convergence problems appear at the beginning of lateral spills from river cells or through break lines. In such cases $Q_{ij}^{(k+1)}=0$ and $Q_{ij}^{(k)} \neq 0$ and the value of the criteria tends to infinity. Consequently, it is possible to locate connections where the algorithm may not converge adequately.

Specific transmissivity equations

Vitalini (1993) implemented adequate expressions for equations (5.4.12) and (5.4.13) applicable to most commonly found hydraulic structures such as weirs, sills, bridges, and sluice gates. Only the weir flow will be further discussed in this paragraph. The remaining cases are well documented (Vitalini, 1993; Sinniger and Hagger, 1989; Henderson, 1966). Therefore they will not be developed in this Section.

Flow over river embankments or dikes or between nodes separated by roads (Figure 5.4.2) can be written as follows (rectangular cross-section):

$$Q_{ij} = C_1 L_w \sqrt{2g}(H_i - H_s)^{3/2} \tag{5.4.16}$$

C_d is the weir loss coefficient, L_w is the length of overflow, H_i is the warter surface elevation at node i and H_s is the elevation of the river bank or that of the break line. For submerged conditions it is necessary to account for the downstream water surface elvation H_j. Consequently the following equation should be used:

$$\begin{aligned} Q_{ij} &= C_2 L_w \sqrt{2g}(H_i - H_s)(H_i - H_j)^{1/2} \\ C_2 &= \frac{3\sqrt{3}}{2} C_1 \end{aligned} \tag{5.4.17}$$

The loss coefficient C_2 is derived from the condition that flows computed with both equations should be equal when:

$$(H_j - H_s) = \frac{2}{3}(H_i - H_s) \tag{5.4.18}$$

In equation (5.4.16) the loss coefficient must be considered as a calibration parameter. It should be selected in order to limit the depth of water above the break line to a reasonnable value. To allow for river bank overflows, river cross sections are extended vertically by 1 meter on the left and right side. The cross section characteristics in equation (5.4.12) are computed accordingly.

For unsubmerged conditions $(H_j-H_S)<2/3(H_i-H_S)$ while for submerged conditions $(H_j-H_S)>2/3(H_i-H_S)$. The above equations assume tthat flows around river embankments or over break lines are subcritical. They can not be applied for supercritical flow. Since the program was developed for flood mapping in flat areas with relatively small depths and low velocities, subcritical flow may be considered to be predominant. The model computes Froude numbers for all links connected to the particular node where equations (5.4.16) and (5.4.17) must be applied. A warning message is produced if supercritical conditions are found.

For irregular river cross sections through weirs, sills or abrupt drops, equations (5.4.16) and (5.4.17) are no longer applicable. The general expression for critical flow and unsubmerged conditions (Figure 5.4.5) can be written as follows:

$$Q_{ij}(H) = C_1\sqrt{2g}\int_0^H L_h(\sqrt{H-h})dh \qquad (5.4.19)$$

Equation (5.4.19) can be expressed as an algebraic sum:

$$Q_{ij}(H) = C_1\frac{1}{2}\sqrt{2g}\sum_{k=1}^{n}\left[(h_{k+1}-h_k)(L_{k+1}\sqrt{H-h_{k+1}}+L_k\sqrt{H-h_k})\right] \qquad (5.4.20)$$

For any water surface elevation H, equation (5.4.20) computes the critical flow Q_{ij} on the basis of the width L_k of the wetted surface for a given intermediate depth h_k. Vitalini (1993) developed a pre-processor to derive the required geometrical characterisitics of an irregular cross-section. For the entire range of H values, the computed flows with equation (5.4.20) are stored in a separate table from which it is possible to interpolate according to the solution of equation (5.4.11).

To account for submerged conditions, the coefficient C_1 is corrected with the following formula (Sinniger and Hager, 1989):

$$C_1 = C_1\sqrt{1-\left(\frac{H_j - H_s}{H_i - H_s}\right)^2} \qquad (5.4.21)$$

Equation (5.4.21) applies when H_j is greater than H_S otherwise the value of C_1 is not corrected.

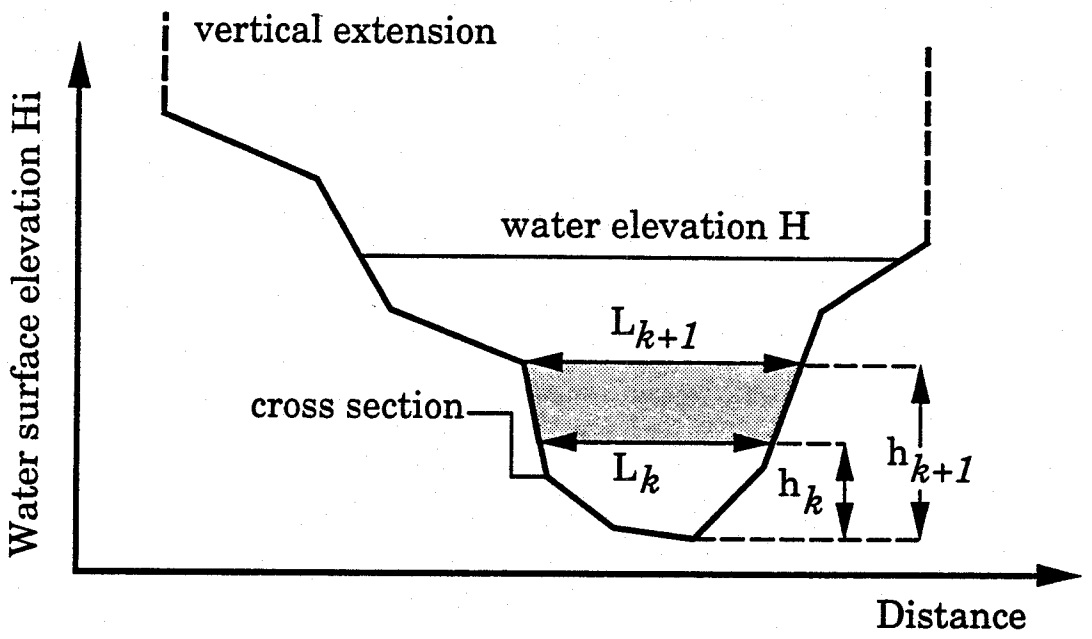

Figure 5.4.5. Computation of critical flow for irregular cross-sections

Further developments

The theoretical background described in this Section allows to implement a hydraulic model for flood delineation. For the purpose of this study, it is considered that the control volume solution of the two dimensional diffusive approximation of the Saint-Venant equations provides sound results and that alternative resolution methods, like finite elements, will not significantly improve the accuracy of the flood impact assessment component of the project. However some theoretical improvements are still needed. They can be summarised as follows:

- A stability criterion and a procedure to optimize the selection of the computational

time step should be developed accounting for the order of magnitude of the computed transmissivities and the size of the polygonal meshes.

- The assumption of the water surface profile between connected nodes should be analysed in more detail. Sound criteria should be derived to select the best profile shape according to hydraulic conditions.

- Flow exchanges between two connected nodes should account for surrounding water surface elevations. Giammarco and Todini (1994) already suggested some improvements in this direction. Their approach incorporates some of the benefits of a finite element resolution while keeping the simplicity of the control volume approach.

- Lateral spill from river cells to flood plain nodes should account for the gradient of the hydraulic grade line. In its actual form, the proposed hydraulic model assumes that the water depth is constant along the length of the embankment.

- The particular transmissivity equations for hydraulic structures need some refinement and should reflect the state of the art of recently developed hydraulic models.

5.4.3. DTM construction and flood delineation

As indicated in the previous paragraph, the solution of equation (5.4.11) requires that the study area should be sub-divided into polygonal cells representing the control volumes in which the mass balance equation is solved at each time step. These polygonal cells can be obtained from an adequate TIN with the Thiessen method. The TIN must account for break lines. The Thiessen polygons are compatible with the derivation of equation (5.4.11) as illustrated in Giammarco and Todini (1994).

To ensure the highest accuracy, the polygon facets must be perpendicular to the lines joining nodal points and must intersect those lines at their median point or close to it. To avoid overlapping of polygonal cells, the triangles should have only acute angles. To meet such conditions, conventional triangulation techniques are not well suited and a specific method was developed.

Defining super-elements

The first step is to define on the basis of traditional topographic maps, preferably at a scale of 1/10000 or higher, large polygonal surfaces or "super-elements" delimited by structure lines (rivers, channels, etc.) and/or break lines (roads, embankments, walls, etc.). The facets of such super-elements must follow the boundaries of all structure and break lines as closely as possible. Mandatory nodal points must be defined at each super-element vertex. Supplementary nodal points can also be defined. Super-elements must be convex polygons. Complex shapes should be broken down into more simple convex polygonal super-elements. Figure 5.4.6 illustrates an example of a super-element lay out.

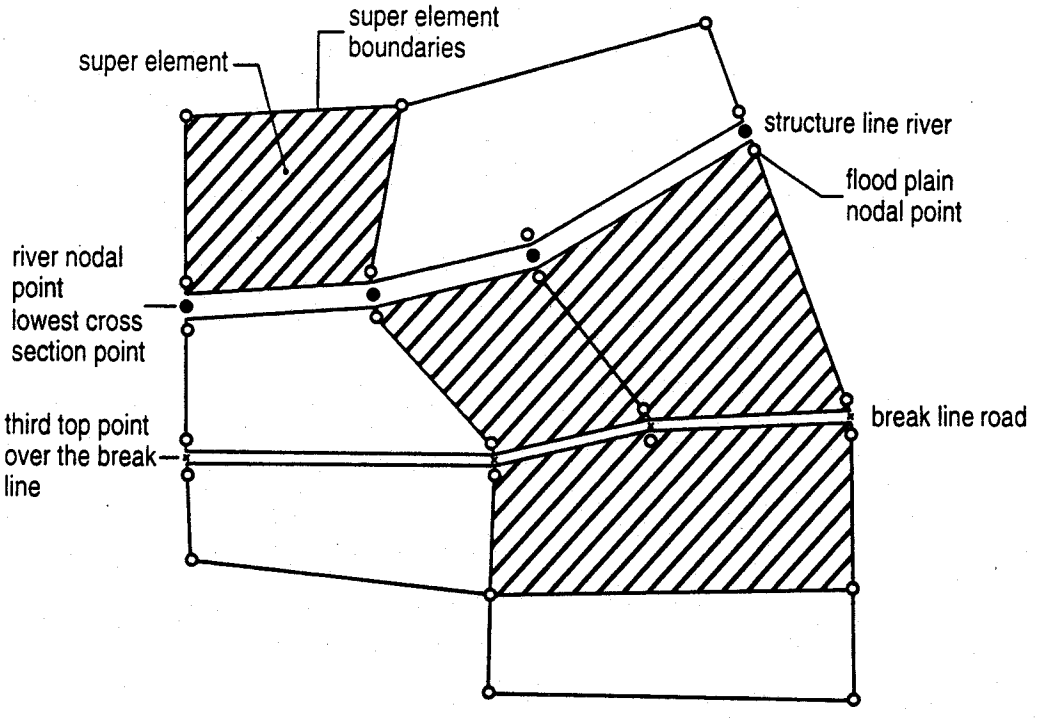

Figure 5.4.6. Layout of super-elements to derive the adequate TIN

The solution of equation (5.4.11) does not require the definition of Thiessen polygons at break lines since the effects of such hydraulic structures are implicitly accounted for in the computation of transmissivities between adjacent nodes. A similar situation applies to river

polygons since their surface is computed from cross-section characteristics and from the control volume length (Figures 5.4.1 and 5.4.2).

Consequently, the proposed triangulation method is only applied within the boundaries of the flood plain super-elements. Two adjacent super-elements have common vertices along their boundary lines. If two super-elements are separated by a break line, they also have counterpart vertices on either side of the obstacle. Along the axis of these two vertices, it is necessary to define a third top-point over the break line (Figure 5.4.6). A similar situation applies for super-elements separated by structure lines. In that case, the third point corresponds to the lowest cross section point (Figure 5.4.6).

Triangulating within each super-element

Within each super-element, it is necessary to locate a central point. The latter should satisfy the requirement that the segments connecting it to the super-element vertices form only acute angles with the corresponding boundary lines. The method must first identify all the obtuse angles of the super-element. Through the corresponding vertex, lines perpendicular to the two adjacent boundaries are drawn. All the segments drawn between the vertex and any point lying between the two perpendiculars will form acute angles with the corresponding super-element boundary lines.

This procedure is systematically repeated for all the obtuse angles of the super-element. The location of the central point lies in the region bounded by all perpendiculars.

Figure 5.4.7 shows an illustrative example of how the proposed triangulation method may be applied. Should this procedure fail to delineate a unique intersection region, it is necessary to arbitrarily split the original super-element.

To increase the number of control volumes, original super-elements may be further broken down. Modifications to original super-elements should not involve the definition of new vertices. Otherwise, it is of course necessary to relocate the central point of the modified super-elements. This procedure ensures that all triangle facets from the central point form acute angles with the super-element boundaries. However, it can not satisfy the condition that at the central point all angles are acute. This situation is illustrated in Figure 5.4.8.

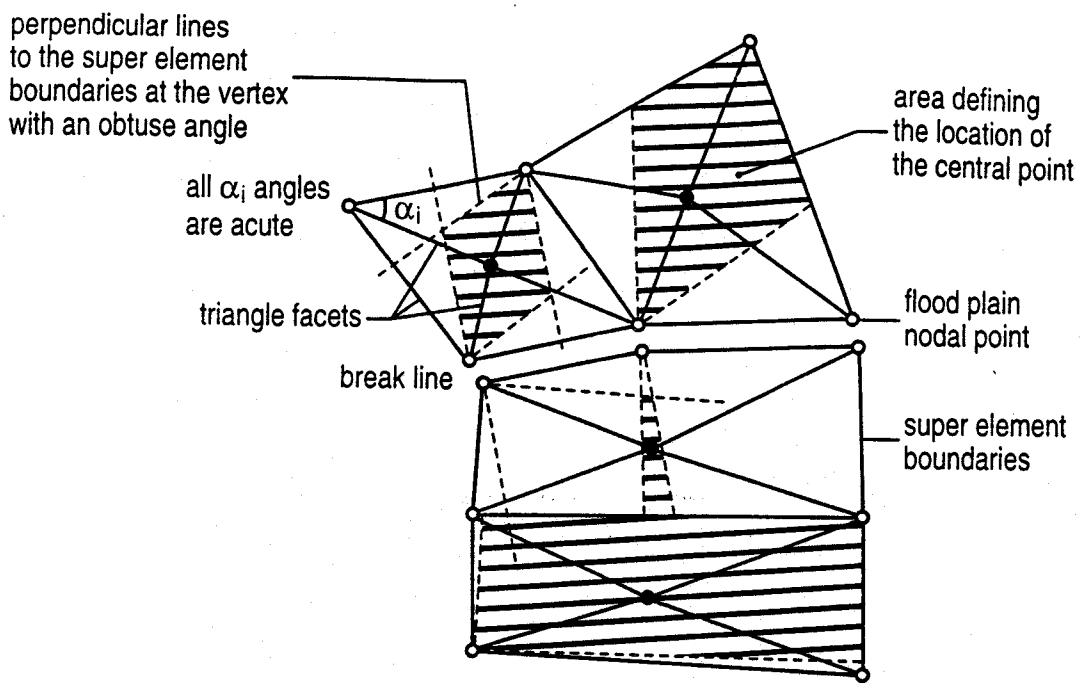

Figure 5.4.7. Location of the central point of the convex super-element

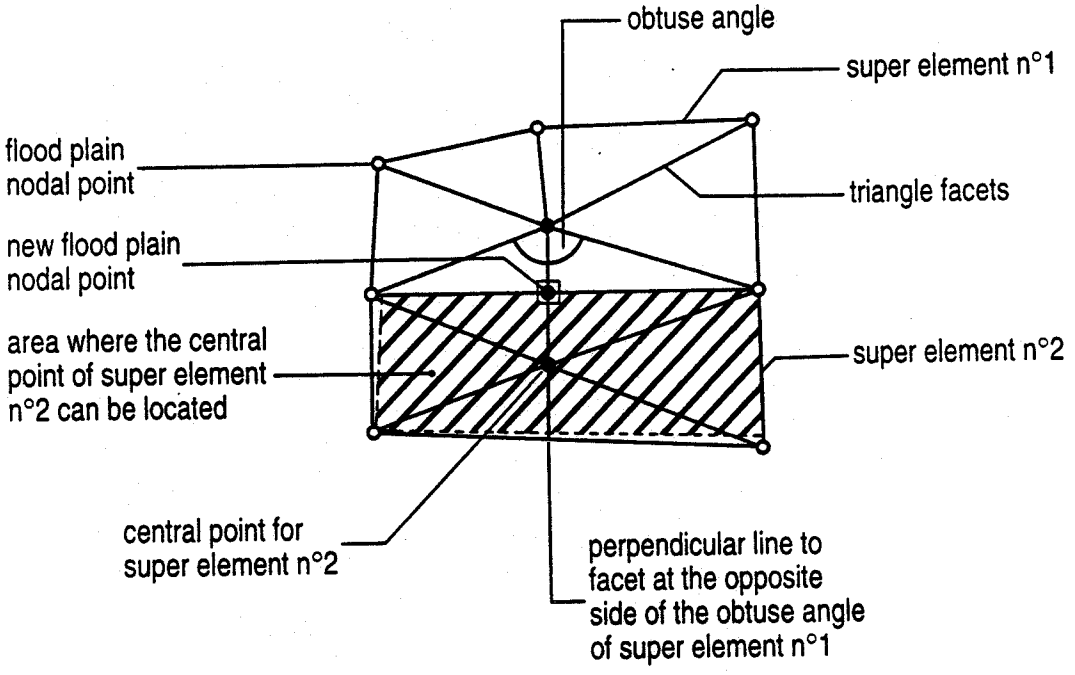

Figure 5.4.8. Definition of new nodal points along the super-element boundaries to ensure that all internal angles of the related triangles are acute

The solution is to draw a perpendicular line to the opposite facet through the central point in order to split the obtuse angle. This necessarily creates a new vertex in the current super-element as well as in the adjacent one. In order to avoid obtuse angles in the adjacent super-element, its central point must lie on the extension of the newly created perpendicular as well as within the already defined intersection region.

Particular cases

Figure 5.4.9 illustrates a particular example in which a break line presents only one intersection point with the super-element boundaries. In such cases the super-element has to be broken down into more convenient convex polygonal shapes. The method requires the addition of two supplementary points (B and C) on either side of the break line. The latter is then artificially extended by a length which is equal to the distance between the supplementary points and the endpoint of the break line. Thus a new end point is created (A) which may be used as a vertex to delineate a new super-element, for which a central point can be located using the above described technique. The original endpoint of the break line cannot be used as a vertex. This procedure ensures that the Thiessen polygon facets between the supplementary points (B and C) and the newly created endpoint (A) will intersect the break line at its end points (O' and O''). The extra surface is added to that of the polygon for node (A) as shown in Figure 5.4.9.

Figure 5.4.10 shows another commonly found special situation where one break line terminates when it intersects another. Normally, the triangulation method used requires the definition of four nodes at a break line intersection. However, in this case this will lead to a unnecessarily short distance between nodes on the side opposite from the terminating break line.

Therefore, only three points are required, A and B, and C which lies on the axis of the terminating break line on the side opposite from A and B. The triangulation method is then applied as described above. The facets of the polygon for node C which are perpendicular to the limiting break line are forced to line up with those of the polygons corresponding to nodes A and B.

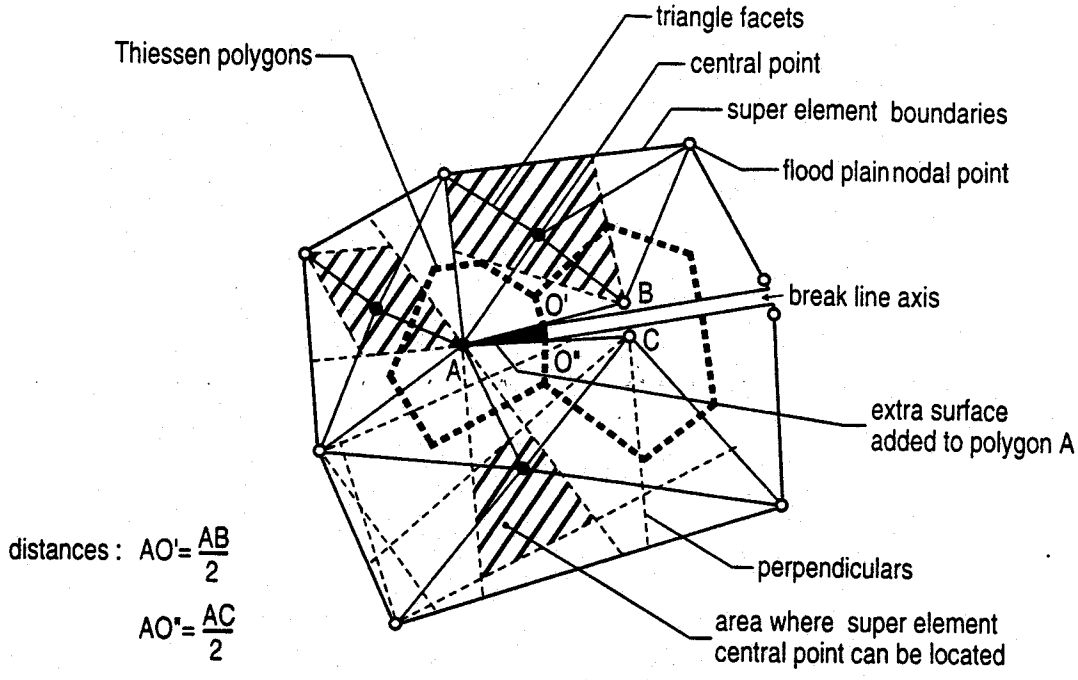

Figure 5.4.9. Particular case where a break line presents only one intersection point with the super-element boundary. Application of the triangulation method

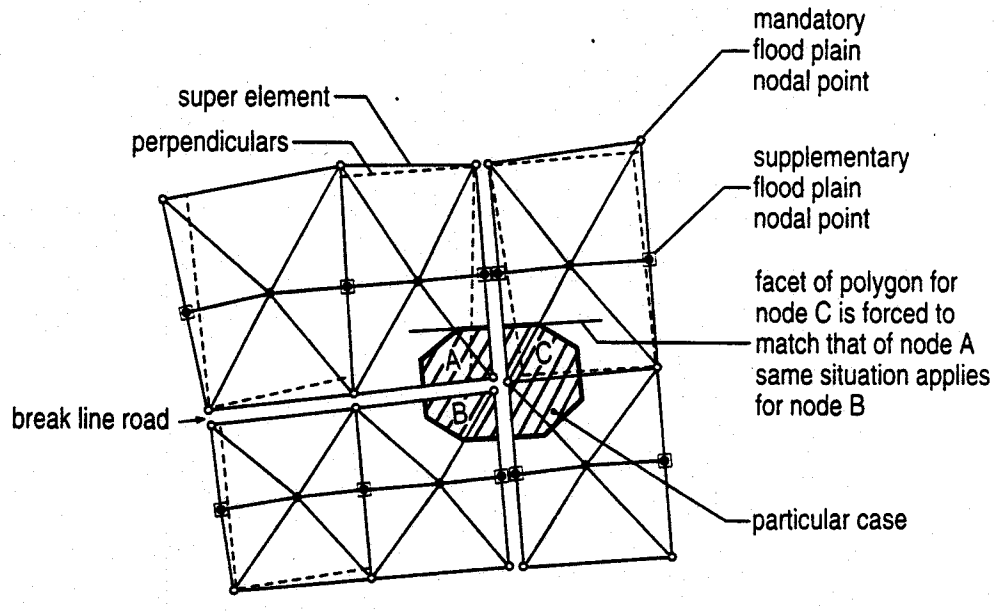

Figure 5.4.10. Particular case where a break line terminates when it intersects another. Application of the triangulation method

Generating the dtm for hydraulic computations

According to the proposed triangulation method, river cells and flood plain polygons will be properly connected. The length of overflow corresponds to the sum of the half way distances between node (i) and those located immediately upstream and downstream. For the case of break lines, the boundaries of the adjacent flood plain cells will also coincide. The length of this common interface is equivalent to that of the overflow width in the weir equation applied between the two nodes located on either side of the break line.

In the near future, the proposed triangulation procedure will be implemented in a semi-automatic algorithm including graphical capabilities for visual inspection of the polygonal mesh and a user-friendly interface to create/modify nodal points and/or split super-elements. The purpose of this development is to assist the engineer in creating several polygonal mesh layouts and comparing the results of the hydraulic calculations. Input data includes the preliminary delineation of super-elements and the locations in the xy co-ordinate system of the nodal points. Delineation of break lines and structure lines is also required.

The generated polygonal mesh is plotted on a conventional topographic map. Nodal points as well as points on the break lines and on the river cross sections are properly identified. This map is finally used to gather all the elevation data. River cross-sections can be defined with conventional topographic methods. The elevations of the flood plain nodal points and break line points can be obtained with Global Positioning System (GPS) equipment using the "Stop and Go" approach (Signer et al., 1993).

With adequate GPS equipment, it is possible to reach high levels of accuracy on the order of a few centimetres for elevation data and of a few millimetres for xy co-ordinates. Since the control volume approach used to derive equation (5.4.11) assumes that the ground elevation of the nodal point is equivalent to that of all the points within the corresponding polygonal grid, it suffices to take one single point within the boundaries of the polygon.

Should the field survey identify new break lines or particular topographic features that were not accounted for in the preliminary delineation of super-elements, supplementary nodal points are located in the field. On that basis a new triangulation can be derived. Such an iterative procedure is needed since the available topographic maps, on which the first

super-element delineation is based, cannot include all topographic particularities of a given study area.

Combining the information used to delineate super-elements with the river cross-section data and the elevations of the flood plain nodal points, a pre-processor derives all the geometric data required to solve equation (5.4.11). This pre-processor also derives input files for the hydraulic model and sets the necessary tables in the GIS framework described later in this Section.

Flood delineation

Figure 5.4.11a shows an example of IDRISI output describing the spatial distribution of water surface elevations for each polygon. For graphical purposes only, this map can be further rasterised. The TIN derived with the proposed triangulation method is modified by creating new smaller triangles whose apices join all the intersection points between polygon sides and the facets of the original triangles as illustrated in Figure 5.4.11b. This procedure is only applied to nodal points in the flood plain. These newly created points belong to the polygon segments defining the interfaces between control volumes. It is reminded that to compute transmissivities between nodes the average depth is calculated at that particular location. The purpose of this minor modification is to obtain "smoothed" flood maps on the basis of computed water depths at the polygon nodes and at the control volume interfaces.

According to the hydraulic model assumptions the ground elevation at the interface points can be linearly interpolated from the altitudes of the upstream and downstream nodes. The water depth at the interface point is directly derived from the assumed water surface profile between these two nodes. A particular procedure was developed to rasterise the newly created triangular network and generate a flood map similar to that shown in Figure 5.4.11c. Obviously, interpolations account for break lines. River pixels are characterised by the elevation of the lowest point of the cross section representative of the control volume and the computed water surface elevation.

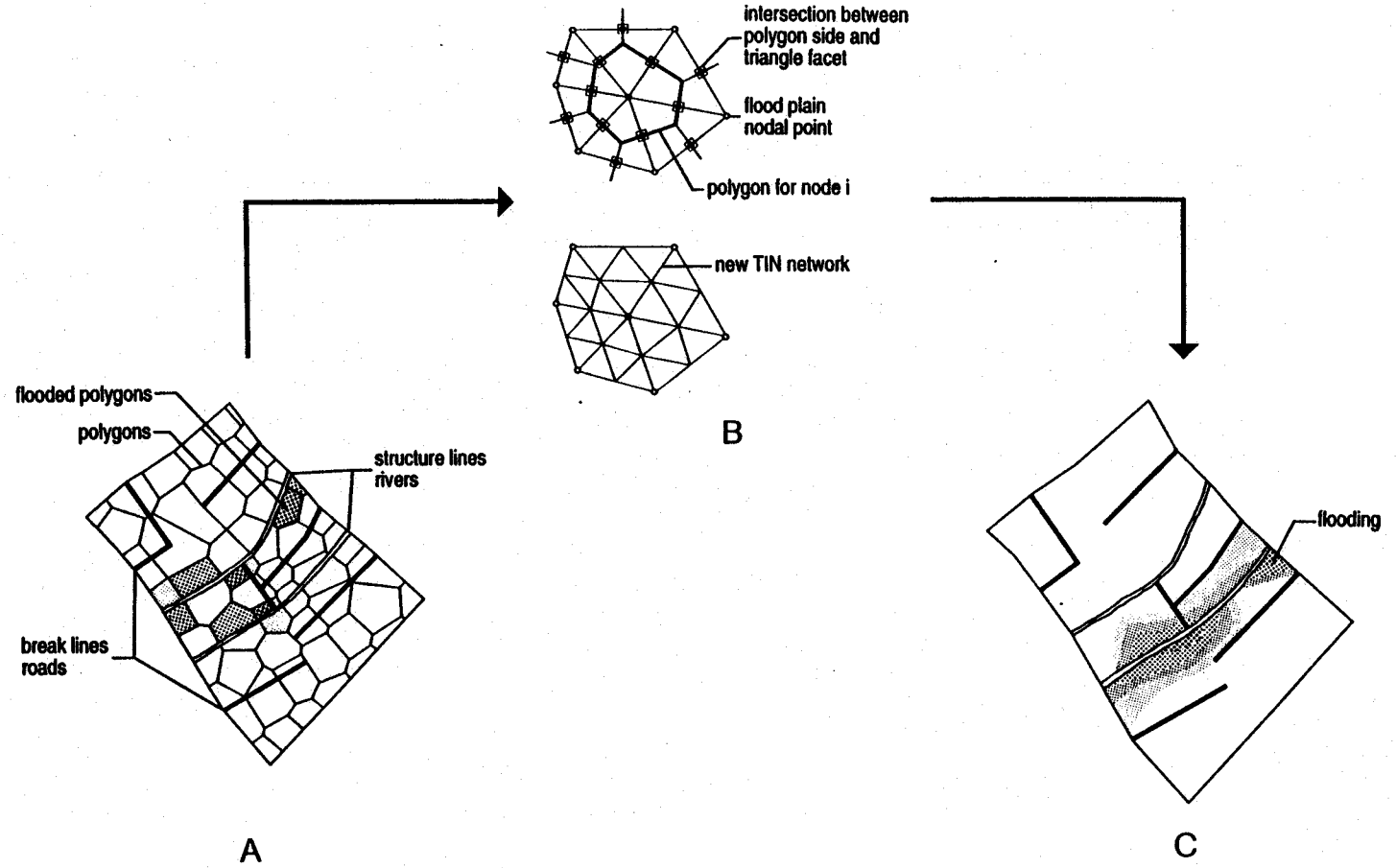

Figure 11. Flood delineation with IDRISI. Water surface elevations for each polygon (A), modification of the original TIN network (B), rasterised flood map (C)

REFERENCES

Abbott, M.B. 1979. "Computational hydraulics. Elements of the theory of free surface flow", Pitman Publishing, London.

Abbott, M.B., Cunge, J.A. 1975. "Two-dimensional modeling of tidal deltas and estuaries", Unsteady flow in open channels,vol.II, 763-812, Edited by Mahmood K., Yevjevich V., Fort Collins.

Abida, H. and Townsend, R. (1992). A numerical model for routing floods through compound channels. In J. Gayer, O. Starosolszky and C. Maksimovic (Editors), Hydrocomp'92 pp 115-122. Proceedings of the international conference on interaction of computational methods and measurements in hydraulics and hydrology held in Budapest, Hungary.

Ahn, S., Kim, G. and Choi, G. (1993). On the applicable ranges of kinematic and diffusion models in open channels. In H. W. Shen, S.T. Su and F. Wen (Editors), Hydraulic Engineering '93. ASCE Proceedings of the Specialty Conference held in San Francisco, California.

Ajiz M., Jennings A. (1984). "A robust incomplete Cholesky conjugate gradient algorithm", Int. Jour. for Numerical Methods in Engineering, Vol.20, pp. 949-966.

Akan A.O., Yen B.C. (1981). "Diffusion-Wave Flood Routing in Channel Networks", J.Hydr.Div.ASCE 107(HY6), 719-732.

Akanbi A.A., Katopodes N.D. (1988). "Model for flood propagation on initially dry land", J.Hydr.Div.ASCE 114(HY7), 689-706.

Bear J. (1979). "Hydraulics of groundwater", McGraw-Hill.

Becker E.B., Carey G.F.,Oden J.T. (1986). "Finite Elements", An Introduction vol.I, Prentice-Hall.

Calo' P. (1987). "Analisi delle conseguenze dello scarico rapido della prevista diga di Elvas (BZ) mediante un modello di propagazione bidimensionale", Tesi di Laurea Università di Bologna.

Chen C., Chow V.T. (1971). "Formulation of mathematical watershed-flow model", J.Mech.Div.ASCE 97(EM3), 809-828.

Cheng R.T. (1978). "Modeling of hydraulic systems by finite-element methods", Advances in Hydroscience, vol.11, 207-284.

Chow V.T., Ben-Zvi A. (1973). "Hydrodynamic modeling of two-dimensional watershed flow", J.Hydr.Div.ASCE 99(HY11), 2023-2040.

Citrini D., NOSEDA G. (1975). "Idraulica", Casa Editrice Ambrosiana, Milano.

Cunge, J.A. 1975. "Two-dimensional modeling of flood plains", Unsteady flow in open channels, vol.II, 705-762, Edited by Mahmood K., Yevjevich V., Fort Collins.

Daubert A., Graffe O. 1967. "Quelques aspects des écoulements presque horizontaux a deux dimensions en plan et non permanents application aux estuaires", La Houille Blanche, 8, 847-860.

De Vries J.D., Hromadka T.V., Nestlinger A.J. (1986). "Applications of a Two-Dimensional Diffusion Hydrodinamic Model", Hydrosoft 86- Hydraulic Engineering Software, Proc.2nd.Int.Conf., Southampton, 393-412.

De Vries, M., Jansen, P. and Van de Berg, J. (1979). Principles of river engineering. Pitman Publishers. London.

Dhatt G., Touzot G., (1985). "The Finite Element Method Displayed", John Wiley.

Di Giammarco, P. and Todini, E. (1994). A control volume finite element method for the solution of "D overland flow problems. In P. Molinaro and L. Natale (Editors), Modeling of flood propagation over initially dry areas. pp 82-101. Proceedings of the Specialty Conference held in Milan, Italy at ENEL-DSR-CRIS.

Di Giammarco, P., Todini, E., Consuegra, D., Joerin, F., and Vitalini, F. (1994). Combining a 2-D Flood plain model with GIS for flood delineation and damage assessment. In P. Molinaro and L. Natale (Editors), Modelling of flood propagation over initially dry areas. pp 171-185. Proceedings of the Specialty Conference held in Milan, Italy at ENEL-DSR-CRIS.

Di Silvio G. (1978). "Modelli matematici per lo studio della propagazione di onde lunghe e del trasporto di materia nei corsi d'acqua e nelle zone costiere", Metodologie numeriche per la soluzione di equazioni differenziali dell'idrologia e dell'idraulica, Ed. Pàtron, Bologna.

Duff I.S., Reid J.K. (1982). "MA-27 - A set of FORTRAN Subroutines for solving sparse symmetric sets of linear equations"", Rep. n. R-10533, AERE Harwell Laboratory, Oxfordshire.

Duff I.S., Reid J.K. (1982). "The multifrontal solution of indefinite sparse symmetric linear systems", Rep. n. CSS 122, Computer Science and System Division, AERE Harwell Laboratory, Oxfordshire.

Fennema R.J., Chaudhry M.H. (1989). "Implicit methods for two-dimensional unsteady free-surface flows", Journal of hydraulic Research, 27(3), 321-332.

Fugazza M., Gallati M. (1977). "A finite element numerical model of the two dimensional shallow water motion", Baden-Baden, IAHR vol.2, 191-196.

Gallagher R.H., Oden J.T., Taylor C., Zienkiewicz O.C., (1975). "Finite Elements in Fluids", vol.1, John Wiley.

Galland, J.C., Goutal, N. and Hervouet, J.M. (1991). A new numerical model for solving shallow water equations. Advances in water ressources, vol. 14, n. 3. pp 138-148.

Grubert J.P. (1976). "Numerical computation of two-dimensional flows", J.Wat.Harbors and Coastal Div. ASCE 102(WW1), 1-12.

Henderson, F. (1966). Open channel flow. Mac Millan Publishing Company. New York.

Higuera F.G., Succi S., Benzi R. (1989). "Lattice Gas Dynamics with enhanced collisions".

Hosseinipour Z., Amein M. (1984). "Finite element computation of two-dimensional unsteady flow for river problems", Proc.5th Int.Conf.on Finite Elements on Water Resources, Burlington, Vermont, 457-466.

Hromadka Ii T.V., Berenbrock C.E., Freckleton J.R., Guymon G.L. (1985). "a two-dimensional dam-break flood plain model", Adv.Water Resour.,8, 7-14.

Hromadka Ii T.V., Nestlinger A.J., De Vries J.D. (1986). "Comparison of Hydraulic Routing Methods for One-Dimensional Channel Routing Problems", Hydrosoft 86-Hydraulic Engineering Software, Proc. 2nd Int. Conf., Southampton, 85-98.

Huyakorn P.S., Pinder G.F. (1983). "Computational Methods in Subsurface Flow", Academic Press, London.

Katopodes N.D. (1980) "Finite element model for open channel flow near critical conditions", Proc.3rd Int.Conf. on Finite Elements on Water Resources, Oxford, Miss., 5.37-5.46.

Katopodes N.D. (1984) "Two-dimensional surges and shocks in open channels", J.Hydr.Div.ASCE 110(HY6), 794-812.

Katopodes N.D., Strelkoff T. (1978). "Computing Two-Dimensional Dam-Break Flood Waves", J.Hydr.Div.ASCE 104(HY9), 1269-1288.

Katopodes N.D., Strelkoff T. (1979). "Two-Dimensional Shallow Water-Wave Models", J.Mech.Div.ASCE 105(EM2), 317-334.

Kershaw D. (1978). "the incomplete Cholesky-Conjugate gradient method for the iterative solution of systems of linear equations", Journal of Comp. Physiscs 26, pp. 43-65.

Labadie, G. (1992). Flood waves and flooding models. In G. Rossi, N. Harmancioglu and Yevjevich (Editors), Coping with Floods. pp 177-218. Pre-proceedings of the NATO A.S.I. held at Majorana Centre, Erice, Italy.

Lai C. (1986). "Numerical modeling of unsteady open-channel flow", Advances in Hydroscience, vol.14, 161-333.

Lapidus L., Pinder G.F. (1982) "Numerical solution of partial differential equations in science and engineering", John Wiley.

Marchi E., Rubatta A. (1981). "Meccanica dei fluidi. Principi e applicazioni idrauliche", UTET, Torino.

Marco, J. (1992). Flood risk mapping. In G. Rossi, N. Harmancioglu and V. Yevjevich (Editors), Coping with Floods.pp 255-276. Pre-proceedings of the NATO A.S.I. held at Majorana Centre, Erice, Italy.

Narasimhan T.N., Witherspoon P.A. (1976). "An integrated finite difference method for analyzing fluid flow in porous media", Water Resour.Res.,12(1), 57-64.

Narasimhan T.N., Witherspoon P.A., Edwards A.L. (1978). "Numerical model for satured-unsatured flow in deformable porous media. 2.The algorithm", Water Resources Research, 14 (2), pp. 255-261.

Ortega J.M., Rheinboldt W.C. (1970). "Iterative solution of non-linear equations in several variables", Academic Press.

Pacciani M. (1987). "analisi comparativa di metodi impliciti ed espliciti per il calcolo della propagazione bi-dimensionale di onde di piena", Tesi di Laurea. Università di Bologna.

Pinder G.F., Gray W.G. (1977). "Finite element simulation in surface and subsurface hydrology", Academic Press, London.

Reddy J.N. (1986). "Applied functional analysis and variational methods in engineering", McGraw-Hill.

Reitano, G. (1992). Flooding vulnerability analysis at basin-wide-scale. In G. Rossi, N. Harmancioglu and V.Yevjevich (Editors), Coping with Floods. pp 301-327. Pre-proceedings of the NATO A.S.I. held at Majorana Centre, Erice, Italy.

Salgado R.O. (1988). "Computer Modelling of Water Supply distribution networks using the gradient method". Ph.D. Thesis, University of Newcastle upon Tyne.

Signer, T., Dupraz, H., Aeschliman, C. and Jolidon A. (1993). Test de la méthode statique rapide avec les récepteurs Wild GPS-System 200. Mensuration Photogrammétrie Génie Rural. 5/346. Société Suisse des Mensurations et Améliorations Foncières (SSMAF).

Sinniger, R. and Hager, W. (1989). Constructions hydrauliques; Ecoulements stationnaires. Traité de Génie Civil de l'Ecole Polytechnique Fédérale de Lausanne, Volume 15. Presses Polytechniques Romandes, Lausanne, Switzerland.

Sloan S.W. (1987). "a fast algorithm for constructing Delaunay triangulations in the plane", Advanced Engineering Software, Vol. 9, n. 1, pp.34-55.

Stoer J., Burlish R. (1980). "Introduction to numerical analysis", Springer Verlag, New York.

Todini, E. (1991). Hydraulic and Hydrologic Flood Routing Schemes. Recent Advances in the Modelling of Hydrologic Systems; Kluwer Academic Publishers.

Vansnick M., Zech Y., (1984). "Fourier analysis for testing a finite elements method in shallow water problems", Proc.5th Int.Conf.on Finite Elements on Water Resources, Burlington, Vermont, 467-476.

Vitalini, F. (1993). Una procedura per la previsione, il controllo e la gestione del rischio di inondazione in forma distribuita sul territorio. Tesi di Laurea. Facolta di Ingegneria, Dipartimento di Ingegneria Idraulica, Ambientale e del Rilevamento, Politecnico di Milano, Milano, Italia, 300 pp.

Xanthopoulos Th., Koutitas Ch. (1976). "Numerical simulation of two dimensional flood wave propagation due to dam failure", Journal of hydraulic research, 14(4), 321-331.

Zatta, A. (1993). Rotture di argini, modelli di rotura, loro inserimento in un programma per l'analisi del rischio di inondazione. Tema di Laurea. Universita degli studi di Pavia, Facolta di ingegneria; Pavia, Italia, 40 pp.

Zienkiewicz O.C. (1977). "The finite element method", 3rd ed., McGraw-Hill, New York.

6. THE DECISION SUPPORT SYSTEM

6.1 INTRODUCTION

6.1.1 The Reno flooding problem and response

The purpose of the man-made portion of the River Reno is to convey water from the mountains of the Apennine range off the land and to the sea as quickly and efficiently as possible. Prior to human intervention, the river discharged its waters to the lowland marshes. Uncontrolled floods off the mountains were dissipated in extensive marshlands.

Over many years, a man-made river has been constructed which takes the waters of the upper Reno from Bologna to the coast, and which has been built up using earth levees. There are two major concerns at present:

- The lower Reno is not capable of carrying all the water conveyed by the upper Reno in times of extreme rainfall;
- The dykes cannot contain water without becoming weakened and eventually breaking.

An attempt to overcome this has been made by building the Canale Napoleone between the Reno and the River Po, so that part of a major flood wave may be passed to the Po in time of crisis. While this has dramatically improved the situation, times still occur when more water is issued by the upper Reno than can be carried by both the Canale Napoleone and the lower Reno, producing flooding downstream of the point of intersection - there are also times when the Po is also in a state of flood and unable to take any of the Reno flow.

The area downstream of the Canale contains industrial units and a sparse population, and recent floods have caused fatalities. The river authorities now seek better ways of operating the system.

An overall flood warning and control system has been defined to meet the needs of the Reno stakeholders. The three groups of people participating in the system are: meteorologists/hydrologists, operational managers and civil response managers.

Overall system

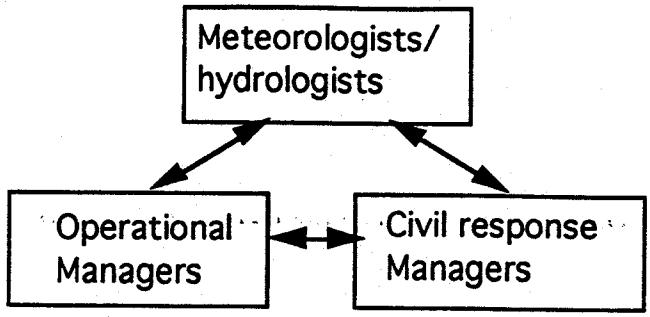

The communications links that will be required between these three groups have been examined. The total warning system consists of two parts: a technological part and a social part.

TOTAL WARNING SYSTEM

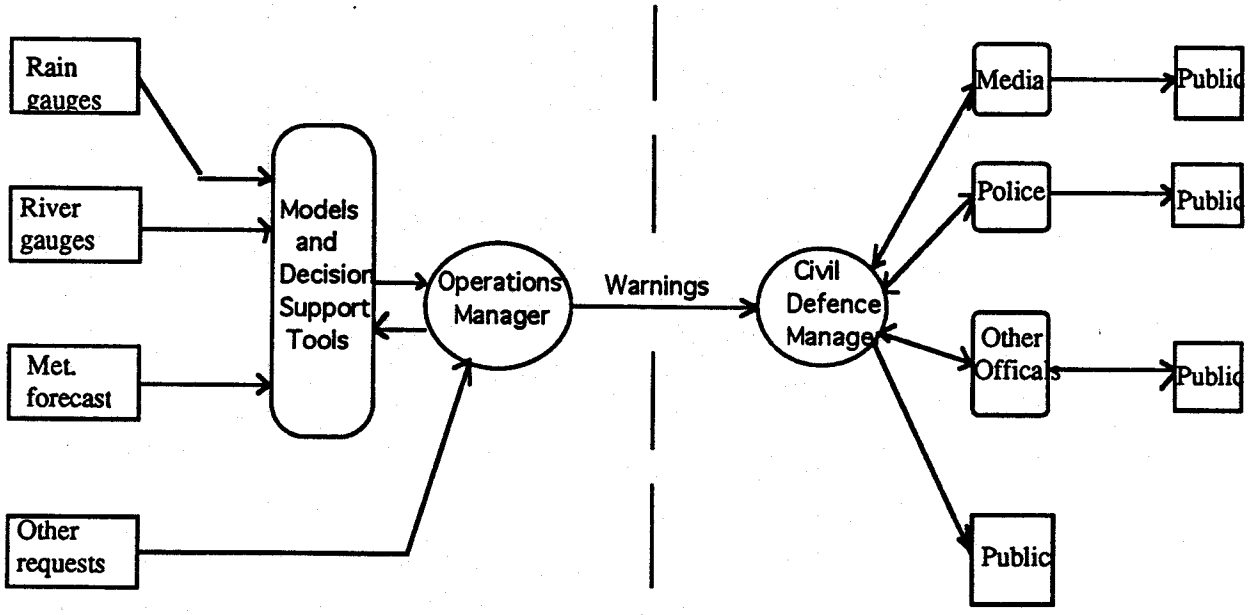

1. TECHNOLOGICAL SUB-SYSTEM

2. SOCIAL SUB-SYSTEM

The *technological subsystem* is run by meteorologists and hydrologists and consists of rain gauges, river gauges, and meteorological forecasting systems, which together provide data for hydrological and flood-forecasting models, and decision support tools. These are, in turn, made available to the *operations managers*. The data, models and decision support tools are interrogated by the operations managers to meet both their own needs and other requests. Relying on this, the operations manager may issue warnings to the *civil defence manager*. The civil defence manager interacts with the media, the police, other officials and the public, both directly and indirectly. This forms the *social subsystem* of the overall total warning system.While AFORISM has not been charged with investigating the social subsystem, the success of the technological system is critically dependant on a clear view of the social subsystem and its needs. Consequently, general lessons from the sociology of hazards must be borne in mind.

6.1.2 Lessons from the Sociology of Hazards

The following lessons from the sociology of hazards are important for the design and operational success of the technological subsystem of AFORISM. These are

- Warnings must be clear;
- Warnings must also specify what is the appropriate response;
- The source of the warnings must be credible;
- Warnings must be reinforced locally;
- The medium used in issuing the warnings must be suited to the circumstances of the specific case;
- The type of appeal to the public must be tailored to the public audience.

The lessons which derive from this for an AFORISM decision support system are two-fold:

- Models, user-interfaces etc., must present clear, unambiguous predictions and courses of action;
- Specific instructions for the appropriate response to be taken, must accompany all warnings.

6.1.3 Outline Design of the Technological Subsystem

Outline data flow diagrams for meteorologists and hydrologists, operational managers and civil response managers have been prepared. These diagrams show the capture, storage, filing, processing, display and delivery of data to the relevant group of managers. They provide the starting point for the detailed design/selection of the operational computer hardware, which is required for the eventual realisation of the decision support and forecasting system. An Expert System is one part of a decision support and forecasting system and was the object of the UCC(Cork) contribution to AFORISM.

6.1.4 Expert Systems

A standard expert system consists of a number of parts:

- a knowledge base (1) of rules and facts,
- stored in a working memory (2),
- accessible to an inference engine (3),
- controlling inferences drawn from the knowledge base, and to which
- a knowledge acquisition subsystem (4) may add knowledge from experts or the system developer.

The basic structure of the expert system is completed with

- a user interface (5), and
- an explanation subsystem (6).

The knowledge acquisition subsystem, the user interface, and the explanation subsystem, all rely on the inference engine.

The limited objectives of the AFORISM project demanded that most attention be given to the knowledge base and the user interface following an analysis of the requirements of the management authority.

6.2 REQUIREMENTS ANALYSIS AND KNOWLEDGE BASE

The first step in constructing an expert system and its user interface in particular, is to determine the requirements which may be placed on the system by Flood Managers. A user requirements analysis has been carried out for two contrasting catchments both subject to flooding, the Reno in Italy and the Lee in Ireland. The most important difference between them is the presence of a relatively large hydro-electric reservoir in the centre of the Lee catchment and the absence of a similar storage reservoir in the Reno catchment. The importance attached to their requirements by the two groups of operations managers and civil response managers, has been estimated on a rough scale from 0 to 10. The results show that the relative importance of the requirements differ substantially between the two catchments. Consequently, no general set of conclusions emerged which is valid for all flood control situations.

However, two tentative conclusions may be suggested:

- large water authorities requiring short warning times, may have the highest need for a formal decision support system, and in contrast,
- small authorities with a long warning time requirement, may have a low demand for a formalised decision support system.

Priority points (out of 10) as perceived by members of the Reno Regional Office and related Consorzio were

Ability to predict aggregation of flood waves below barrier	9
Ability to predict aggregation of flood waves above barrier	9
Ability to predict traffic access route (Consorzio)	8
Support for ecological aspects of decisions	6

Priority points (out of 10) as perceived by civil response managers in the Reno were

Integrated data bank of potential hazards	8
Data bank/risk maps for flooding	7
Support for response action i.e. list of contractors	7
Identification of response priorities e.g. the elderly	6

The project has made important contributions to a decision support system which addresses most of these requirements. The contributions are described in the remaining

sections of chapter 6. Further work remains to be done. Providing all the means to satisfy these requirements was not the major objective of AFORISM.

6.2.1 A tentative Reno Knowledge Base

A knowledge base for the Reno would consist of all the sets of rules (and facts) which are followed in its operation as a water resource. A set of rules has been established for the issue of a pre-alert notice and the operation of the Reno Barrier. These are presented below, together with three further tentative sets consisting of:

- three ecological rules derived from the general ecology literature of northern Europe on the possible effect of river flow variations on plants, invertebrates, fish and birds,
- a set of channel and bank maintenance rules for enhanced conservation derived from the general ecology literature of northern Europe, and
- two legal rules applicable under Common Law.

6.2.2 The Reno Pre-alert and Barrier Rule Set.

Pre-alert rules:

IF level at Casalecchio
> or = 0.8 meters
THEN the flood service of the Reno Special Office is activated.

IF level at Casalecchio
> or = 1.4 meters
THEN give Pre-Alert.

IF level at Casalecchio
> or = 1.00 meters
AND River high downstream
THEN give Pre-Alert.

IF aggregation of flood waves upstream,
even small waves
AND river high downstream
THEN give Pre-Alert

IF Pre-Alert given
THEN consider using Reno Barrier.

Rules for Barrier Operations:

IF Reno level at Barrier
> or = 22.00 meters
THEN Adjust Barrier to minimise aggregation risk.

IF level high upstream for many hours
THEN adjust the Barrier to
keep level even > 22.00 meters downstream.

IF level > 22.00 meters downstream
for many hours
THEN consider possible overflow
though GALLO spillway.

IF want to use flow diversion
into NAPOLEON CANAL
THEN adjust the Barrier quickly
to provide an overflow level,
irrespective whether the level in the
downstream Reno is stabilised
at 22.00 meters or not.

6.2.3 Ecological Rules

Rule 1. Mitigate high flows as much as possible.

Rule 2. Ignore normal variations

Rule 3. Keep up a minimum base flow.

These rules are based on the general effect which normal and extreme variations in flow have on the different numbers of species of riverine plants, invertebrates, fish and birds in northern Europe.

		Flow Variations	
	Number of species	**Normal**	**Extreme**
Plants	1000s	Positive effect	Very Negative effect
Invertebrates	1000s	No effect	Very Negative effect
Fish	10s	No effect	Very Negative effect
Birds	10s	No effect	Very Negative effect

6.2.4 Channel & Bank Maintenance Rules for enhanced conservation:

Can, or should, the channels be left entirely untouched?

If **YES:**

consider

structural solutions

flood banks,
flood storage areas,
flood bypass channels, and
multi-stage channels.

consider

biological solution

tree planting to shade out plant growth

If **PARTIALLY:**

consider

structural solutions

partial dredging,
conserving riffles and pools, and
meander conservation.

consider

biological solutions

weed cutting and
dredging.

If **NO:**

consider

structural solutions

reinstating pools, riffles, and shallow bays,
shallow water berms, groynes and water deflectors,
low stone weirs.

consider

biological solution

establishing aquatic plants.

Can, or should, the banks be left entirely untouched?

If **YES:**

consider

structural solutions

flood banks,
flood storage areas,
flood bypass channels, and the
off-site dumping of spoil

consider

biological solutions

fencing, and
the bank-top planting of alders

If **PARTIALLY:**

consider

structural solutions

multi-stage channels,
partial dredging,
meander conservation,
working from one bank,
vertical earth bank protection,
islands,
soil spreading,
spoil disposal in banks, and
spoil disposal and trees

consider

biological solutions

timing the mowing of bank vegetation,
patch cutting of bank vegetation,
working through scrub,
hedges,
marking trees to be treated,
working between and around trees,
coppicing trees and scrub,
retaining trees within flood banks,
minimal tree and scrub removal for otters,
marking and retaining holt trees for otters.

If **NO:**

consider

structural solutions

reinstate shallow water berms
and shallow bays,
stumps and logs,
spiling,
wire mesh and willow,
hurdles,
natural stone,
gabions,
fabric and mesh revetment materials,
cellular concrete revetment materials
fish shelters,
artificial otter holts,
bat roosting boxes,
nesting banks for kingfisher and
sand martin.

consider

biological solutions

reed planting for bank protection,
natural re-colonisation,
seed mixtures,
transplanting turf,
tree and scrub planting

6.2.5 Legal Rules

1. "The authority owes a duty of care to all persons, members of the public and others, that may be effected by its actions."

2. "Provided the effect of the actions of the authority have a mitigating effect on the severity of a natural hazard, then the authority can claim the defence of *inevitable accident.*"

6.2.6 Further rules

A rule base with 20 rules has been defined, which is far below the power of current computerised KBS (knowledge base/expert system) technology.

Rule Set	Number of Rules	Remarks
Operations	10	Reno alert rules.
Ecology	2	Does not give rules for each species.
Maintenance	6	Relevant for day-to-day activities.
Legal	2	Does not include individual cases.

Further rules may be envisaged covering

- integrity of the dykes,
- aggregation and propagation of flood waves,
- overtopping of banks, and the
- growth and decline of flooded areas,

all of which require extensive modelling and the collection of field data. Preliminary work on the first three of these problems has been carried out at Newcastle and is reported in sections 6.3 and 6.4. The Lausanne group has carried out extensive work on the growth and decline of flooded areas and their socio-economic impacts. While the Lausanne approach, reported in section 6.5, has been developed on a flood-prone area in the Basse Broye region of Switzerland, it is clearly applicable to the Reno.

However, further work is required before the corresponding rule sets can be formulated for routine use by the Reno managers.

6.3 SYSTEM DESIGN - FLOOD CONTROL STRATEGIES

6.3.1 The "heuristic policy"

The river authorities currently employ a policy - hereafter referred to as the 'heuristic policy' - which, during the initial rise of a flood wave, allows the streamflow downstream of the barrier to reach its maximum level, and thereafter proportions the flow between the lower river and the canal in the same ratio as the ratio of the maximum lower river flow and maximum canal flow. This situation is maintained until either the flow recedes to a safe level or the system comes into saturation. In the latter case, both the lower river and the canal are carrying as much water as possible, and any more water ensuing from the upper part of the river will result in an unavoidable flood. The flow to the canal is reduced significantly at this point as it will no longer be of any benefit to continue with attempts to divert the flood water, and consequently the lower river goes over saturation and floods.

The operation of the policy just described is made on the basis of currently observed river levels upstream of the canal. The policy makes no use of forecast streamflow information, and hence no attempt to look ahead is made. No attempt is made either to conserve the lower dykes or the canal in readiness for a big flood wave. Hence it is seen that a policy which can make use of forecasted information, and which can look ahead to determine an operating policy producing the best operation over at least the foreseeable future must be able to perform better than the heuristic policy described.

6.3.2 Short- and long-term flood control strategies

It is clear that the requirements of a new operating policy are

- to use the barrier and flood canal - the Canale Napoleone - to pass as much water as quickly as possible from the land to the sea, before dyke breakage and ensuing spillage occurs,

- to perform this operation in a way that maintains the strength of the dykes, so that when an extreme flood wave does eventually come and a flood becomes inevitable, the dykes will still have strength in reserve to hold the water back as long as possible.

Dynamic Programming is a mathematical technique for finding optimal control strategies for dynamic systems. All current dynamic programming applications to hydraulic control have been to systems containing a reservoir. The lack of this feature on the Reno means that there is no buffering between the input to the control system and its output, so that some of the stochasticity inherent in the input will also show itself in the output. Thus the output is beyond direct control; human operators can only influence the transition probabilities of the downstream flows, i.e. to make downwards transitions in the lower streamflow state more probable by partly closing a barrier than they would otherwise have been the case. Consequently, much of the literature is irrelevant to the Reno system. However, many aspects of different schemes have been noted and included in the new proposal developed at Newcastle.

The work at Newcastle has sought new theory for the control of the system for both the short-term mechanical preservation of the dykes, and also for the long-term minimization of the amount of flood damage in a situation when breakage of the dykes becomes inevitable.

The two approaches are complimentary in that the former considers the short-term flow forecast as input and seeks to minimise the exposure of the dykes to the water, whereas the latter considers the operation of the river system over a period of many years, and attempts to determine an operating policy that will minimize the amount of flood damage over this period of time, when, at some stage, such damage must inevitably occur. In the latter case the strength of the dykes is considered to be a function of the history of water levels, whereas the former simply seeks to minimise the exposure in the short term.

The remainder of section 6.3 presents a brief introduction to dynamic programming followed by an investigation of its use for the minimization of long-term flood damage. Section 6.4 presents the causes and effects of water-damage to dykes and development of methodology for short-term operations.

6.3.3 Dynamic programming

Dynamic programming is essentially an efficient mathematical technique for searching through a set of possible paths which a process may take through its state space, and

finding that path which has an optimal characteristic. For example, the set of paths between two points on the surface of a cone may be considered, and that which has the shortest length found. It gives the same result as would be obtained using the calculus of variations.

The necessary parts of a dynamic programming problem are:

- an **objective function** - the cost or value of each path - which is to be optimised over all feasible paths;
- a **recursive equation** describing the evolution of the objective function - how its value at time t+1 can be determined from the value at time t;
- **boundary conditions** - specification of the initial and final states of the system.

There are many variations on the above theme: for example, if the process has a random element, then the path is sought which has the largest probability of meeting some objective, or which has the largest expected return - so-called stochastic dynamic programming; if, instead of enumerating all state transitions between time t and time t+1, all paths through the state space which are adjacent to some trial path over the entire planning horizon are considered, then we are in the realm of differential dynamic programming.

In this work a novel dynamic programming algorithm is developed to compute (a) the expected path taken by a stochastic system, and (b) that set of controls on the system for which the expected path based on those controls has an optimal value.

6.3.4 Minimization of long-term flood damage

The theory has produced new working which derives the expected path taken by a river system through its state space, rather than a most probable path. This may be advantageous because it may represent a more natural assessment of the future course of events, and deviations are likely to be less from this than from the most probable path.

While the above work has been done on purely theoretical grounds, much effort has also

been spent in making the final result applicable in a general real-time situation, and in particular has considered its implementation on the Reno river with all the benefits that AFORISM brings to the problem, i.e. rainfall forecasts, streamflow forecasts, damage assessment, etc. In particular, the complementary nature of the different forecasting systems as regards temporal scale and lead-time has been used to full advantage by designing a system which takes forecasts at different lead times and uses them in a cascade of dynamic programming algorithms nested within one another.

However, unlike traditional approaches, the outer dynamic programming does not dictate the boundary conditions of the nested programmes, rather backwards chaining is used so that the inner programmes can select, or optimally match up to, the outer programmes.

Once the expected path taken by the river system is known, starting from the currently observed state and based upon forecasted rainfall and river flow scenarios, then the optimal operating policy can be derived, either the one which produces the lowest maximum flood damage, or the lowest total flood damage over the entire planning horizon. Again, this is achieved through the use of dynamic programming, and the steps involved here are intertwined with those which produce the expected path above.

6.3.5 Simplifying assumptions

The dykes are assumed to break as soon as the water level integral over some previous window of time exceeds a certain value, and are assumed to be overtopped when the streamflow exceeds some threshold. The only control available on the system is a simple determination of the proportion of upstream flow passed to the downstream part of the river and the canal. This has been programmed in a form suitable for the input of control policies derived from different sources, so that they can be compared in terms of total amount of water actually spilled in a long simulation.

The simplifying assumption is made that the flow from the upstream part of the river is divided between the canal and the lower part of the river in some ratio, and the level of the river upstream is beyond the scope of human control. This does not actually do justice to the intricacy of the control structures which are present on the Canale Napoleone, but has been made to simplify the mathematics, making the analysis tractable.

Damage to the dykes is considered a monotonic function of the integrated water level of the river over some previous window of time. Thus minimising dyke damage amounts to minimising the water level integral.

Also, in order to test any proposed control policy, a test-bed model river system is required on which the policy can be imposed, and which approximates the current operation of the Reno by the river authorities.

The test-bed model has an upstream and downstream river component, and where these meet a canal is available to take excess water. Rather than model the carrying ability of the canal separately, it is assumed to be a perfect vessel with dykes on either side, with the same mechanical properties as those on the lower river.

6.3.6 Transition probabilities between stream-flow states

The dynamic programming algorithm requires knowledge of transition probabilities between streamflow states. Since the records available for the case study catchment, the Reno, are no longer than three years, a long-term streamflow model is required which will describe the probability distribution, and ultimately the transition probability distribution, of the streamflow states.

The model developed was designed to reproduce explicitly an average streamflow, a daily cycle, a standard unit hydrograph, and an extreme runoff hydrograph, such as would be observed in time of flood. The model has been used to generate ten millennia of data, from which the transition probability matrices can be inferred.

6.3.7 Limitations and conclusions

While the theoretical basis of the model is believed to be correct, there is a serious implementation difficulty which prevents its immediate use and forbids proper evaluation of the consequences of the theory: the state variables used by the dynamic programming algorithm are the streamflow and the water level integral over some previous window of time in both the canal and the downstream river. The response of the river system to flood

waves implies a time-scale of around 15 minutes. But compared to this, the memory inherent in the dykes and the containing ability of the canal is very long, of the order of 1344 intervals, or two weeks. If these state variables are discretized, then it is found that the maximum river flow is not enough to produce, in one time-step, a large enough volume of water to cause a transition to occur in the water level integrals' states.

Thus the dynamic programming does not foresee any change in the strength of the dykes, hence will never anticipate breakage. It is not possible to resolve it simply by changing the scales of measurement. Thus the problem remains unresolved, and it is therefore not possible to make any recommendations as regards the operation of the Reno River system at this stage, other than to stay with the heuristic policy currently adopted by the Reno authorities.

Much discussion among the scientists on the AFORISM project has highlighted possible routes for the continuation of the pursuit of the optimal operating policy, namely to intertwine the considerations of the streamflow states and water level integral states in the dynamic programming scheme, and to work in continuous time. Both these suggestions merit further attention, but the goal of a truly optimal operating policy for the Reno system will remain elusive until a substantial amount of further original development has taken place.

Subsequent work should concentrate on the "heuristic operating policy". It should be modified in small ways in search of improvements. This would lead to recommendations about what the most significant (for better or for worse) modifications to the current policies are, and may come up with a significantly improved, almost optimal policy.

6.4 SYSTEM DESIGN - DYKE FAILURE

6.4.1 Dyke failure modes

Traditional flood control systems consider the height of the levee as the principal measure of flood protection. It has been observed by Wood (1977), however, that most flood control systems do not fail by overtopping but by structural weakness of the levee or the soil around it. The failure of levee systems has been divided into four common modes by

Bogardi et *al.* (1977):

- overtopping due to elevation of the water exceeding that of the levee,
- structural failure of the levee resulting from embankment failure,
- structural failure resulting from subsoil failure,
- wind wave action causing scour of the levee.

The system fails by the first occurrence of any one of the failure modes mentioned. Bogardi (1968) and Bogardi and Szidarovszky (1975) found that the duration of the flood above some critical discharge level affected levee resistance. It is possible to consider the levee resistance as a function of soil properties and through detailed modelling of the soil mechanics, a probability density function for the resistance could be found. Other parameters such as construction method, type of facing, and so forth could be included in the probability density function.

This study at Newcastle presents an objective function for the river/dyke system based on the above. It is demonstrated by running simulation experiments, that this alternative framework theoretically leads to a "better" flood protection policy, notwith standing the conclusions drawn in Section 6.3.7 above.

Only overtopping and infiltration collapse are considered below.

6.4.2 Minimization of dyke damage

The trade-off which must be reconciled in deriving the optimal policy is that between (a) passing the water off the land and to the sea as quickly as possible, and (b) holding the water back as much as possible so as to conserve the strength of the dykes for as long as possible.

The optimum policy is then the one which passes the most water to the sea before the dykes break.

The consequence of this would be two-fold:

- the frequency with which the dykes actually break would be reduced, and
- the amount of spillage after any breakage would be minimised.

It must be understood that when more water comes down from the upper Reno than can be carried by the canal and the lower part of the river, a flood is unavoidable under any operating policy. The policy described above, however, would ensure that the dykes remain intact for as long as possible before the breach is finally made.

6.4.3 Flood simulation using PAB

A flood routing program - PAB (Todini and Bossi, 1986) based on the parabolic approximation to the de Saint Venant partial differential equations for gradually varied unsteady flow in open channels is available to AFORISM. The advantages of the PAB procedure over alternative methods of unsteady flow simulation in an open channel are well known.

In this section a modified version of PAB is used so that its output relevant to the flood control operation of the Canale is available to the objective function which represents the flood control policy.

6.4.4 The Objective Function

A literature survey of current optimization models for surface water management revealed a shortage of methods that could be applied directly to rivers having no reservoirs. Where earth levees are employed as the protective mechanism against flooding, the emphasis has been on their elevation or on their structural resistance to the forces generated by the probable maximum flood.

The objective function adopted here considers a levee resistance based on the concept of a flood exposure index.

The Reno system states relevant to the proposed optimal flood control policy are

- the inflow forecast at Panfilia,
- the current water surface levels from Casalecchio to Bastia,
- the current storage level in the Canale Napoleone, and
- the proportion of diverted water eventually transferred to the river Po.

The cross-sectional configuration of streams and rivers in general are highly irregular. For the computation of flood losses, the cross-section is assumed to have a simplified and idealized geometry. The channel cross-sectional geometry and location of the levee are considered symmetrical to the centre of the channel.

It is assumed that the hydraulic characteristics of the reach are the same on both sides of the flood plain. If the capacity of the channel at a section is exceeded, overflow is assumed to be as serious as if it occurred on either levee. The associated loss is evaluated on the basis that the water surface elevation exceeds the safe elevation. This loss is accumulated over the flood forecast horizon T.

The weighted volume of water spilt is accumulated over the entire length of the river. The safe levee elevation need not be the maximum levee height. An allowance equal to a constant clearance can be assumed and a lower level specified.

The presence of water with a pressure head adjacent to a porous embankment, progressively increases the pore water pressure in the embankment medium due to seepage, with a corresponding reduction in its effective shear strength. The volume of water seeping into a porous medium is given by d'Arcy's relation.

6.4.5 Simulating the Current Policy

A pre-alert is issued when the water depth at Casalecchio is greater than 1.0 m. Flow rates exceeding 700 m^3/s at Panfilia are diverted into the Canale Napoleone if flow levels in the Po permit. The maximum rate of diversion is 500 m^3/s. In the unlikely event that the River Po is also in flood, then the maximum rate of diversion is reduced to 150 m^3/s as

flow is transferred to secondary canals in the system. The travel time of the flood wave from Casalecchio to Panfilia is 12 hours. The pre-alert is simulated by the pre-emptying of the Canale into the Po, which (on average) accepts the Reno flood 70% of the time.

6.4.6 Results and Discussion

Three schemes were devised and examined in detail in this study:

- A flood wave whose peak flow at Panfilia is less than 700 m^3/s (the critical value) is routed through the system and both the current and the proposed optimal policies are applied. This is a calibration exercise as no water should be introduced into the Canale with either policy;

- The same flood wave is routed through the system but the critical flow rate at Panfilia is assumed to be 200 m^3/s. The two policies are applied in turns;

- The flood wave which occurred in November 1990 and whose peak at Panfilia exceeded 700 m^3/s is routed through the system.

The outputs from the two modes of operation are compared on the basis of volume diverted and the period of diversion:

- The existing method of operation results in a strict limitation on the downstream discharge rate. The proposed policy is flexible, determining the downstream discharge rate at every time interval after considering the current levels in all 202 cross-sections.

- It is observed that the actual volume transferred to the canal is lower when the proposed policy is applied. This is considered beneficial because it uses the canal less frequently. Incipient problems of bed erosion upstream is thought to be connected to the frequency of use of the canal although the mechanism is not yet fully understood.

- The period of diversion is shorter with the proposed policy and starts earlier. The early start permits lower levels downstream which later permit higher releases.

- The total system losses, as defined above, over the simulation period are lower with the proposed policy. The new policy reduces the exposure of the dykes to the flood

water in any discrete period and over the whole flood duration. This reduces their risk of failure.

- For the two flood waves considered, the canal approached full capacity but did not fill up. In either case, only 70% of the volume diverted in every time step is eventually transferred to the Po.

6.4.7 Conclusions

The results of the simulations show that the objective function which considers the damage to the dykes as a function of the integrated water level of the river over some interval of time theoretically, leads to a superior method of operation them the heuristic rule however this observation is negated by the disappointing realisation that the chosen objective function is inappropriate in the context of the Reno. Should the method become feasiblen the application of this method in real time would require that flows for the upstream site of Casalecchio and all the confluence points be made available continuously to the real-time operator.

6.5 IMPACT ASSESSMENT MODELS

6.5.1 Methodology - GIS

The following methodology developed by EPFL-IATE at Lausanne has been used for flood impact assessment. The hydraulic model, which is a mixed one-and two-dimensional model developed at UNIBO-ICI and extended at EPFL-IATE, transforms flow forecasts into water surface elevations at any point in the study area. Flow magnitudes, velocities, directions and durations of submersion can also be computed at any location. On the basis of a DTM (Digital Terrain Model), the GIS (Geographical Information System) derives maps showing the spatial distribution of these hydraulic variables.

A pre-processing module extracts the parameter of interest for the particular damage assessment procedure. Direct flood damages to built-up areas are evaluated on the basis of

maximum instantaneous water depths. Indirect costs may also require the total duration of flooding. The danger of building instability may be evaluated with maximum flow velocities. Traffic disturbances require the location of road cut-offs where the depth of water prevents normal circulation. Agricultural damages are essentially related to the duration of submersion.

Combining the required flood map with land use information identifies the objects (plots, buildings, road stems, etc.) affected by flooding. Flood impacts on each object can be evaluated on the basis of social, environmental and economic criteria. Any change in the control strategy, such as source runoff control, implementation of a reservoir or canalization, modifies the flow forecasts and leads to a new flood impact map. An objective comparison of several flood control alternatives is therefore possible.

Various hydrologic and hydraulic models were used to compute flow forecasts and the spread of flooding respectively. These are external to the GIS framework. The results of the hydraulic calculations are imported into the database by means of adequate pre-processing interfaces.

The study started with the development of three prototypes for traffic networks, built-up areas and agriculture. The purpose of each prototype is to assess data requirements and accuracy. For instance, damages to agricultural practice can be evaluated for each plot individually or on the basis of homogeneous areas according to data availability. In the first case, the detailed cadastral survey is required while in the second damage figures can be worked out on the basis of representative areas where the same crop rotations are implemented. In Switzerland, the detailed location of each plot is available on a digital format. In other countries this information may be rather difficult to gather and it is preferable to start from the crop rotations which are easier to identify.

To ensure a large spectrum of applicability, it was decided that all prototypes should use different levels of data aggregation. The same applies to built-up areas or traffic network. In most countries detailed land occupation plans are seldom available. Field surveys and areal photograph interpretation generally involve prohibitive costs. Therefore it is preferable to work on the basis of land use plans to define average worth values for each land use category. For the traffic network, it is important to answer questions such as:

- Should one consider one or more links between departure and arrival points within the

road network? or

- Should one account for secondary and third class networks such as agricultural tracks?, etc.

The prototypes were developed to answer questions of this type. They were initially considered to be learning tools capable of increasing and improving experience and knowledge of the problem.

The prototypes were also used to compare, evaluate and develop damage assessment procedures on the basis of land use information and calculated hydraulic parameters. Available flood damage statistics are usually established after a specific flood episode. The relationship between hydraulic conditions and the amount of damages is a difficult task. For instance the destruction of a building may have occurred because of high erosion velocities at the basement level and/or unsustainable water depths. Agricultural damages are related to the type of crop flooded and the growth state of the plant. The spatial distribution of crops varies with time. Crop yield losses vary significantly from one season to another. For these reasons, it is felt that the extrapolation of damage statistics at a regional scale is questionable. On-site procedures are more suitable because they can be calibrated on the basis of past experience and local constraints.

Different GIS software systems were also compared. A combination of GIS systems is definitely required including a database system and both a raster and a vector oriented support. To develop the prototypes, simple and easy to use software systems were preferred; dBaseIV for the database management system, IDRISI for the raster GIS and MapInfo for the vector support were finally selected. All these packages run on personal computers under MSDos-Windows environments.

The prototypes were tested, modified and presented for illustrative purposes to concerned agencies and experts in the Basse Broye river region in Switzerland. Each time, the prototypes were improved to satisfy new requests or correct serious defects.

Once the acquired expertise and the knowledge about the problem were considered to be satisfactory, a Conceptual Data Model (CDM) was designed (Joerin, 1993). This CDM allowed one to organise the database and to manage the time evolution of the stored information. The CDM is independent of software and hardware specifics. It must be

regarded as the basis on which the system should be implemented in any GIS framework. The prototypes were also developed using standard GIS operators in order to ensure transportability to more sophisticated platforms. It is felt that any migration to a more powerful system will probably increase the performance of the system. Most powerful systems already include operators that had to be developed separately in the prototypes. However, in most cases the prototypes use commonly available GIS operators that can be found in practically every package available in the market.

A More Detailed Over view of the Flood Delineation and Impact Assessment Study

The remainder of Section 6.5 is extracted from the report by Joerin prepared as part of the EPFL-IATE contribution. A flood map is of little help to planners unless it is combined with land use information. It is not possible to assess flood impacts exclusively on the basis of flood delineation maps. A small extent flooding in an urban area may have larger impacts than submersions in rural areas covering much larger zones. Since the spatial distribution of crops varies from one growing season to another and the plant sensitivity to submersions varies within a single growing season, a static flood risk map will not provide the necessary information to properly assess flood damages to agricultural productivity. Similar considerations apply to road cut-off resulting from flooding because the related impacts may vary significantly with traffic density which is a function of time.

For the purpose of flood impact assessment a detailed description of land use is necessary. Such level of detail leads to large volumes of data space and time dependent. Consequently the application of Geographical Information Systems (GIS) is probably the best means to establish impact assessment maps. The spatial analysis tools included in a GIS are certainly capable of providing improved estimates of flood impacts.

Flood impact assessment is a multi-criteria problem. Flood impacts must be considered on an economic, social and environmental basis. Each one of this three components needs to be evaluated separately. Moreover, flood impacts need to be derived for each and every anthropogenic sector (traffic, agriculture, industrial areas, etc.). It is also noted that each individual sector will not be sensitive to the same hydraulic variables. Consequently, the assessment of flood impacts requires a large number of operations and important fluxes of data. It is obvious that such operations can only be done efficiently within a Data Base

Management System (DBMS) combined with a GIS to integrate the spatial component of the problem.

GIS and decision making processes is a promising research field. Chevallier (1994) proposed an integrated approach combining GIS capabilities and multi-criteria analysis within a common computer platform. He suggests using the GIS to simulate system states before and after any anthropogenic modification in a given territory. Several research efforts have also been directed towards identifying the ideal location for human infrastructures. Interesting studies related to land suitability evaluation can be found in Pereira and Duckstein (1993) and Eastman et al. (1993). However, very few applications of GIS technology to assess flood damages have been published. One important problem is that flood damage assessment methods (including economic, social and environmental impacts) are still approximate. Yevjevich (1992) indicates that only economic flood damages to built-up areas have been given full attention. They generally rely upon damage-stage curves resulting from post flood evaluations and various extrapolations according to land use characteristics (commercial, residential, etc.).

The objective of this study is to assess the potential applications of GIS technology to evaluate flood impacts in agricultural areas, built-up areas and traffic networks. This chapter will describe for each case the flood damage assessment procedures and their implementation within the selected GIS framework. The flood maps are established on the basis of the developed hydraulic model presented in the previous chapter. Applications of the GIS framework will also be illustrated by means of prototypes.

6.5.2 Methodology and study area

Figure 6.1 illustrates the overall methodology for flood impact assessment. The hydraulic model transforms flow forecasts into water surface elevations at any point in the study area. Flow magnitudes, velocities, directions and durations of submersion can also be computed at any location. On the basis of a DTM, the GIS derives maps showing the spatial distribution of these hydraulic variables. A pre-processing module extracts the parameter of interest for the particular damage assessment procedure. Direct flood damages to built-up areas are evaluated on the basis of maximum instantaneous water depths. Indirect costs may also require the total duration of flooding. The danger of

building instability may be evaluated with maximum flow velocities. Traffic disturbances require the location of road cut-offs where the depth of water prevents normal circulation. Agricultural damages are essentially related to the duration of submersion.

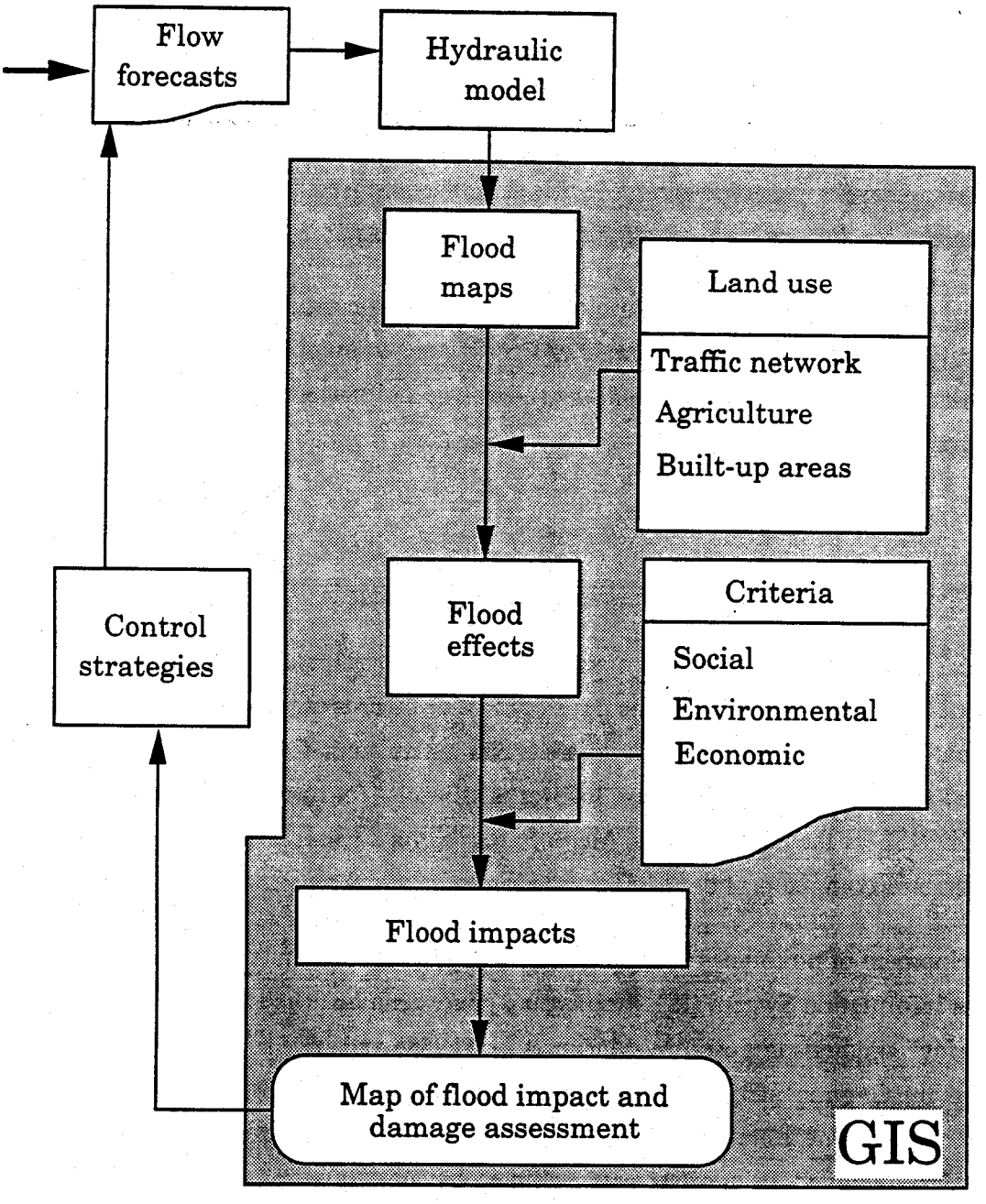

Figure 6.1 - Flood impact assessment methodological framework

Combining the required flood map with land use information identifies the objects (plots, buildings, road stems, etc.) affected by flooding (flood effect map). Flood impacts on each object can be evaluated on the basis of social, environmental and economic criteria. Any change on the control strategy modifies the flow forecasts and leads to a new flood impact map. In the framework of AFORISM, the proposed system should provide system operators with an objective comparison between possible control strategies in real time. From a planning point of view, the proposed methodology is still applicable and provides the necessary information to assess flood control measures (source runoff control, river reclamation, detention reservoirs, etc.). In this case, the proposed methodology should be seen as a valuable tool for land use planning and risk delineation.

Figure 6.1 also shows that the hydrologic and hydraulic models used to compute respectively flow forecasts and the spread of flooding are external to the GIS framework. The results of the hydraulic calculations are imported into the database by means of adequate pre-processing interfaces.

Development of prototypes

Figure 6.2 illustrates the approach to design the overall methodology shown in Figure 6.1. The study started with the development of three prototypes for flood impact assessment on traffic networks, built-up areas and agriculture. The prototypes has been developed with simple and easy to use softwares: dBaseIV for the database management system, IDRISI for the raster GIS and MapInfo for the vector support. All these packages run on personal computers under MsDos-Windows environments.

The development of prototypes is suggested by a large number of authors as a first step to design an Information System (IS). Prototyping phases can be found in the "Information Engineering" method proposed by Martin et al. (1988) and in the Modul-R approach described by Gagnon (1993). Three distinct approaches to develop prototypes are currently applied. These are the "Prototypage rapide", the "Prototypage Evolutif" and the "Double Prototypage". In the first approach the prototype is developed in the analysis phase before the system design and implementation. An iterative loop allows to evaluate and enhance the prototypes. In the second method, the prototype development and enhancement is achieved after the system design and directly leads to the implementation.

The third one is a combination of the first two. Burns et al. (1985) use two main criteria to define the adequate prototyping approach: the complexity and the uncertainty of the system to be designed.

The methodological framework of AFORISM is obviously complex and includes sophisticated operations with the data. The uncertainty is also significant mainly because the users of the AFORISM system are still to be determined and the functionalities of the overall framework might change according to the design stage. These considerations fully justify the development of prototypes and allow the selection of the approach called "propotypage rapide". Consequently, the prototypes presented hereafter have been developed with simple and user-friendly software. They allowed to design the Conceptual Data Model (CDM).

This prototyping phase allowed to easily analyse the different components of the AFORISM system with minimum efforts for data acquisition, for software manipulation and programming developments. The prototypes were also considered to be learning tools capable of increasing and improving our experience and knowledge of the problem. Consequently, the required data accuracy, the procedures, the type of software and the interfaces with the hydraulic model could be fully tested.

The prototypes were tested and demonstrated on a small portion of the Basse Broye river flood plain (~3 km^2) in Switzerland. The area is essentially drained by two rivers: the Petite-Glâne and the Fossé Neuf. The first one has a capacity of around 30 to 40 m^3/s while the second is able to convey some 5 to 10 m^3/s. Channel slopes are low, around 0.1%. Flood plain slopes are even lower. River banks are at higher elevation than the surrounding land. Flooding occurs by lateral spilling from the main channels. There is no evidence of dike failure problems.

Land use is essentially rural with relatively high profit margins. There are also a few isolated built-up areas and a quite complex traffic network with a high density of rural tracks for agricultural machinery. This extensive road network delineates low depression compartments in which flooded water may remain stagnant or overflow. The flood progresses by the sequential filling of juxtaposed compartments.

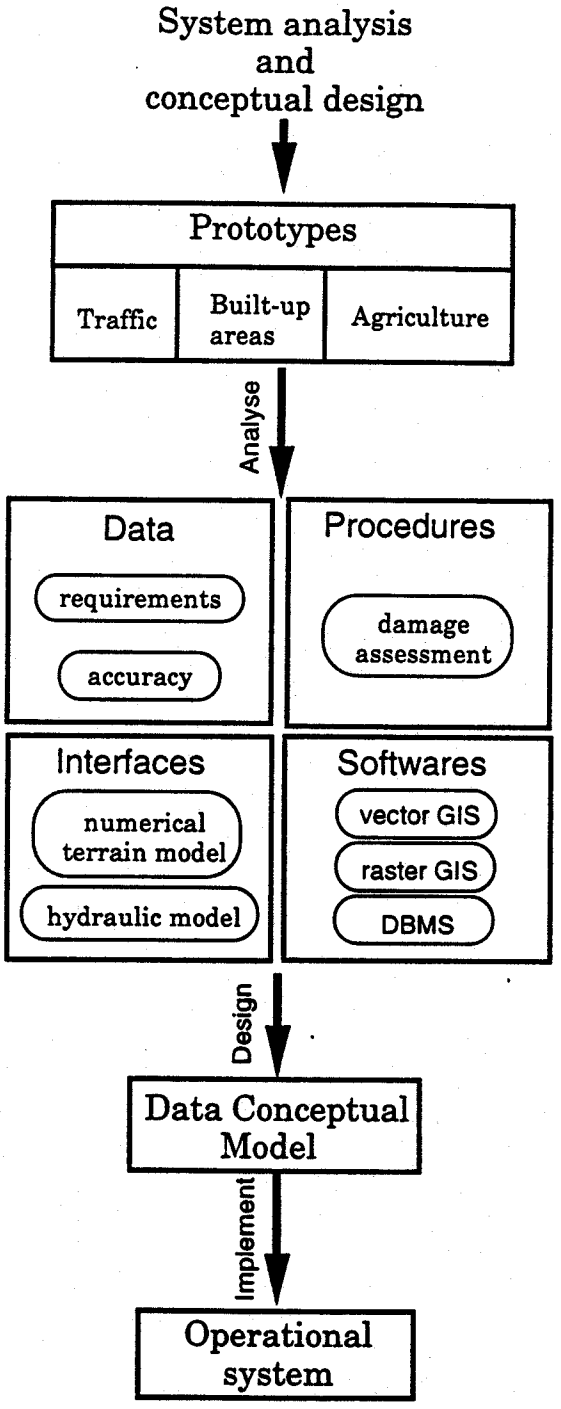

Figure 6.2 - Methodological approach for prototype development

Data

The prototypes allow to assess data requirements and accuracy. For instance, damages to agricultural practice can be evaluated for each plot individually or on the basis of homogeneous areas according to data availability. In the first case, the detailed cadastral survey is required while in the second damage figures can be worked out on the basis of representative areas where the same crop rotations are implemented. In Switzerland, the detailed location of each plot is available on a digital format. In other countries this information may be rather difficult to gather and it is preferable to start from the crop rotations which are easier to identify.

To ensure a large spectrum of applicability, it was decided that all prototypes should use different levels of data aggregation. The same applies to built-up areas or traffic network. In most countries detailed land occupation plans are seldom available. Field surveys and air photograph interpretation generally involve prohibitive costs. Therefore it is preferable to work on the basis of land use plans to define average worth values for each land use category.

Damage assessment procedures

The prototypes were also used to compare, evaluate and develop damage assessment procedures on the basis of land use information and calculated hydraulic parameters. Available flood damage statistics are usually established after a specific flood episode. The relationship between hydraulic conditions and the amount of damages is also difficult to establish. For instance the destruction of a building may have occurred because of high erosion velocities at the basement level and/or unsustainable water depths.

Agricultural damages are related to the type of crop flooded and the growth state of the plant. The spatial distribution of crops varies with time. Crop yield losses vary significantly from one season to another. For these reasons, it is felt that the extrapolation of damage statistics at a regional scale is questionable. On-site procedures are more suitable because they can be calibrated on the basis of past experience and local constraints.

For the traffic network, it is important to answer questions such as: a) should we consider one or various links between departure and arrival points within the road network? or b) should we account for secondary and third class networks like the agricultural tracks?, etc.

Softwares

Different GIS softwares were also compared. A combination of GIS systems is definitely required including a database system and both a raster and a vector oriented support. The prototypes were developed using standard GIS operators in order to ensure transportability to more sophisticated platforms. It is felt that any migration to a more powerful system will probably increase the performance of the system. Most powerful systems already include operators that had to be developed separately in the prototypes. However, in most cases the prototypes use commonly available GIS operators that can be found in practically every package available in the market.

Conceptual modeling

The prototypes were tested, modified and used as demonstrators for illustration purposes to concerned agencies and experts. Each time, the prototypes were improved to satisfy new requests or correct serious defects. Once the acquired expertise and knowledge about the problem were considered to be satisfactory, a Conceptual Data Model (CDM) was designed (Joerin, 1993). This CDM allowed to organise the database and to manage the time evolution of the stored information. The CDM is independent of software and hardware specificities. It must be regarded as the basis on which the system should be implemented in any GIS framework.

6.5.3. Interface with the hydraulic model

The used hydraulic model requires a particular discretization of the flooded area on the basis of polygonal cells derived from a Triangular Irregular Network (TIN) accounting

for structure lines and break lines. The present paragraph will briefly describe the interfaces between the GIS framework and the hydraulic model to derive flood maps. All GIS components, vector and raster, and the DBMS are required and interact between each other by several exchanges of information.

Figure 6.3 illustrates the interface between the GIS framework and the hydraulic model. The DBMS stores most of the input data required by the hydraulic model to route floods through the main channels and over the flood plain. These input parameters are stored in various tables within the DBMS and can be graphically displayed with the cartographic capabilities of a GIS. Moreover, modifications to subsets of input information in selected spatial locations are also possible.

The most important tables are those including the basic description of each polygon ("Polygons" table), the links between nodes ("Polygon links" table) and the water surface elevations for each polygon ("Polygon flooded" table). The table "Polygons" includes a polygon ID, the surface (S), the ground elevation (Zs) and the type indicating a flood plain polygon or a channel polygon. For the latter, cross section co-ordinates must be specified in the "X-Section" table. They are used by specific post-processors to derive the essential hydraulic characteristics (stage-discharge-area relationships, cross-section interpolations).

In the "Polygons" table shown in Figure 6.3, type "1" refers to a cross section while type "0" relates to a standard flood plain polygon. The table "Polygon links" stores all the connections between polygons including the distance between nodes (L) and the width of the interface (B). This table also contains the type of transmissivity equation to be used in the hydraulic model "FH". When FH=0 the shallow wave Manning equation must be used while FH=3 indicates that a weir flow equation has to be applied between nodes "2" and "8". The parameters required by specific hydraulic equations can be derived in most cases from the information stored in the tables "Polygons" and "Polygon links". The table "Polygon flooded" includes the information necessary for flood mapping, specially the water surface elevations computed by the hydraulic model at any time (t) and the depth of flooding (D). Other hydraulic variables like flow or velocity can also be included in a table similar to that describing the links between nodes. Specific post-processors for channel nodes have been developed to produce graphical cross-sectional and longitudinal profiles at desired locations.

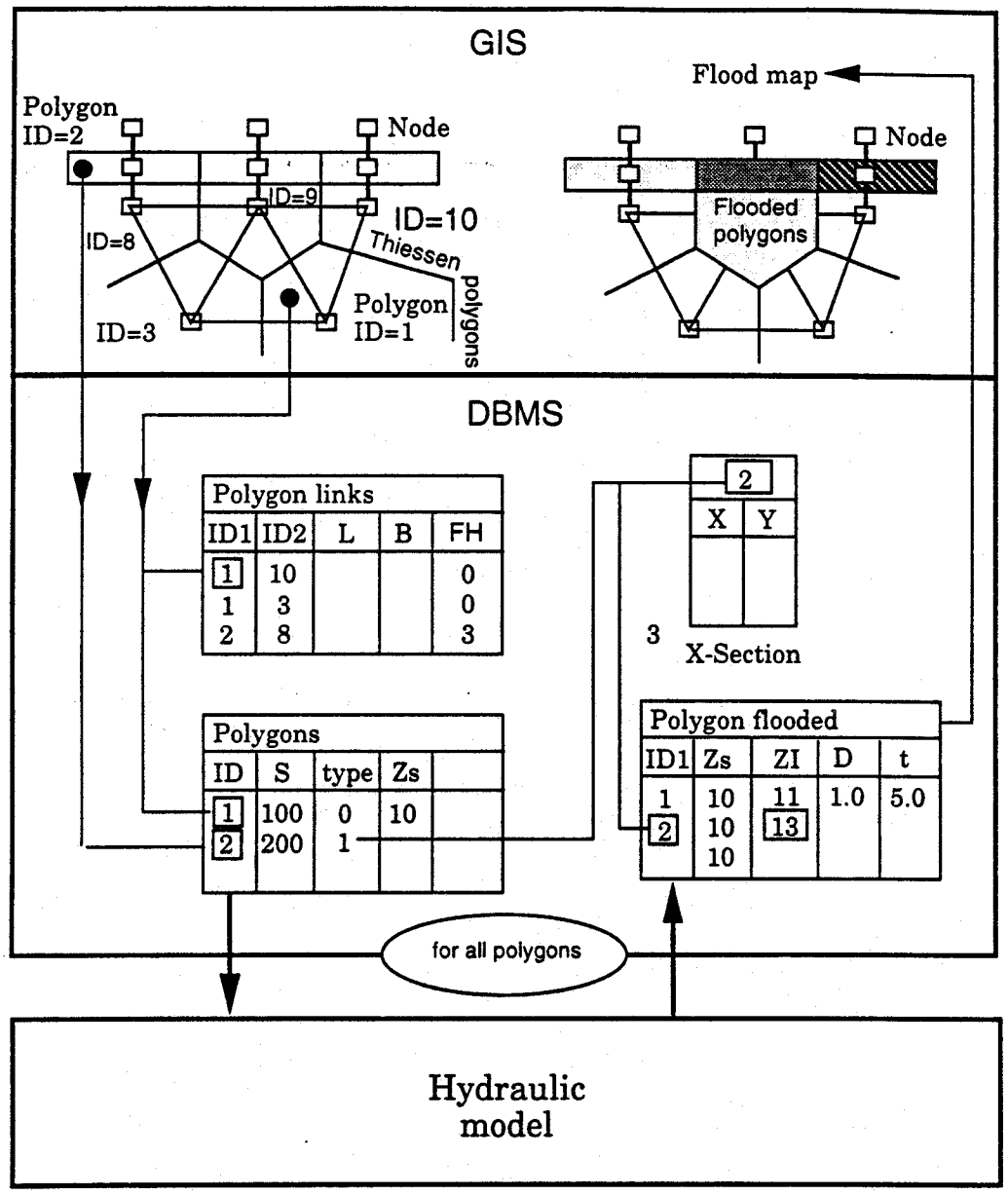

Figure 6.3 - Interface between the GIS framework and the hydraulic model

6.5.4 Flood Impacts and GIS Implementation

This paragraph describes for the three selected anthropogenic sectors: agriculture, built-up areas and traffic conditions, the proposed damage assessment procedure and the related implementation within the GIS framework. For the moment, damages are evaluated on an economic basis except for traffic conditions where the assessment of flood impacts required the development of a specific index.

6.5.4.1 Flood damages to agriculture

Flood damages to agriculture result from more or less prolonged submersion affecting the normal growth rate of plants. According to the period of flooding and the duration of submersion, the farmer may decide to accept either a partial, even complete damage or seed a replacement crop if the season and/or the soil conditions allow for it. The duration of submersion is defined as the time span between the beginning of flooding and the drying out of the soil. Until then, the soil and the plants may be damaged by labour or heavy machinery.

Evaluation of damages

The proposed damage assessment procedure can be applied to a wide variety of agricultural schemes in humid temperate climates. However, yield losses and economic figures result from on site inquiries involving local farmer associations in the Basse Broye region (Consuegra, 1992). It was then possible to identify crop types, rotation characteristics and to draw a map indicating the areas where similar crop rotations are followed. Profit margins and yield losses could also be estimated from local sources of information.

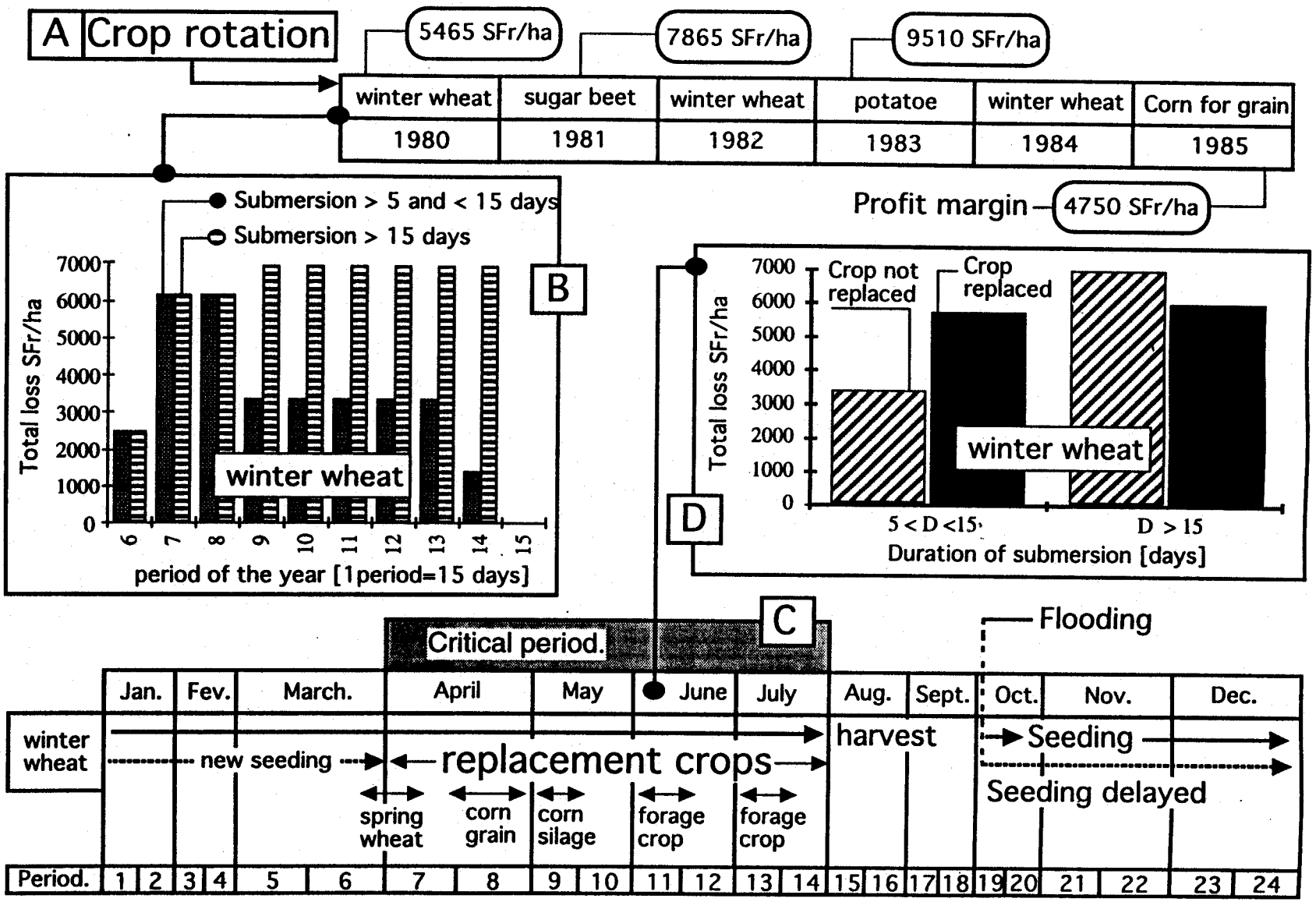

Figure 6.4 Damage evaluation for agricultural areas. Crop rotations (A), sensitivity to flooding (B), replacement crops (C), comparison of yield losses with and without replacement (D).

Crop rotations and crop sensitivity

Figure 6.4a shows a typical crop rotation in the study area. The cycle covers a period of 6 years. At a given plot, winter wheat will be followed next year by sugar beet and by winter wheat again two years later. Winter wheat is then followed by potatoes, winter wheat again and finally corn for grain. The profit margins for each individual crop are also shown. This crop rotation corresponds to average weather conditions and guarantees adequate overall profit margins. The crop sensitivity changes during the growing season from seeding to harvest periods. For each single type of crop, the total damages were estimated on the basis of the duration of submersion and the period of the year. For instance, Figure 6.4b shows the time evolution of total losses for winter wheat according to the season and the duration of submersion without considering replacement options.

Damages have been assigned to the period where the flooding occurs even if the consequences may appear later during the year (indirect costs). For durations between 5 and 15 days the crop sensitivity is higher at the beginning of the growing season and decreases until harvest. From April to harvest, durations of submersion higher than 15 days lead to a total loss equivalent to the gross product. The latter includes profit margin, seeding and soil treatment expenses, marginal fees as well as indirect costs, which vary from one season to another.

Seeding delays and crop replacements

Flood damage computations must also account for eventual replacement crops which are intended to minimise yield losses. Flooding in the study area does not occur, on average, more than once a year. More frequent flooding would prevent economically feasible agricultural practice. For this reason, the crop replacement policy shown in Figure 6.4c can only be derived on the basis of one single flooding event per year. However, there are no restrictions regarding the period of occurrence of submersions. Obviously, each crop replacement is associated with a yield loss. The growth cycle of winter wheat in the study area starts at the beginning of October (seeding) and finishes at the end of July (harvest). If winter wheat seeding was done in normal conditions the crop will be sensitive to submersions from the beginning of April until harvest (critical period in Figure 6.4c).

Submersion durations higher than 5 days between October and March will postpone

sowing to the end of March or the beginning of April at the latest. Related yield losses are equivalent to 30% of the profit margin plus the re-seeding expenses. During the critical period, seeding of winter wheat can not be postponed and farmers in the study area have to implement a replacement crop. During the first two weeks of April, submersion for a duration between 5 and 15 days will ruin the winter wheat seeded in October and force replacement with corn for grain sowed during the last two weeks of the same month. During the second fortnight of April, submersion durations higher than 5 days will force the replacement of the crop and the seeding of corn for silage in early May. During the month of April, submersions no longer than 5 days will not generate substantial yield losses. Figure 6.4c illustrates the remaining crop replacement options until the harvest period. It is always necessary to compare the damages to the actual plant with those involved with the crop replacement. Figure 6.4d shows that for winter wheat and submersions between 5 and 15 days, the farmer will prefer to sustain losses instead of sowing a forage crop. A different decision will be taken for submersions higher than 15 days.

GIS implementation

Figure 6.5 illustrates the overall set-up within the GIS framework of the flood impact methodology. The procedure requires the flood map describing the duration of flooding for each polygon and that showing the spatial distribution of individual crops. Both maps are on a vector format. However a raster support can also be used. In the DBMS, the following tables are also needed: a) the "Plot" table describing for each plot the current crop in the field and b) the "Potential Losses" table indicating the yield losses per hectare for each crop type and for several submersion durations at the moment of flooding. The "Potential Losses" table includes yield losses for both the replacement and the no replacement options. The "Plot" table is updated at the beginning of each agricultural season. For each plot, the crop type is determined according to rotation rules similar to that shown in Figure 6.4a. The "Potential Losses" table is updated every 15 days to follow the evolution of crop sensitivity to flooding.

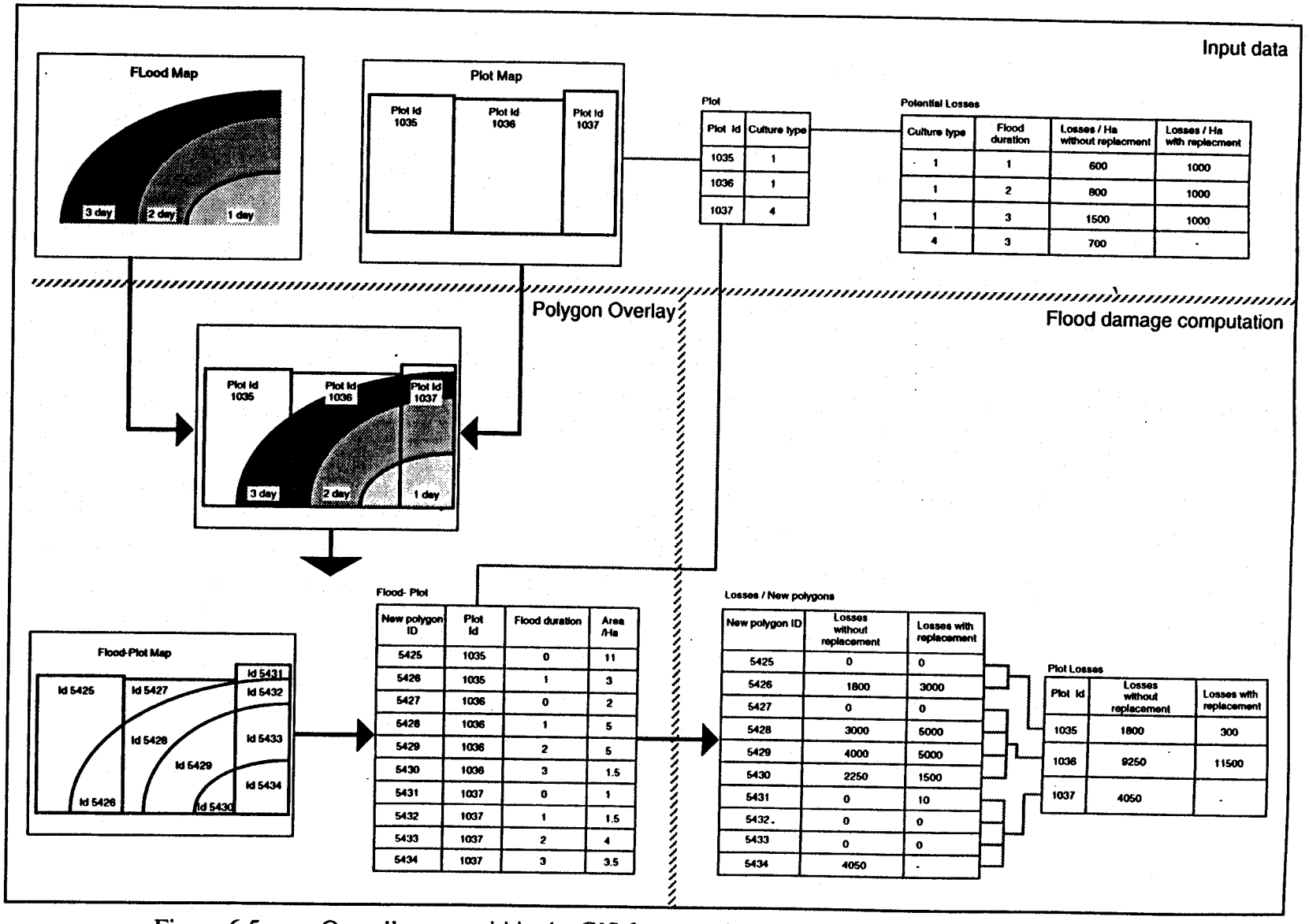

Figure 6.5 Overall set up within the GIS framework to assess flood damages to agriculture. Polygon overlay operations, relational tables, input data and resulting yield loss estimates

The procedure starts with a "polygon overlay" operation between the map showing the durations of submersions for each control volume and that describing the spatial distribution of plots and crop types. Each plot will be broken down into smaller polygons covered by one single duration of submersion. For instance, figure 6.5 shows that plot # 1035 will be broken down into two polygons # 5425 and # 5426. Polygon # 5425 corresponds to the non flooded surface of plot # 1035 while polygon # 5426 relates to the surface of that same plot which is submerged for 3 days.

This splitting procedure leads to a new table "Flood-Plot" indicating the number of the newly created polygons, the plot number to which it belongs, the corresponding submersion duration and the area flooded. The "polygon overlay" operation can be done on both the raster and the vector GIS. Since the available MapInfo version does not have this option, the prototype uses IDRISI for this purpose.

The computation of flood damages uses the "Flood-Plot" table as the main source of information and is entirely achieved within the DBMS. For each newly created polygon (# 5425 for instance) and on the basis of the plot identifier (ex: #1035) it is possible to find the crop type on the field at the beginning of flooding in table "Plot". On the basis of the crop identifier, the duration of submersion and the surface flooded, damages can be computed with the information included in table "Potential losses".

Computations are done for both the replacement and the no crop replacement options. The resulting economic damages are stored in the "Losses-New Polygons" table (Figure 6.5). To obtain the flood damages for each plot (#1035) it is necessary to cumulate economic losses for all the corresponding sub-polygons (# 5425, 5426, etc.).

The results are stored in the "Plot-Losses" table for both the replacement and the no replacement options. The cheapest alternative is selected. In case of replacement, it is assumed that the entire plot surface will be seeded again with the new crop.

Flood damages to all plots can be easily mapped with the vector GIS. Figure 6.6 illustrates a typical output from MapInfo. The first map illustrates the spatial distribution of plots and crop types. Polygonal lines indicate the limits of the plots while the colours relate to a particular crop type. The flood map with the duration of submersions has been overlaid. Dark blue indicates long duration of flooding while the lighter shades correspond to shorter submersions.

The second map illustrates the spatial distribution of flood damages. The green parcels present low damages, the blue ones moderate losses and the red ones sustain the largest destructions. Interactive query information can be gathered directly from the second map to visualise the calculated flood damages for each single plot.

6.5.4.2 Flood damages to built-up areas

Evaluation of damages

Economic damages to buildings are based upon standard stage-damage relations similar to that shown in Figure 6.7. These relations only consider submersion effects and do not account for nearby velocities or debris transport which may be an important cause of destruction. The relationship between these hydraulic variables and the economical damages are not easy to establish (Torterotot, 1994). However, if future studies derive such kind of relations, it will be relatively easy to include them in the prototype described hereafter. The flood damage computation is based on a evaluation of the depth of water around each building ("Height of submersion"). If this value is higher than a critical height, the building is completely destroyed. Losses are equal to the value of the structure and that of the building content. If the water depth is less than the critical value, losses are proportional to the value of the building content. The exponent "a" allows to parameterise the stage-damage relation according to the building type. If $a<1$ small flood depths will be strongly penalised while $a>1$ indicates that the expensive contents of the building are located in the upper stories.

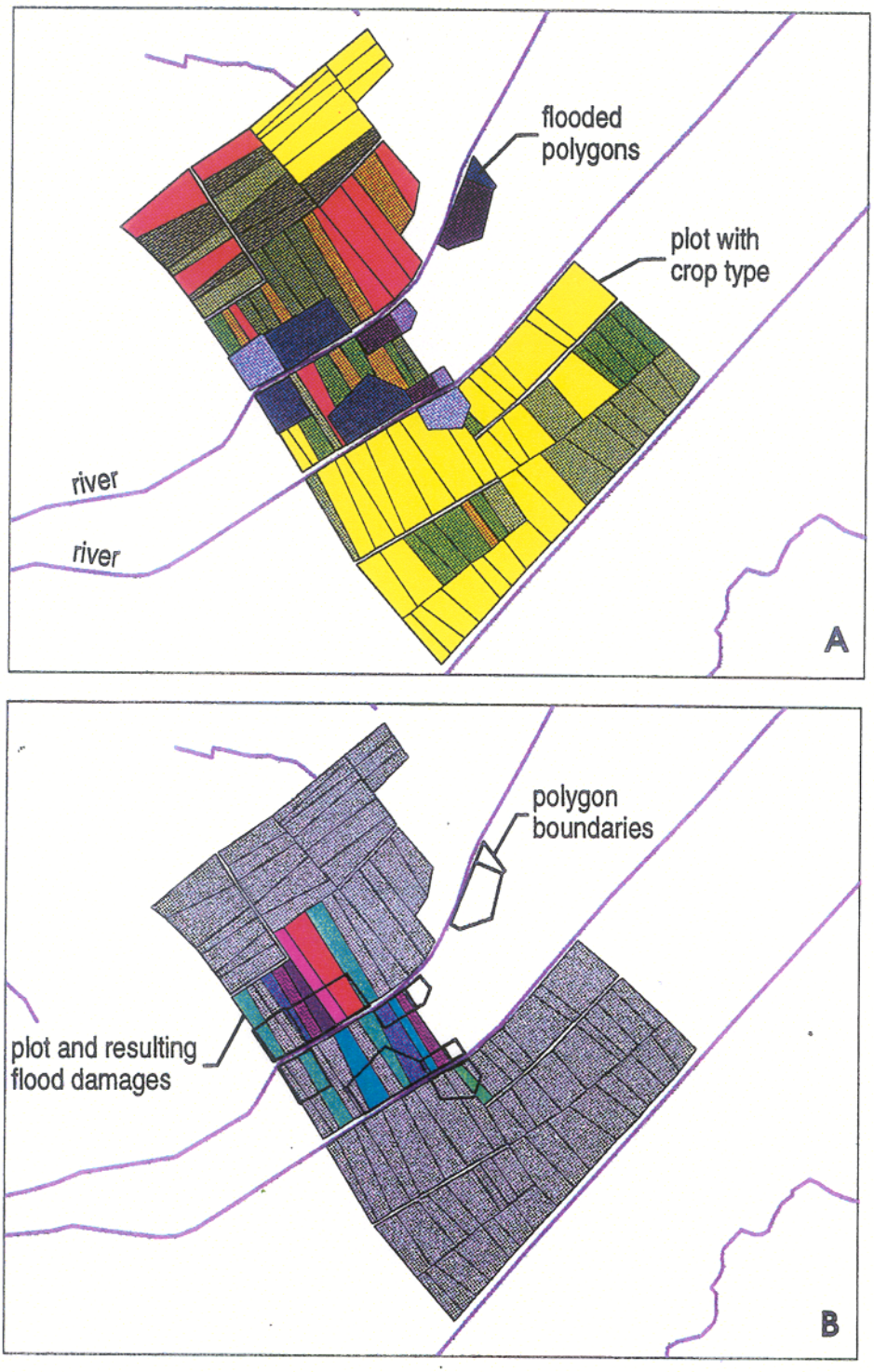

Figure 6.6 MapInfo outputs illustrating the duration of flooding for concerned polygons, the plot and crop type spatial distribution on the resulting yield losses.

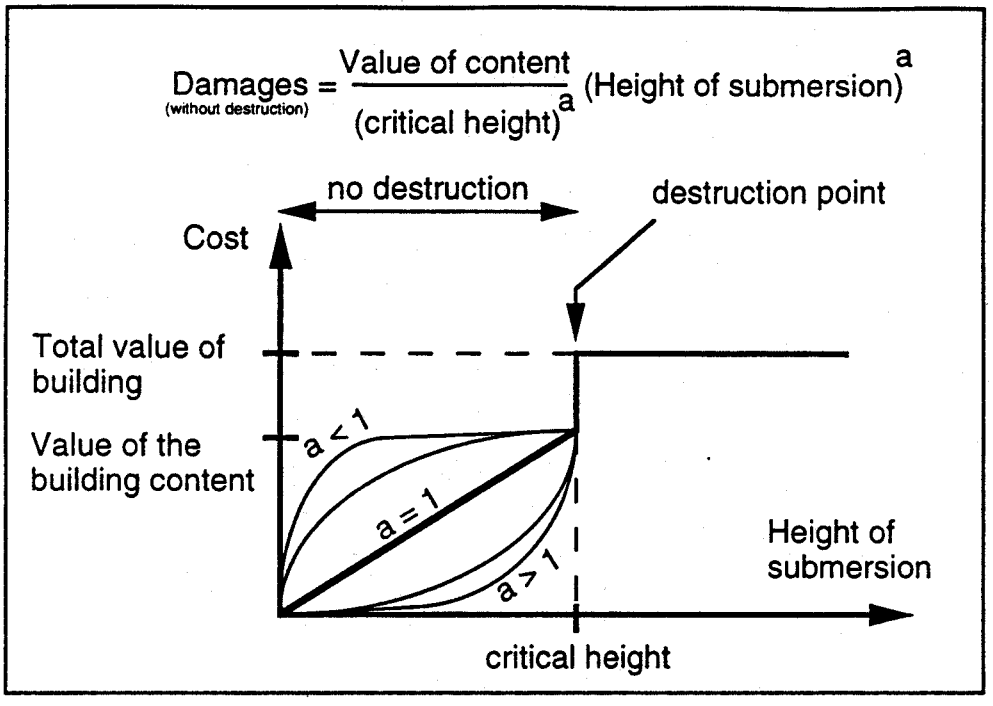

Figure 6.7 - Typical stage-damage relation for built-up areas

GIS implementation

For a given flood episode, the pre-processing routine in the DBMS identifies for each node the maximum water depth during the entire flood event. This information is transferred to the GIS to produce a map showing the spatial distribution of maximum water surface elevations. Figure 6.8 illustrates the subsequent operations to assess flood impacts on built-up areas.

The flood map mentioned above is first overlaid with that delineating the boundaries of individual buildings (Building map) to identify all the constructions affected by flooding (Buildings and Flood map in Figure 6.8). The GIS is then able to compute the average depth over the surface covered by each single building. This information is stored in the "Building and flood depths" table.

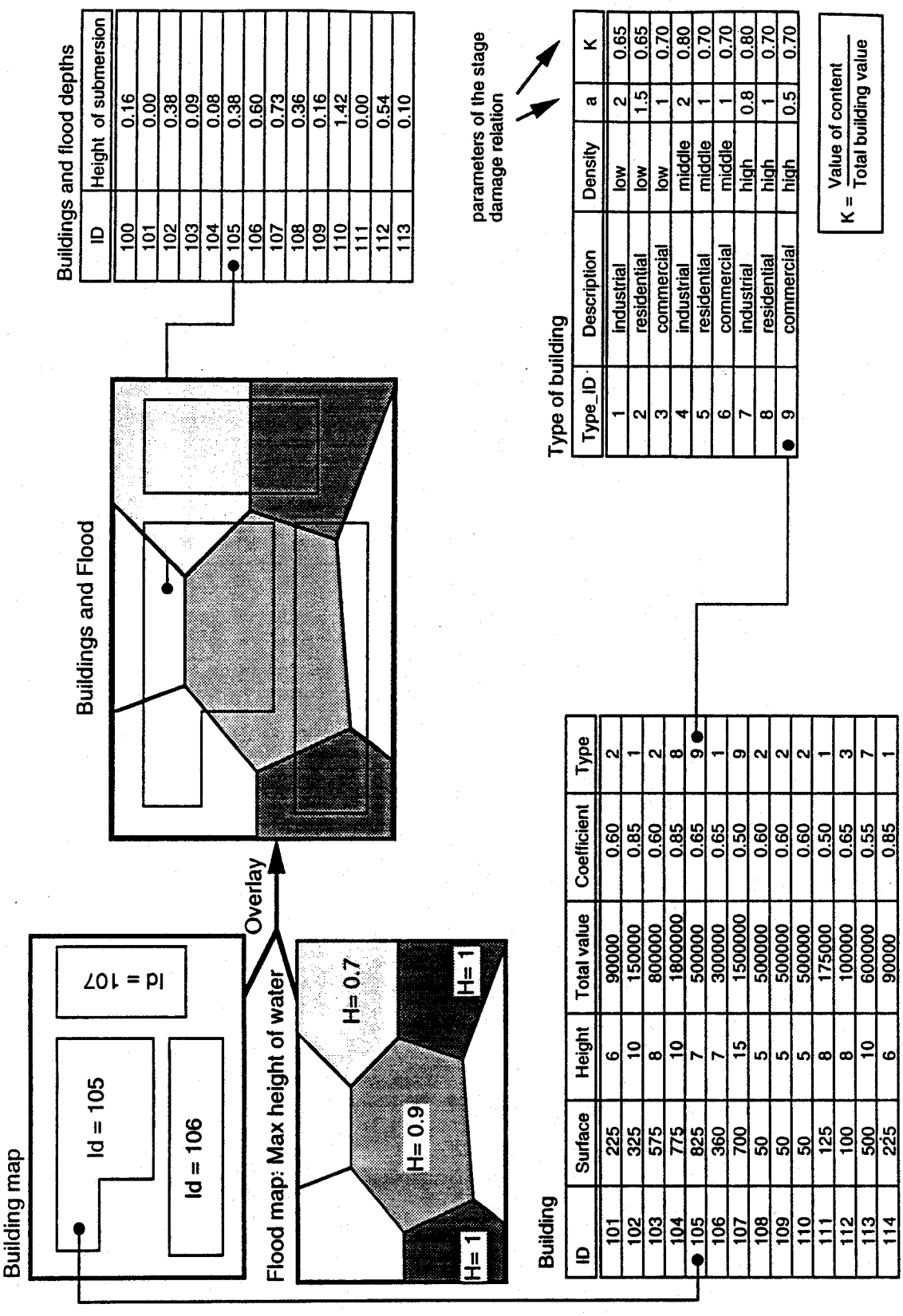

Figure 6.8 Operations within the GIS framework to assess flood damages to built-up areas.

In this example, the building #105 is partially flooded. According to the "Building" and the "Type of building" tables, building #105 belongs to a commercial area and the corresponding stage-damage relation can be approximated by a polynomial equation in which the exponent "a" is equal to 0.5. Using the "Type of building" and the "Building and flood depths" tables damages can be computed for each single building. These damages are then transferred to the GIS to produce a map showing the spatial distribution of economic losses. Cumulating individual damages leads to the global economic flood impact on built-up areas.

Typical output maps produced by IDRISI are shown in figure 6.9. Figure 6.9a shows the spatial variability of maximum depths for each polygon and indicates all the buildings affected by flooding. Figure 6.9b illustrates the resulting damages expressed as a function of the total value of each single concerned building.

6.5.4.3 Flood impact on traffic conditions

Traffic damages relate to flow interruptions and to reduced circulation speeds. In case of road cut-off, the search for the fastest alternative path between two points is definitely an important question for rescue services. For the purpose of AFORISM it is also required to derive an overall index representing the spatial distribution of traffic density resulting from road cut-off. These evaluations can be done on the basis of minimum travel times between departure and arrival points in the road network (Dopt).

The road network is subdivided into a series of stems (Figure 6.10). A stem represents a piece of road between to cross-roads. Each stem can be characterised by a travel time according to traffic conditions and speed limits. The network analysis operators in the GIS system allow to determine the fastest link between two connected points which are typically considered to be major urban agglomerations (Figure 6.10).

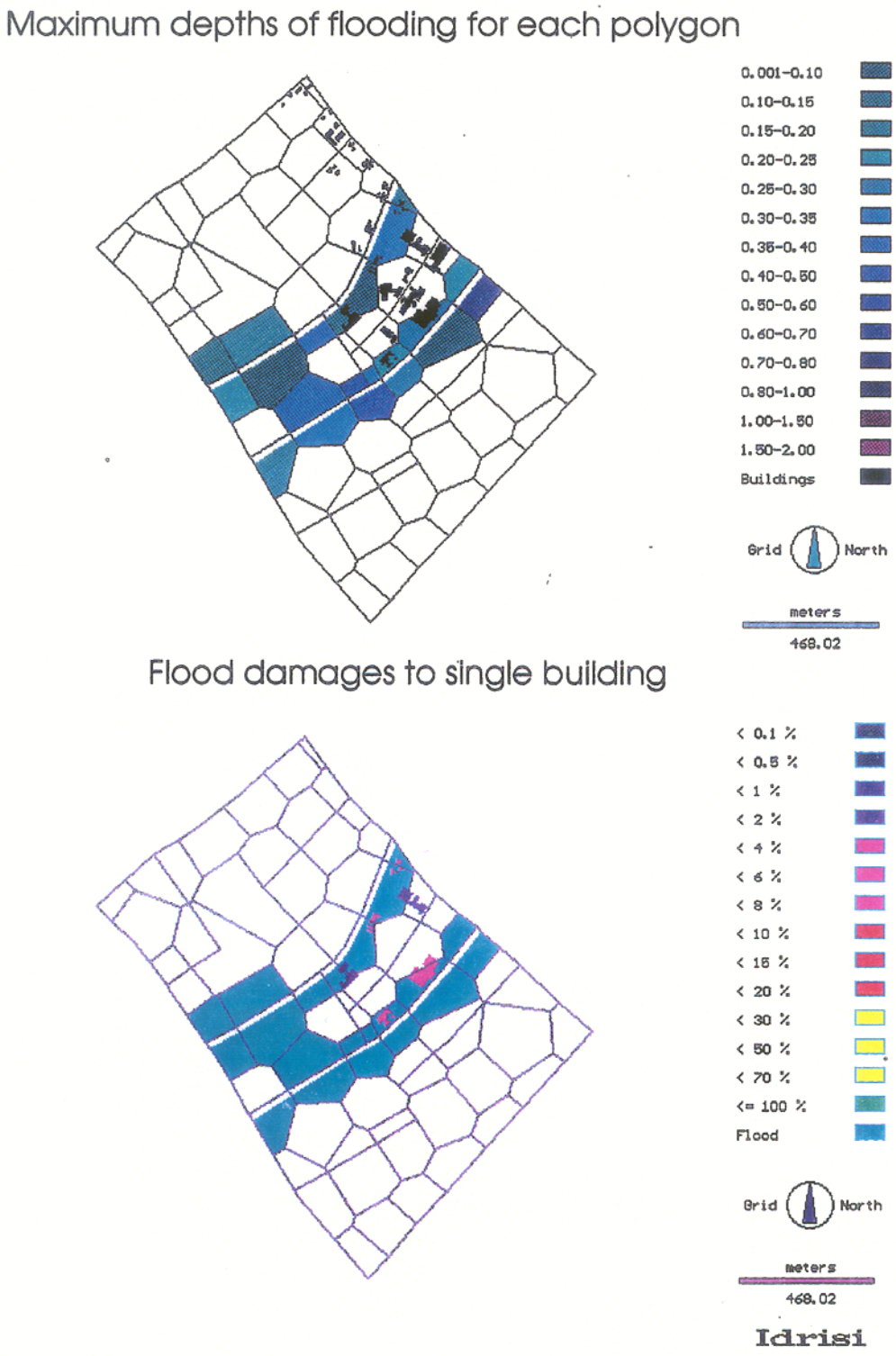

Figure 6.9 Typical IDRISI output maps showing the maximum water depths for all polygons and the resulting flood damages to single buildings

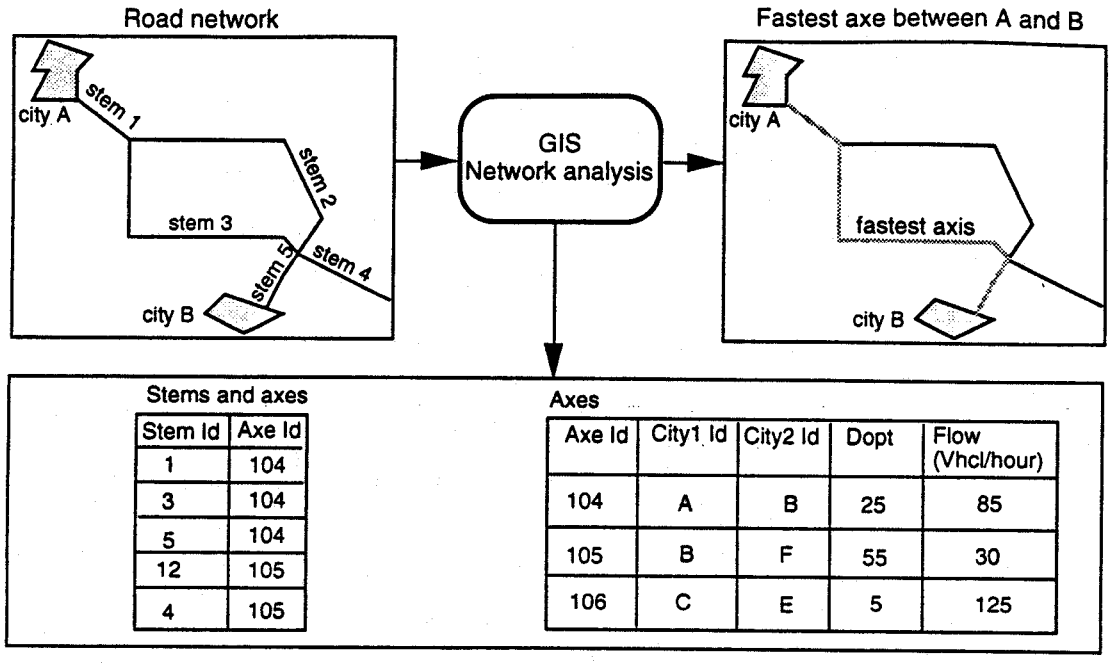

Figure 6.10 - Description of toad network in the GIS framework

The set of stems describing fastest links between two cities is called an axis (table "Stems and axes" in Figure 6.10). Theses axes are also characterised by an average daily traffic flow derived from regional development plans commonly available in Switzerland (table "Axes" in figure 6.10). The proposed methodology assumes that travel times are equal in both directions of circulation. The average flow per axis is equal to the sum of those in each traffic direction.

In case of flooding, the system identifies the road sections where circulation is no longer possible. Traffic cut-off occurs if the depth of submersion on the road is higher than a given value and lasts longer than a pre-specified interval.

For selected departure and destination points, the system re-computes new travel times and identifies the fastest links between connected cities. For each axis the impact of flooding on traffic flow can be computed with the following formula:

$$N = \left(1 - \frac{Dopt}{Dino}\right) F.D \qquad (6.1)$$

where Dino is the travel time in case of flooding, F is the average vehicle flow in normal conditions and D the duration of flooding. N is computed for each axis. It represents the number of vehicles that could not reach destination during the flooding period. If N=0, the axis is not concerned with flooding. The maximum value of N is equal to FD indicating that the axis between the two concerned cities can not be used during the entire flooding duration.

The overall impact of flooding is derived by cumulating the individual values of N for each axis. The system will also compute the new spatial distribution of traffic density resulting from flooding. This allows to identify overloaded stems and to suggest alternative paths.

Figure 6.11a illustrates the database architecture to identify the major axis concerned with traffic cut off due to flooding.

Two cities are connected by one single axis (the fastest one). The latter is described by the attributes shown in table "axes". The fastest travel time (Dopt) is determined within IDRISI using the COST and PATHWAY functions. COST computes travel times from a given origin to all destination points. PATHWAY identifies the fastest paths between selected departure and arrival points. The stems corresponding to a given axis are stored in table "Stems-axes". If flooding prevents normal circulation through a given stem (table "Flooded-stems" coming from IDRISI), dBaseIV looks for all the concerned axes in table "SStems-axes". For each selected axis, the concerned cities can be found in table "Links-Cities". City and axes identifiers are stored in table "Concerned axes".

For each disturbed axis, IDRISI calculates the new fastest travel times (Dino) in a similar manner as that used to compute Dopt and stores the results in the table "New travel time" shown in figure 6.11b. With query type operations, dBaseIV finds in table "Axes" traffic flow and Dopt for all concerned axes and calculates the effects on traffic flow (N) according to equation (6.1). For each single axis, the corresponding value of N is stored in the table "Impact on axis". The new spatial distribution of traffic is computed by cumulating for each single stem the vehicle flow of all axes passing through it. Figure 6.12 shows a typical output produced by IDRISI comparing traffic densities for both normal and flooding conditions.

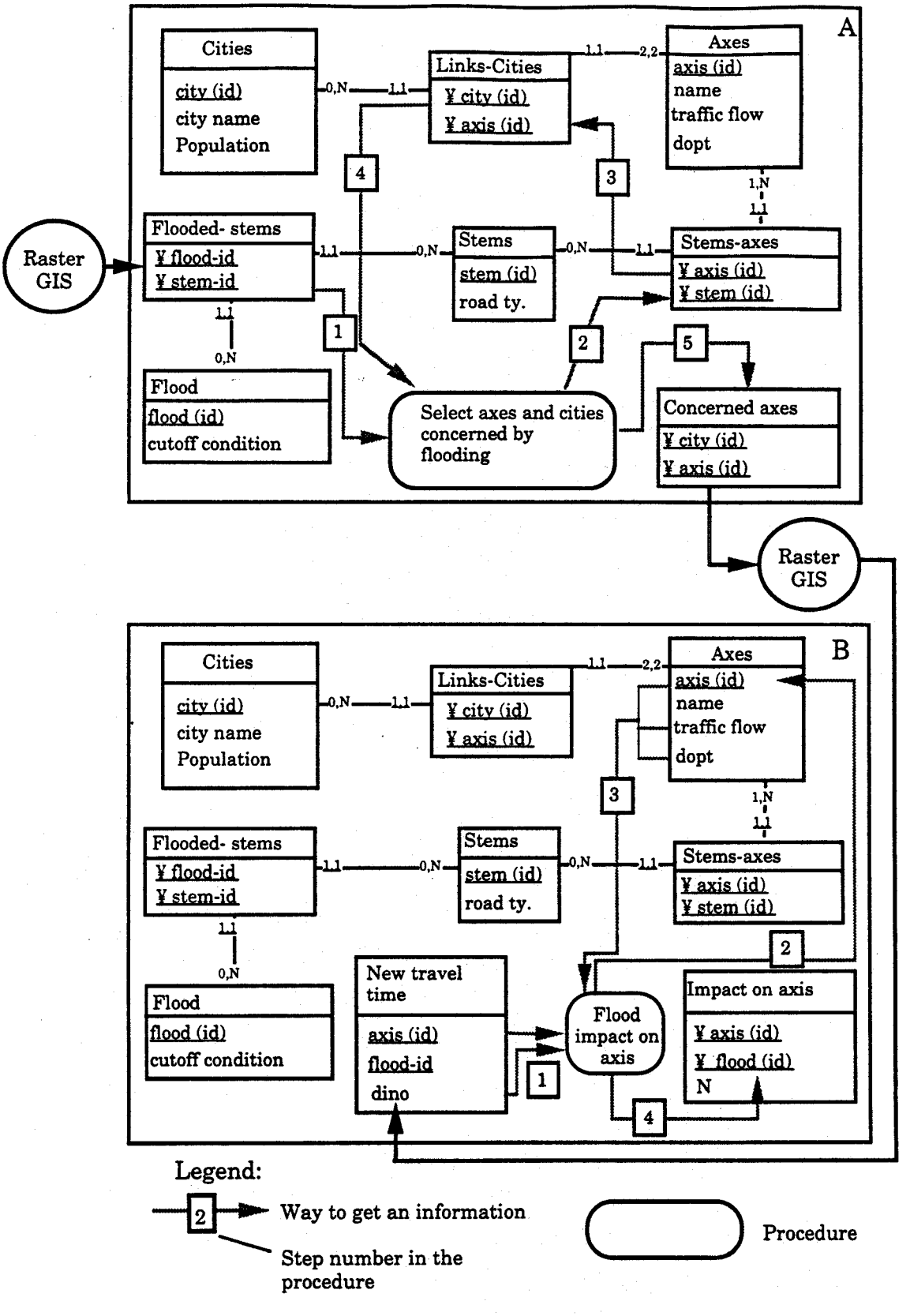

Figure 6.11 Logical data model and procedures to assess flood impacts on traffic conditions

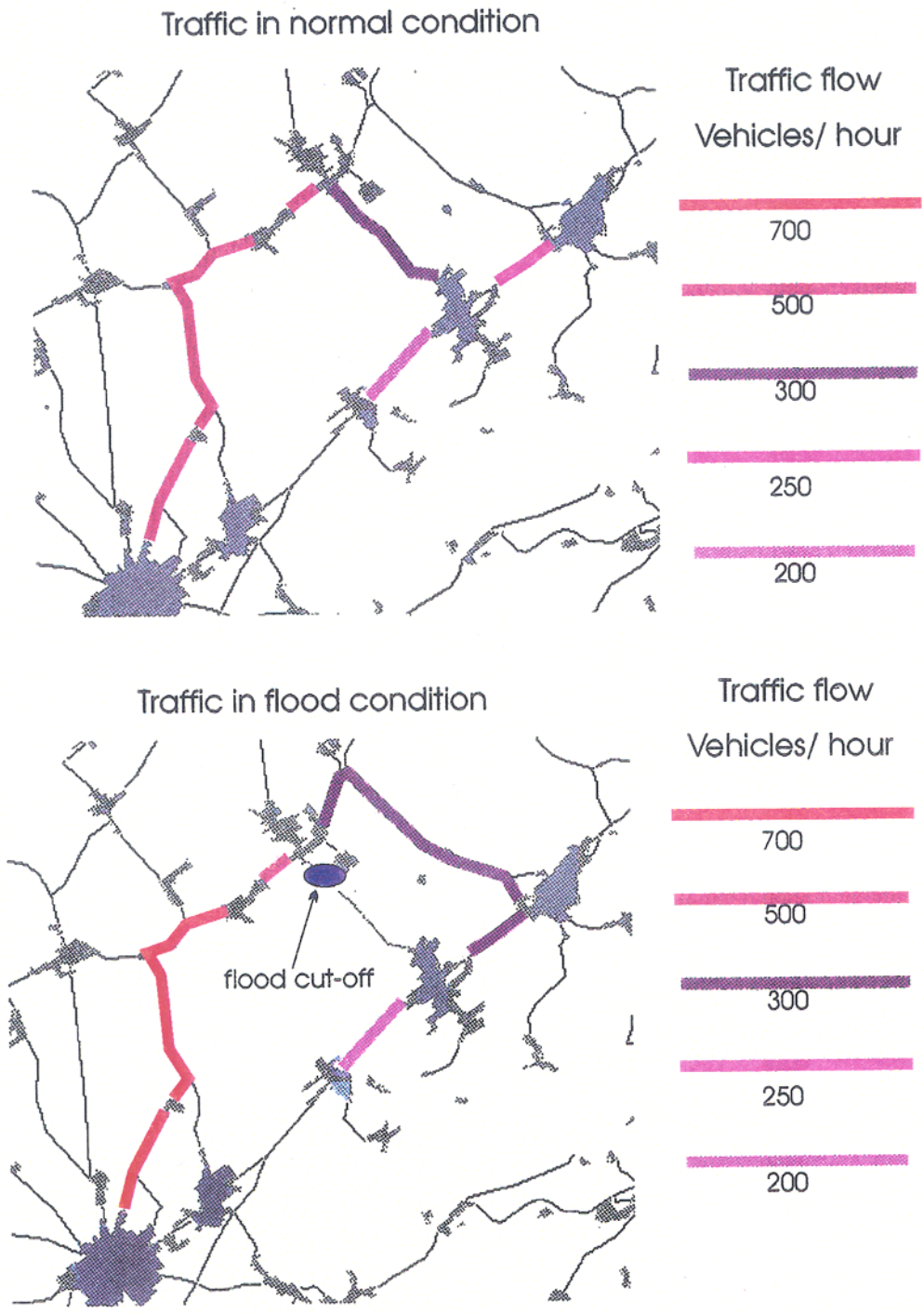

Figure 6.12 IDRISI outputs comparing traffic densities for normal and flooding conditions

6.5.5. Data Base Requirements

The GIS system required by the AFORISM framework presents a wide spectrum of utilities. First, the system manages the data required by the hydraulic model. The Data Base Management System (DBMS) must provide updated information describing the state of the hydraulic network when a flood forecasting is issued. Moreover, the stored information should be updated when modifications of land use occur or when new hydraulic structures may be implemented.

6.5.5.1 Dynamic Modeling

The dynamic component of the DBMS and that of the GIS framework is evident. A first data flux occurs when the GIS provides the parameters required by the hydraulic model. The results are then returned to the GIS to produce flood maps. Flood maps are subsequently combined with land use information to derive flood effects and finally flood impacts. Such operations produce new types of information composed of spatially variable numerical damage evaluations to be used in the decision making process. If we consider that all these operations have to be done to evaluate several control strategies, it is easy to realise that the management of such data fluxes is not an easy task. The main dangers of such a dynamic data base are to corrupt the data base because of inadequate updates, to loose data and/or to use the wrong information for a given type of operation.

To model the dynamic character of the database, we propose to use the static and dynamic conceptual approach REMORA (Rolland et al. 1988). This method is based on three concepts linked together with three relationships. Those concepts are "objects, "events", and "operations". The relationships which link them are "an event activates an operation", "an operation modifies an object", and "an object modification is noticed by an event" (Figure 6.13). Using those three concepts, the database evolution can be modeled and managed. The dynamic conceptual model illustrates for all events which updating operation(s) have to be activated, and which object(s) will be modified. A simple example is shown in Figure 6.14.

These concepts have been implemented within AFORISM and the related implications can be found in Joerin (1993). For illustration purposes, the dynamic component will be described hereafter in conjunction with the evaluation of flood impacts to agricultural practice.

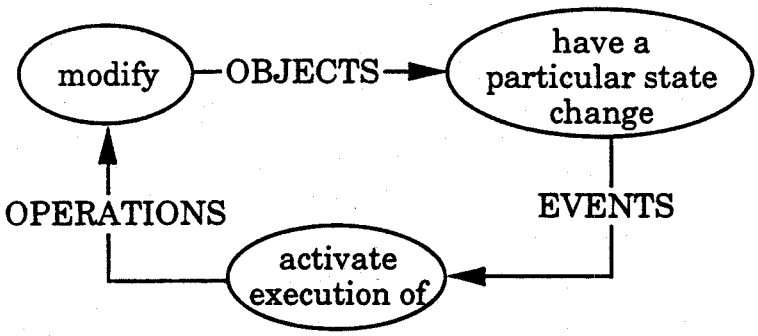

Figure 6.13 - Concepts used for dynamic modelling

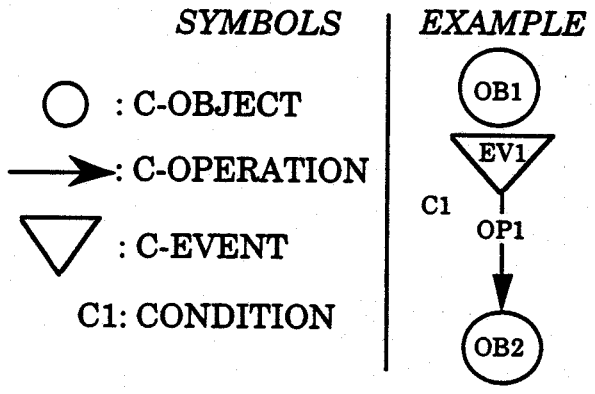

Figure 6.14 - Symbols for dynamic modelling

6.5.5.2 Integration of the Dynamic aspect in the Database

In the context of agricultural practice, time may be represented by the following hierarchy of events (Figure 6.15). First, time is constituted by a sequence of crop seasons (Sc). Each crop season begins with a winter season, during which farming is limited to field work. Then, as spring approaches, the agricultural activity starts (A) and crops grow. When a crop reaches the optimal state of growth, it is harvested (H). This period is critical, because at that time crops have the greatest worth. Finally, after the harvest, new crops are sowed and the spatial distribution of crops is again modified (S). Crop season duration is not fixed. Indeed, it depends on the region's climate and the specific meteorological conditions of the period. In Switzerland, a crop season lasts for one year, in warmer countries its duration can be just a few months. Moreover, the harvest period might be delayed for a few weeks if meteorological conditions are not favourable. Nevertheless, the proposed time structure is not modified by these fluctuations because the sequence of events is always the same.

This illustrates the interest of a time reference system that is not based on exact time positioning. It is worth noting that this time perception is well suited to a non gradual evolution (with abrupt changes), but not to a phenomena presenting gradual changes like crop sensitivity to flooding. Crop sensitivity is of interest during the agricultural activity period (A). To follow this gradual behaviour, it is necessary to discretize the time evolution of crop sensitivity and define each interval as a pseudo-event. This concept is illustrated in Figure 6.16. This may not be the optimal solution since it is not always easy to define events on the basis of a gradual evolution of a given phenomena. Using this hierarchical time structure it becomes possible to clearly identify the most important events, which will determine the evolution of the geographical database. Each of those events correspond to a modification in the real world. Obviously the database needs to be modified accordingly, this is achieved using updating operations.

Modifications resulting from operations are governed by rules. In this application, three rules determine the database evolution. The first expresses the rotation process, the second models the crop sensitivity evolution, while the last manages the replacements of crops after a flood. Figure 6.17 represents the dynamic conceptual model which "translates" these three rules of evolution. The first one describes the rotation process, the second models the crop sensitivity evolution while the third one manages the replacement

of crops after a flood. The latter indicates that when flooding occurs the modification of OBJ4 is noticed by EV3 and activates the execution of OP3 that updates OBJ5 introducing the resulting flood damages in his attributes. EV3 also activates OP4 that updates OBJ1 introducing an eventual replacement crop. It is also noted that operation 2 (OP2) is activated by a temporal event. The latter occurs regularly (in our case every two weeks) independently of outside conditions as opposed to an external event such as a flood. In this application the temporal event is used to update the crop sensitivity data with a regular time step. This example illustrates the potential of the REMORA method to develop a Conceptual Data Model for AFORISM. The REMORA approach has been adapted to develop the static and dynamic CDM. The static CDM specifies the required information, the data structuring and organisation to fully satisfy the wide variety of operations required by the AFORISM system. The dynamic CDM describes the content and the ordering of the required operations to update the Data Base and to extract the necessary information when a flood forecast is issued.

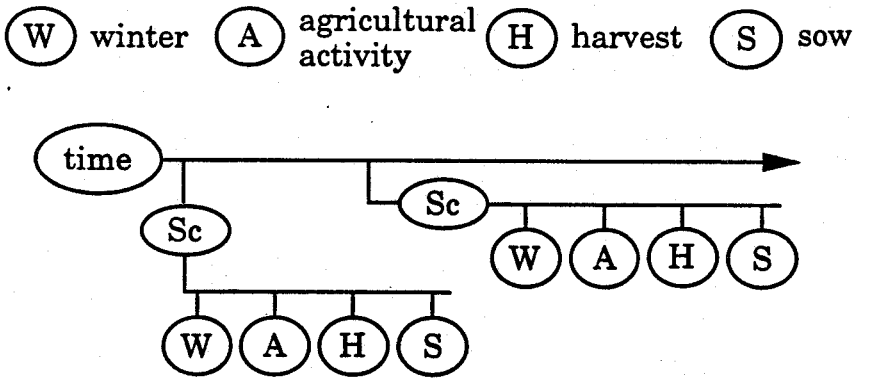

Figure 6.15 - Time perception in agricultural practice

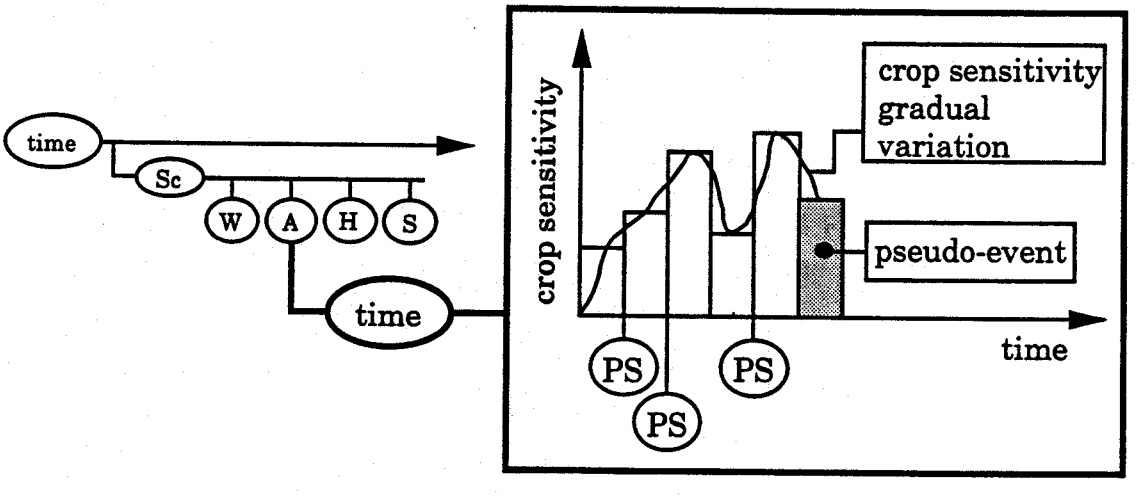

Figure 6.16 - Time representation of crop sensitivity

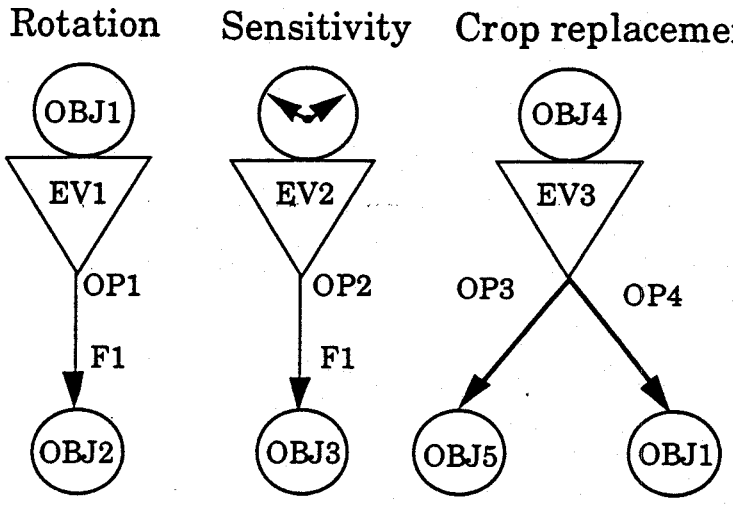

Legend:

Events

EV1: Sow
EV2: Temporal event
EV3: Flood impact

Objects

OBJ1: Crop on parcel (in the field)
OBJ2: Crop on parcel (planned)
OBJ3: Sensitivity
OBJ4: Flood impact
OBJ5: Parcel

Operations

OP1: Updates data on crop according to the rotation rule.
OP2: Updates crop sensitivity data.
OP3: Updates data on economic loss.
OP4: Updates data on crop in the field after the destruction of the planned crop.

Figure 6.17 - Data dynamic model

6.5.6 Summary of Impact Assessment Modelling

The main results of this Impact Assesment study can be summarised as follows:

- An overall framework to assess flood impacts combining GIS capabilities and a suitable hydraulic model has been developed.

- Adequate procedures to evaluate flood impacts in agricultural areas, in built-up zones and for traffic conditions have been developed. Damages for the first two are computed on an economic basis while the third one required the derivation of a particular index.

- The prototypes described in this report fully demonstrate the usefulness and the suitability of GIS to tackle flood impact assessment problems.

- A Conceptual Data Model has been derived for the purpose of AFORISM. It describes data requirements and organisation within a DataBase Management System (DBMS). A dynamic component was also included to account for the large number of data exchanges between the hydraulic model and the GIS as well as during the operations related to the damage assessment procedures.

The prototypes presented in this report provide a sound basis for impact assessment. However, some further developments are required:

- Implement the developed procedures and interfaces into more efficient softwares and platforms. Apply the overall methodology to a real large scale flood delineation study.

- Improve the damage assessment procedures including the social and environmental components.

- Explore the link with expert systems to ensure the applicability of the developed methodology in real time flood forecasting problems.

6.6 CONCLUSIONS

The results presented in this chapter provide the starting point for the detailed design of the operational decision support and forecasting system for the the Reno.

AFORISM has produced a knowledge base with 20 rules, which is far below the power of current computerised KBS (knowledge base/expert system) technology.

Further rules may be envisaged in the areas of

- aggregation and propagation of flood waves,
- overtopping of banks,
- growth and decline of flooded areas, and the
- integrity of the dykes,

While much has been achieved, further extensive computer modelling, optimization and the collection of field data is required, before rule sets can be formulated for routine use by the Reno managers. This work might be carried out in a follow-on phase of AFORISM.

Subsequent work should concentrate on the "heuristic operating policy". It should be modified in small ways in search of improvements and tested on the PAB and GIS simulators of Reno floods. This would lead to recommendations about what the most significant (for better or for worse) modifications to the current policies are, and may come up with a significantly improved policy.

Here, use should be made of the rainfall simulation model in conjunction with the ARNO rainfall-runoff model to produce possible flooding scenarios

The GIS flood impact assessment models and procedures are ready for transfer to the Reno, since it has been shown to be an effective toll for visualization of the problems besetting flood-phone areas. This imprimation transfer methodology should be of particular use to planners and decision-makers.

REFERENCES

Ball , M.O., W.F. Balas , and D.P. Loucks, 1978, Structural flood control planning - *Wat. Res. Res. 14(1),* pp 62-66.

Barton, 1969, *. *"Communities in Disaster: A Sociological Analysis of Collective Stress Situations"* ; Doubleday and Company: Garden City, New York.

Bogardi, I., 1968, Flood exposure recommended as a parameter for describing the fatigue loading on flood control structures - *Bulletin of the IAHS, No. 3* pp 14-24.

Bogardi , I. and F. Szidarovszky, 1974, nduced safety algorithm for hydrologic design under uncertainty - *Wat. Res. Res.* 10(2), pp 155-161.

Bogardi, I., A. Casti , J. Casti , L. Duckstein, 1977 - Optimal flood levee designs by dynamic programming - *International Institute for Applied Systems Analysis, RM-77-12, 13* pages.

Bone ,Q. and Marshall N.B., 1982, *"Biology of Fishes""*: Blackie: Glasgow, UK.

Bras , R.L., R. Buchanan and K.C. Curry, 1983, Real time adaptive closed loop control of reservoirs with the High Aswan Dam as a case study - *Wat. Resour. Res.* 19(1), pp 33-52.

Brennan , M.M., 1992a, AFORISM: Reno Management problem - *University College, Cork, Ireland.*

Brennan , M.M., 1992b, Proposed initial set of rules as used by managers for decision making in flooding stations on the River Reno, Italy - *University College, Cork, Ireland.*

Burns, R.N. and Dennis, A.R. (1985). Selecting the Appropriate Application Development Methodology. Databse, Fall, pp: 19-24.

Chadwick , A. and J. Moffet, 1984, Hydraulics for Civil Engineering - *Butterworth,* London.

Chevallier J.J. (1994). De l'informatique à l'action: vers des systèmes d'aide à la décision à référence spatiale (SADRS). Proceedings of EGIS MARI'94 held in Paris; Published by the EGIS Foundation, Utrecht, the Netherlands.

Consuegra , D., 1992, Concept de Gestion des Eaux de Surface:Aspects méthodologiques et application au bassin versant de la Broye en Suisse. Thèse No 1064. Département de Génie Rural, Ecole Polytechnique Fédérale de Lausanne; Lausanne, Suisse, 200 pp.

Drabek , Michael A., 1986, *Human Systems Responses to Disaster.* Springer-Verlag: New York.

Duckstein , L., I. Bogardi , F. Szidarovszky and D.R. Davis, 1975, Sample uncertainty in flood levee design: Bayesian versus non-Bayesian methods *Wat. Res. Bulltn.* 11(3), pp 426-435.

Eastman R., Kyem Peter A.K.and Toledano J. (1993). A procedure for multi-objective decision making in GIS under conditions of conflicting objectives. Proceedings of EGIS 93 held in Genoa; Published by the EGIS Foundation, Utrecht, the Netherlands.

Edwards ,R.W. and Brooker M.P., 1984, *"The Ecology of the Wye"*: W. Junk Publishers: The Hague.

Emilia Romagna Regional Authority, 1992, The Napoleonic Channel: River Reno Flood Channel.

Fhrc, 1993, "EUROflood-1st Annual Report-March 1993"; Prepared by Flood Hazard Research Centre, Middlesex University, Enfield, Middlesex, UK.

Fritz & Marks, 1954, *"The NORC Studies of Human Behaviour in Disaster"*; Journal of Social Issues; vol. 10, no. 3, pp 26-41.

Fritz , C.E. et al., 1957, *"The Human Being in Disasters: A Research Perspective"*; The Annals of the American Academy of Political and Social Science, 309, Jan., pp. 42-51.

Frost ,W.E. & Brown M.E., 1972, *"The Trout- The New Naturalist Series"*. Collins: London.

Gagnon P.D., 1993, Modul-R version 2.0. Centre de recherche en géomatique, Département des Sciences Géodésiques et de Télédétection. Faculté de foresterie et de géomatique, Université Laval, Ste-Foy, Québec, Canada.

Haimes , Y.K., K.A. Loparo , S.C. Olenik and S.K. Nanda 1980, Multiobjective statistical method for interior drainage systems - *Wat. Resour. Res.* 16(3), pp 465-475.

Joerin, F., 1993, Conceptualisation statique et dynamique d'un système d'information géographique, utilisé comme outil de simulation. Mémoire pour l'obtention du certificat postgrade en informatique, Laboratoire de Bases de Données, Département d'informatique, Ecole Polytechnique Fédérale de Lausanne; Lausanne, Suisse, 90 pp

Lewis , Gill and Gwyn Williams (1984) *"Rivers and Wildlife Handbook: A guide to practices which further the conservation of wildlife on rivers"*: The Royal Society for Nature Conservation, The Green, Nettleham, Lincoln LN2 2NR, UK.

Macdonald, T.C., and J. Langridge -Monopolis, 1984, Breaching characteristics of dam failures - *Journal of the Hyd. Div., ASCE,* 110(5) pp SC7-596.

Martin, J. and Mc Clure, C. (1988). Structured Techniques: the Basis for Case, revised edition, Prentice Hall, 776 p.

Mellor , D., 1992, Review of Dynamic Programming applications in hydrology with discussion relevance to AFORISM - *University of Newcastle upon Tyne.*

Mileti , Dennis S., T. E. Drabek and J. E. Haas (1975) *"Human Systems in Extreme Environments"* The University of Colorado, Institute of Behavioural Science: Boulder, Colorado.

Morla Catalan , J., and C.A. Cornell, 1976, Earth slope stability by a level-crossing method *Journal of the Geotech. Div. ASCE,* 102(GT6), pp 591-604.

Peck , R.B., 1967, Stability of natural slopes - *Journal of the Soil Mech. and Found. Div. ASCE,* 93(SM4), pp403-417.

Pereira J. M. C.and Duckstein L., 1993, International Journal of Geographic Information Systems, Vol. 7, No 5, pp:407-424.

Perry , R.W. et al.1980 *"Enhancing Evacuation Warning Compliance: Suggestions for Emergency Planning"*; Disasters Vol. 4 No. 4, pp. 433-449.

Perry , W.W., 1982, *"The Social Psychology of Civil Defence"*; Lexington Books: Lexington, Massachusetts, USA.

Plate , E.J., and L. Duckstein, 1988, Reliability-based concepts in Hydraulic Engineering - *Wat. Res. Bulltn.* 24(2), pp 235-245.

Quarantelli , *. (1982): *"Inventory of Disaster Field Studies in the Social and Behavioural Sciences: 1919-1979"*; Disaster Research Centre, The Ohio State University, Columbus, Ohio.

Rolland,C., Foucaut, G. and Benci, G. (1988). Conception des systèmes d'information: la méthode REMORA. Edition Eyrolles, Paris, France.

Simonovic , S.P., 1989, "Application of Water Resources Systems Concept to the Formulation of a Water Master Plan", Water International, 14, 37-40, 1989.

Simonovic , S. P., 1993, "Expert Systems for Water Resources Management" Technical Report n. 9/93. Centro IDEA. Bologna.

Sttendinger , J.R., 1983, Confidence intervals for design events - *Journal of Hyd. Eng ASCE,* 109(1) pp 13-27.

Szidarovsky , F, L. Duckstein and 1. Bogardi, 1975, Levee system reliability along a confluence reach - *Journal of the Eng Mech. Div. ASCE,* 101(EM5), pp 609-622.

Todini, E., Bossi, A;, 1986. PAB (Parabolic and Backwater) an unconditionally stable flood routing scheme particularly suited for real time forecasting and control, J; of Hydraulic Res., Vol. 24, n. 5, pp. 405-424.

Torterotot, J.P. (1994). Les coûts des dommages dûs aux inondations: Estimation et

analyse des incertitudes. Thèse de Doctorat de l'Ecole Nationale des Ponts et Chaussées, spécialité Sciences et Techniques de l'Environnement, Paris, France.

Tung , Y.K., and L.R. Mays 1980, Risk analysis for hydraulic design - *Journal of the Hyd. Div. ASCE,* 106(HY5), pp 893-913.

Tung , Y.K., and L.R. Mays, 1981, Risk models for flood levee design - *Wat. Resour. Res.* 17(4), pp 833-841 .

Tung , Y.K., and L.R. Mays, 1981, Optimal risk-based design of flood levee systems - *Wa~. Resour. Re.s.* 17(4), pp 843-852.

Tung , Y.K., 1987, Effect of uncertainties on optimal risk based design of hydraulic structures *Journal of the Wat. Res. Plan. and Mgt. ASCE,* 113(5), pp 709-722.

Vanmarcke, E.H., 1977a, Reliability of earth slopes - *Journal of the Geotech. Div. ASCE,* 103(GTl l) pp 1247-1265.

Vitalini, F., 1993, Una procedura per la previsione, il controllo e la gestione del rischio di inondazione in forma distribuita sul territorio. Tesi di Laurea. Facolta di Ingegneria, Dipartimento di Ingegneria Idraulica, Ambientale e del Rilevamento, Politecnico di Milano, Milano, Italia, 300 pp.

Yevjevich, V. (1992). Floods and society. In G. Rossi, N. Harmancioglu and V. Yevjevich (Editors), Coping with Floods. pp 11-18. Pre-proceedings of the NATO A.S.I. held at Majorana Centre, Erice, Italy.

7. THE RENO RIVER CASE STUDY

The following chapter describes the combined experiment on the Reno River catchment which was conceived of with the purpose of aggregating the different components of the AFORISM project.

The Reno river has a very long history of floods, going back in time to the age of the Etruscans. Only recently was an integrated monitoring system implemented on the catchment for the purpose of monitoring the river and trying to control the flood waves travelling along the flat reaches in the plain.

After a brief geographical and historical overview of the river Reno, the chapter continues with a description of the cascade of models implemented in collaboration with the local Authorities, in particular with the Reno River Basin Authority and with the Bologna branch of the Hydrographic and Marigraphic National Services.

The chapter concludes with a description of he first experiment on the use of a Limited Area Atmospheric Model precipitation forecast as the input to a rainfall-runoff model in order to extend the forecasting lead time, will be presented together with a discussion on further research needed to improve the quality of quantitative flood forecasts.

7.1 DESCRIPTION OF THE RENO RIVER SYSTEM

Situated in Italy, the river Reno rises north of the Apennines and flows down to the Po Valley, where it turns east and empties into the Adriatic sea north of the town of Ravenna (see Figure7.1).
The river extends over a total length of 210 Km and has a basin of approximately 4017 Km^2.

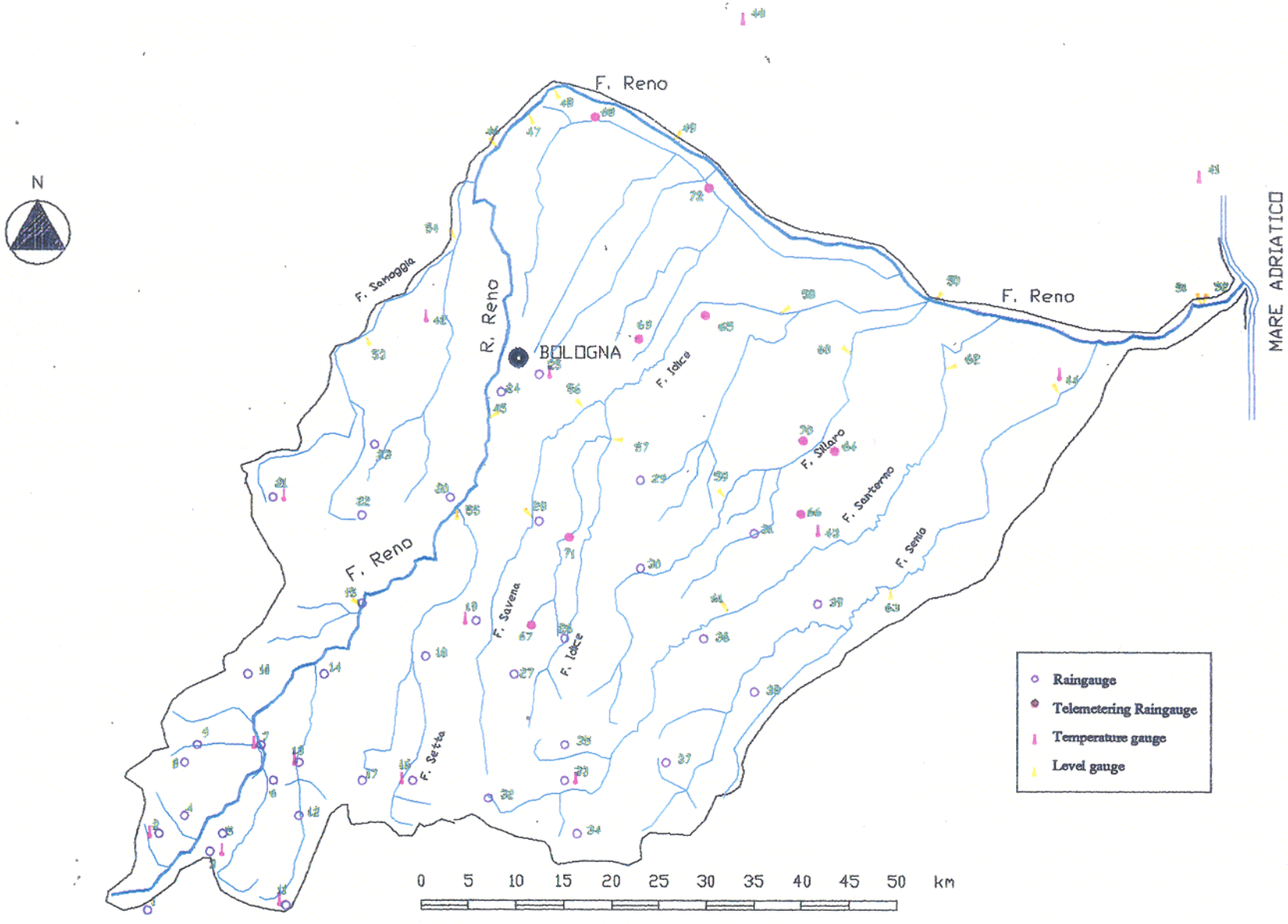

Figure 7.1 - The Reno river basin showing sites of the gauging stations.

7.1.1 History of the development of the course of the river

The flow characteristics of the river Reno lie behind an enormous number of disastrous events which, down the centuries, have altered the course of the river and the lowland basin between the Via Emilia and the district of Ferrara. Indeed, it is worth remembering that since ancient times the authorities designated to control the waters of Ferrara always regarded the river Reno as an inveterate problem that was difficult, if not impossible, to solve. A brief history of the river is therefore warranted.

Before the end of the first millennium, according to extant documents, the situation on the Bologna-Ferrara lowland plain was relatively stable. At Ferrara the river Po divided into two branches, the Volano that headed north, and the Primaro that flowed south. Below the Primaro, on the right bank, lay a large marsh, known as the "Padusa", into which emptied the rivers and streams that ran down from the Apennines. One of these was the Reno. In the Padusa, the waters deposited their solid particles and, thus clarified, flowed into the Primaro and from there to the sea. The lowland plain between the districts of Bologna and Ferrara was slowly filled and raised.

This state of balance was shattered by two major breaches of the Po at Ficarolo, first in 1152 and again in 1192. The Po opened up a new channel, called Po Grande and Po di Venezia, with a wider, shorter and swifter course (because of the steeper slope) towards the sea. The waters flowing into the branch that then split into the Volano and Primaro greatly diminished and this in turn led to a drop in the marshy waters on the right bank of the Primaro and the depletion of the Padusa. The Apennine water courses drew nearer and nearer to the Primaro.

This led the Bologna City Authorities in the fifteenth and sixteenth centuries to embank the rivers and direct them into the Primaro, thereby freeing vast areas from the waters. The Santerno, Lamone, Senio, Sillaro, Quaderna, Gaiana and Savena suffered this fate in 1460. They were followed by the Reno, which in 1522 was directed into the short reach of the Po upstream of Ferrara that then split into the Primaro and Volano below the town. This canalisation had dire consequences for Ferrara as the waters of the Reno silted up the Primaro Po.

The attempts made to excavate the channel, first by the Este family and later by the

Papal Government (the Great Clementine Excavation) did not succeed in restoring the lost balance. In fact, at the end of the sixteenth century, the Apennine rivers and streams entering the Primaro escaped their channels and the marsh once again occupied the areas which had been given over to cultivation. The economic damage caused to the district of Bologna was massive and, among other things, occasioned the interruption of direct navigation between Bologna and Ferrara along the shipping canal or "Canale Navile".

What is more, the advantage accruing to Ferrara did not last long. In fact, early in the seventeenth century the Papal Government, in exchange for recognition of its rights over the city of Ferrara (taken from the Este family) by Venice, agreed to the cutting off of the Po Grande at Porto Viro. With this, the Venetians shifted the principal mouth of the Po further south so that its turbid waters, being conveyed to the Ferrara coast, would not silt up the Lagoon (as they had previously done). This led to the raising of the coast at Ferrara, impeded the outflow of the waters in the coastal lowlands, and compromised the Major Ferrara Land Reclamation Project.

The water situation in the districts between Bologna and Ferrara was the subject of heated debate between those in favour of directing the Reno into the Po Grande (as had been done with the Panaro in 1622) and those who preferred to direct its waters along the line of the lowlands on the right bank of the Primaro. However, very little was actually done until 1749, when after yet another breach of the Reno, a new rehabilitation project was drawn up for the Reno-Primaro area, entailing the construction of the Cavo Benedettino or "Benedictine Channel" which was to convey the clarified waters of the Poggio and Malalbergo valleys into the Primaro and receive the waters of the canalised Savena and Idice. The disastrous breach of the Reno in 1750 (Panfilia) rapidly silted up the Channel which soon proved to be inadequate.

Finally, in 1767, permission was granted for work to begin on the Lecchi-Boncompagni project, which entailed directing the Reno along the line known as "lowland to lowland", from Panfilia to the sea, using the re-excavated Benedictine Channel and the Primaro below the Traghetto. In the course of the works the Primaro was strengthened with new banks, the T. Savena was fed into the Idice, immediately downstream of S.Lazzaro, and major works were carried out to divert the Idice into the Marmorta lowlands and the Correcchio into the Sillaro. Thus, at the end of the eighteenth century,

a good portion of the Bologna lowlands was freed of dead-water, albeit at the cost of a massive public debt.

A short time later Napoleon's army entered Italy and threw the country's existing states into confusion. Bologna became the capital of the Reno district, Ferrara capital of the Po district, and both were subsumed under the Cispadane Republic, which later returned to the Kingdom of Italy.

In the years following the establishment of the Napoleonic government in Bologna, the Lecchi-Boncompagni reclamation project revealed grave shortcomings. The turbid waters of the Reno raised the channel bottom and as a result the waters of the Bologna lowlands could not be permanently accommodated within it. The lowlands started to expand once again. For this reason, the government agreed to the idea to direct the Reno into the Po Grande along a canal (ten miles long) which, beginning at Panfilia, near S.Agostino, was to terminate in the Palantone (the outlet actually chosen was the Panaro, at Bondeno, and from there to the Po Grande). Excavation work began in 1807 and proceeded with various ups and downs.

In 1813 the Idice was diverted at S. Martino in Argine and, from there, together with the Quaderna, was directed into an embanked area east of Molinella that was called the Idice and Quaderna Fill. A short time later, the work on the major channel was interrupted at Bondeno due to the ruinous defeat of Napoleon Bonaparte and the fall of his empire. Thereafter, for the whole of the nineteenth century, works on a smaller scale were undertaken, some of them with the involvement of private parties.

The second half of the nineteenth century witnessed the development of hydraulic machines for the mechanical lifting of water. These altered the plight of lowland areas by ensuring the permanent drainage of water. Works which formerly had been precarious, and therefore uneconomical, became cost effective thanks to the mechanical raising of water. Moreover, the progress made in electrical technology with the development of electric pumps that were far more efficient - and therefore less expensive - than the steam and internal-combustion engine variety, paved the way for mechanical reclamation projects in circumscribed areas (the most depressed).

The Napoleonic structure only became really operational in the second half of the twentieth century. Today the main purpose of the canal (known as the "Napoleonic

Channel") is irrigation, though it is used in some cases to divert part of the discharge of the river Reno towards the Po during exceptional flood events.

Due to the fact that most of the river Reno, after it has crossed the city of Bologna, is confined within dikes that are virtually suspended in relation to ground level, the Reno does not receive water by gravity from the catchment basins in this area. The runoff in this area is fed into the Reno by mechanical lifting.

7.1.2. Description of the upland basin

The upland basin of the river Reno covers an area of 1051 Km^2 measured at the Casalecchio outlet, of which some 178.5 Km^2 are situated in Tuscany; this part of the basin reaches elevations of over 2000 metres in the Apennines (see Figure 7.2).

A series of tributaries characterises the upland reaches of the Reno basin. A sub-basin may be identified for each of the larger tributaries, and each sub-basin has its own tributaries.

The main tributaries on the left bank of the Reno are, from upstream to downstream: the Maresca and Orsigna (in Tuscany), the Randaragna, Rio Maggiore, Silla, Marano, Vergatello, Croara and Venola. The right bank tributaries are, again moving downstream: the Limentra di Sambuca, Limentra di Treppio, Camperolo and Setta, their sub-tributaries being the Brasimone (left bank), the Gambellato, the Voglio and the Sambro (right bank).

Situated in this part of the basin are several reservoirs serving a variety of purposes (electrical power generation and drinking water supply). The system of reservoirs comprises:

- the Molino del Pallone dam;
- the Pavana dam;
- the Suviana dam;
- the Brasimone dam.

Figure 7.3 shows the system described, while the scheme in Figure 7.4 shows how the reservoirs are connected to each other.

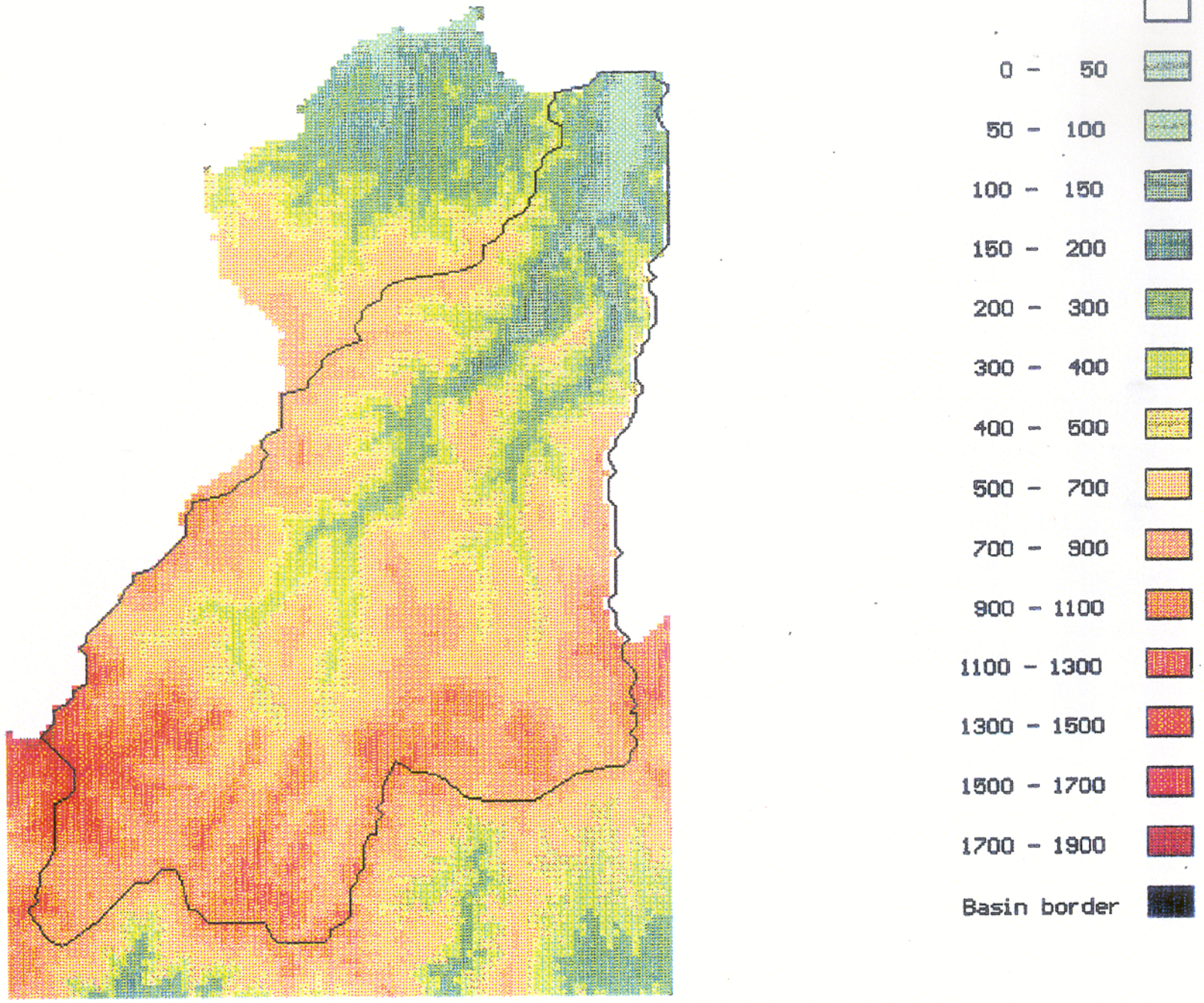

Figure 7.2 - Digital Elevation Model of the Reno river basin to the Casalecchio weir

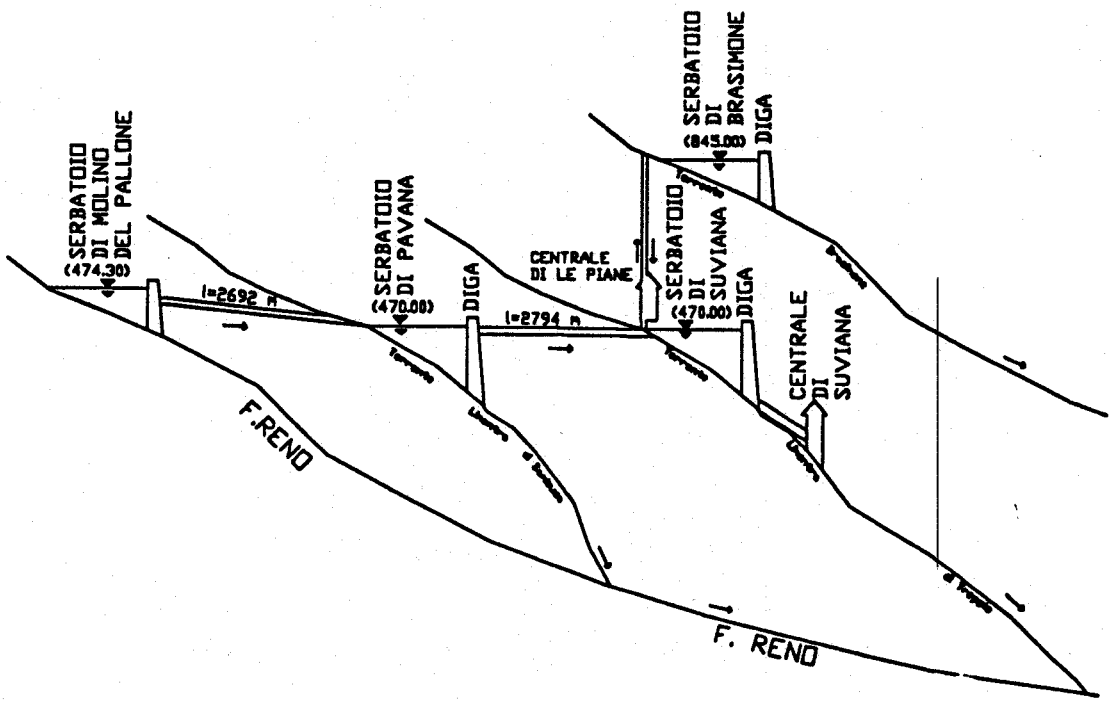

Figure 7.3 - Diagrammatic vertical section of the reservoir system of the upper Reno

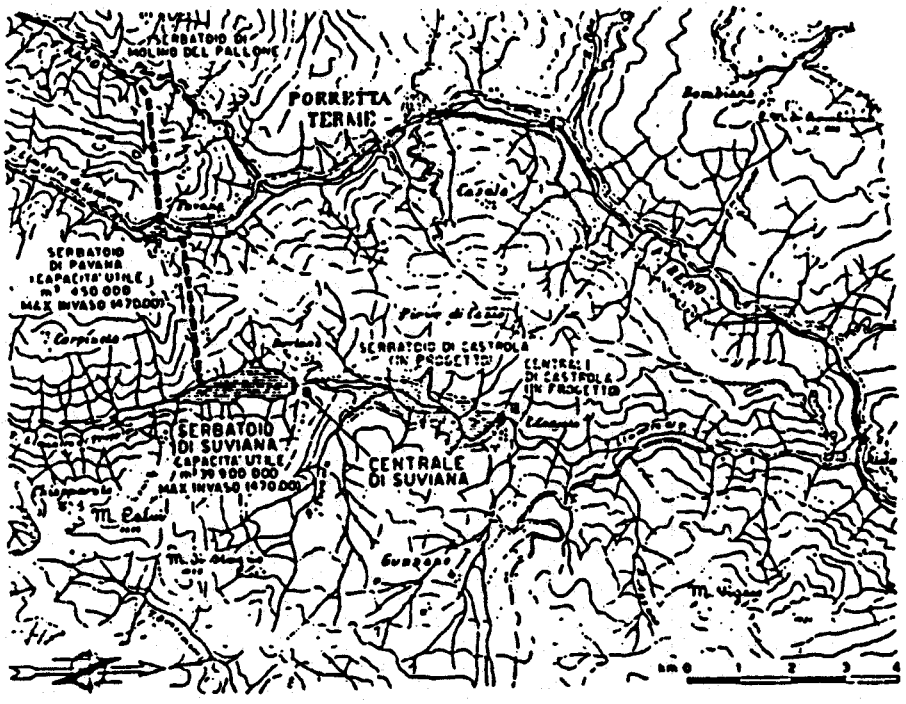

Figure 7.4 - Plan of the reservoir system of the upper Reno